Mechanisms of HIV-1 Persistence and Post-Treatment Control

Mechanisms of HIV-1 persistence and post-treatment control

A dissertation presented

by

Radwa Raed Sharaf

to

The Division of Medical Sciences

in partial fulfillment of the requirements

for the degree of

Doctor of Philosophy

In the subject of

Virology

Harvard University

Cambridge, Massachusetts

April 2019

Dissertation Advisor: Daniel Kuritzkes & Jonathan Li Radwa Raed Sharaf

Mechanisms of HIV-1 persistence and post-treatment control

Abstract

The typical course following HIV-1 infection has been well-documented throughout numerous research studies. In this thesis, we focus on the mechanistic understanding of two atypical contrasting phenotypes that have not been well-studied; namely post-treatment control and persistent low-level viremia. The former, post-treatment control, was demonstrated in treated individuals who interrupt therapy, yet maintain viral suppression. We explored their proviral landscape and determined that levels of total, as well as intact, proviral genomes are significantly lower in post-treatment controllers, compared to non-controllers. Interestingly, the proportion of various proviral classes did not significantly differ between the two groups. We identified total proviral genomes as a biomarker to predict post-treatment control before therapy is interrupted. Additionally, to determine whether limited treatment interruptions led to an irreversible increase in the viral reservoir, we measured levels of integrated HIV-1 DNA before and after interruption and found that levels of integrated HIV-1 DNA returned to pre-treatment interruption levels after therapy was resumed. Furthermore, we studied the mechanism underlying persistent low-level viremia, which occurs in a subset of treated individuals with documented high levels of adherence, absence of drug-resistant viral variants and inability to suppress the viremia by treatment intensification. We found that plasma viremia is largely clonal and identified the matching proviral clone. Integration site analysis showed that transcriptional interference from the host gene into which the provirus was inserted regulated expression of the viral transcripts. Future studies of post-treatment controllers and individuals with persistent low-level viremia are needed to further our understanding of the mechanisms underlying HIV persistence and virologic control.

Table of Contents

In Appreciation Of My Parents

Raed Sharaf and Eman Hanafy

For everything they did and still do

&

In Loving Memory Of Raghda Eltagoury

She lived and laughed and loved and left

(1987-2014)

Acknowledgments

To Jonathan Z. Li, also known as “El Jefe,” who took a risk by adopting a third-year graduate student into his lab family. I will forever be grateful to you for supporting me on a daily basis, professionally and personally, and for giving me the freedom to pursue various projects without objection. Thank you for being my number one advocate and for having a vested interest in my future. Thank you for showing me that science is a collaborative endeavor. You have taught me that research lies in the technical details as much as in the hypothesis behind the experiments. And of course, thank you for the many jokes, laughs, pranks and bets over the years.

To Daniel Kuritzkes for his insightful help and guidance. Thank you for your patience, words of encouragement and teaching me intricate details about the English language. In addition, I am grateful for the many helpful comments you made throughout my dissertation work and the preparation of this manuscript.

To my past and present lab mates who were my family away from home: Rachel, Zach, Jesse, Colline, Behzad, Layla, Golnaz, Elmira, Nick, Ying, Xin, Sara, Ruth, Françoise, Zixin and Tracy. The warmth that everyone has shown made up for all the snowy days in Boston.

To my companions along the PhD journey: Fernanda and Phil, senior and older grad student, respectively. I couldn’t have asked for a better company. I am grateful for current and former students in the virology program for the comradery.

To Mathias Lichterfeld and Xu Yu for the numerous discussions, assistance and feedback on my work. I am grateful for the chance to learn from and work with you.
To Guinevere Lee and Charlie Gao, who helped me analyze the proviral sequence data and sparked my interest into the world of bioinformatics.
To Xiaoming Sun, Stephane Hu, Chenyang Jiang and Kevin Einkauf for their help with our projects.

To Todd Allen, Joseph Sodroski and Alejandro Balazs, who have taken time out of their busy schedules to give me invaluable advice on my work during the DAC meetings.

To David Cordozo for his incessant support and heartfelt conversations over lunch. You are the dean every graduate student needs, but only a lucky few were so fortunate to have had.

To Athe for his $1.

To Lora Maurer, Maria Bollinger and Catherine Dubreuil who ensured everything ran smoothly.

To Karl Munger for his words of encouragement and advice.

To James Chodosh for our stimulating lunch discussions.

To Maud, Shariq and Thomas. I don’t think I would have survived the early years had you not been there for me. I appreciate you taking the time to teach and guide me.

To Julie, I can proudly say: I am done writing :)

To Aly who always greets me with a smile in the morning.

To Ramy Karam Aziz. You believed in me from the beginning. Every time I open PubMed, I remember when you first showed it to me.

To my friends within science who have experienced - or are still experiencing - the life of a graduate student: Ali Ellebedy, Sara Serag, Rania Sulaiman, Eslam Samy, Bassem Mostafa, Douaa Mugahid, Sara Amr and Aya Almarsafawi. Thank you for understanding, for listening and for visiting.

To Yossr and Manar. You were and still are my backbone.

To dear friends in Berlin: Mona, Nada and Andrea.

To Hala, Dina, Mai, Sarah, Mariam and the wonderful tante Gigi. You kept me laughing.

To the movie night / board game / matcha-is-ok-but-when-is-the-strawberry-coming-out clan, Cherry, Sherif, Karim, Rana, Ahmed, Moemen, Rana & Lina: You guys are a true blessing!

To Sara Mohsen, Doaa Abdallah, Rahma Kasem, Radwa Kamal, Samira Mahmoud, the microbiology department and the wonderful alum of FOPCU. Our chats brightened my days.

To Nada, Mostafa and the entire squash team: Thanks for making the tournaments possible and introducing me to the courts.

To Sara and Khaled: Thanks for dragging me to the gym.

To an amazing group of Egyptians in Boston.

To my former roommates Giulia, Natalia and Sara.

To my friends and family in Egypt. I am fortunate indeed. You always had my back.

To my brother Khaled and his wife Menna for their moral support, the food and most importantly for bringing into life our bundle of joy, Maryam.

To my beloved parents, Raed and Eman. The thanks I owe you cannot adequately be expressed. It is through your constant guidance and devotion to my education that I am able to express the ideas set forth in this thesis.

Lastly, I would like to thank HIV-1 post-treatment controllers for their existence, without whom this dissertation would not have been possible.

CHAPTER 1

INTRODUCTION

Introduction was partly published as a review in Curr HIV/AIDS Rep. 2017 Apr;14(2):72-81.
doi: 10.1007/s11904-017-0355-y.

Human immunodeficiency virus (HIV-1) is a lentivirus, a genus of retroviruses. HIV-1 preferentially infects activated CD4 T cells of the adaptive immune system. If untreated, HIV-1 infection progresses over time to the acquired immunodeficiency syndrome (AIDS). AIDS is precipitated by a decline in CD4 count and is characterized by progressive failure of the immune system, allowing life-threatening opportunistic infections and cancers to occur (Figure 1.1A). Within bodily fluids of an infected individual, HIV-1 is present as both cell-free viral particles and virus residing within infected immune cells. The virus is acquired through sexual or blood transmission. Vertical transmission can also occur from an infected mother to her infant. Since the beginning of the epidemic, the World Health Organization estimates that more than 70 million people have been infected with HIV and about 35 million people have died of HIV. Globally, almost 37 million people were living with HIV at the end of 2017. In most HIV-1 patients, antiretroviral therapy (ART) effectively controls the infection, suppressing plasma viremia and reversing the CD4 count decline (Figure 1.1B). ART is crucial for the patient's wellbeing and preventing transmission. Suppression of plasma viral load (VL) below the quantification limits of clinically accessible assays (20-50 copies/mL) is a widely accepted indicator of successful ART. Despite the success of antiretroviral therapy in suppressing HIV and its dramatic impact on the HIV epidemic, it is not curative.

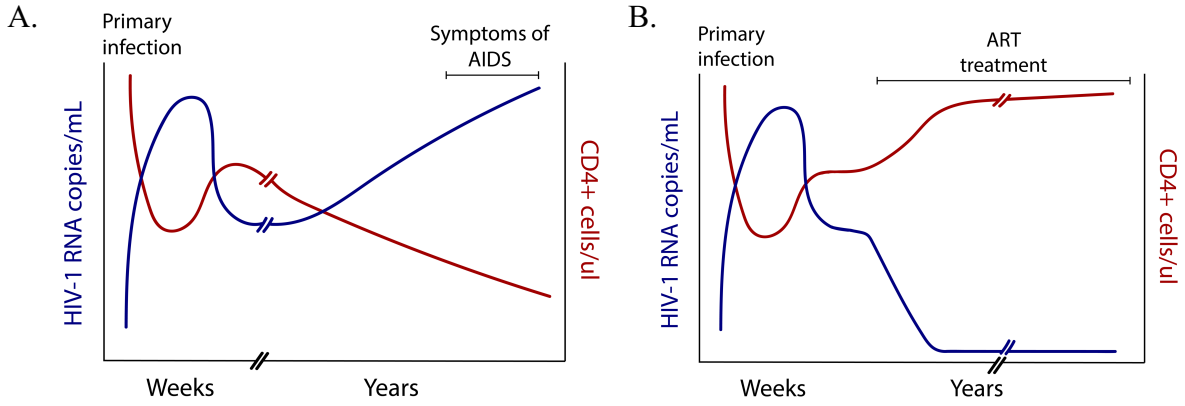

Figure 1.1: Viral load and CD4 changes in an untreated infected individual (A) and an individual on ART (B).

1.1: Replication cycle of HIV-1

HIV-1 requires the attachment of its viral protein envelope (ENV) to a cellular receptor (CD4) and a co-receptor (either CCR5 or CXCR4) to allow for entry (Figure 1.2). This promotes membrane fusion between viral and target cell membranes, enabling the viral core to enter the host cell cytoplasm. This is followed by uncoating, which releases the viral nucleoprotein complex. HIV, like other retroviruses, encodes the enzyme reverse transcriptase (RT), which reverse transcribes the single-stranded RNA genome into linear double-stranded DNA. HIV-1 RT lacks proofreading activity and has a high error rate estimated at 3-4 $\times$ 10^{-5} per base per round (1, 2). This allows for the accumulation of mutations with every replication cycle. In addition, the retroviral genome is packaged into the virion as two copies of single-stranded RNA. During reverse transcription, RT frequently switches from one template to the other, a phenomenon referred as template switching. When cells are infected with more than one copy of HIV, such switching can generate viral recombinants. In addition, RT can also undergo intramolecular jumps, leading to a myriad of mutations, such as deletions, insertions, duplications and internal inversions. One of the fundamental challenges to effectively controlling HIV-1 is the genetic heterogeneity of the viral populations, which is largely a consequence of rapid virus replication rates and an error-prone RT, coupled with frequent template switching.

Once the genome is reverse-transcribed, the linear double-stranded DNA is imported into the nucleus and inserted into the host genome by the process known as integration. Integration is a distinguishing feature of retroviral replication and is catalyzed by the enzyme integrase (IN). The integrated viral DNA, also known as provirus, serves as the template for synthesis of viral transcripts by the host transcriptional machinery. Viral transcripts comprise genomic RNA that is packaged into virion particles and viral mRNA that is translated to make viral proteins. Most

integrated proviruses are defective and only a small proportion are intact, potentially coding for replication-competent virus (3–5).

Integration is a critical and, as yet, irreversible step of HIV replication. The pre-integration complex (PIC) consists of viral DNA, IN and other components that facilitate nuclear import and subsequent integration. The PIC interacts with one or more host factors that help the PIC associate with host chromatin (6–12). Overall, HIV integration is favored in introns of actively transcribed genes (13–15). There is a weak sequence conservation at the integration site, which is determined by interactions between the viral integrase enzyme and host DNA (16, 17). Given that the integrated provirus is part of the host cellular DNA, when an infected cell replicates, all the daughter cells will harbor the same exact provirus integrated at the same site as the parental cell. Thus, integration sites can be used to track the clonal expansion of infected cells.

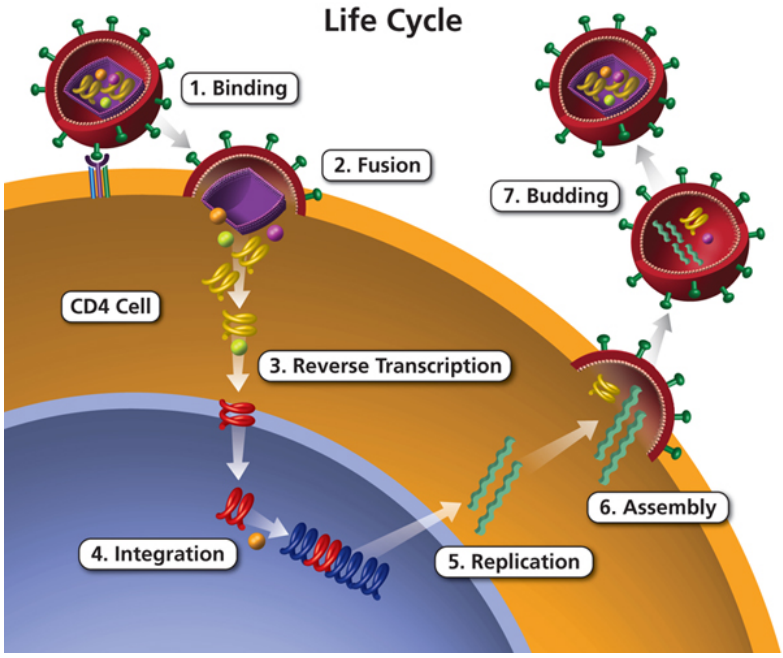

Figure 1.2: Replication cycle of HIV-1.
Source: AIDSinfo - NIH

1.2: HIV-1 reservoir

Productively infected CD4 T cells can revert to a resting memory state in which there is minimal transcription of viral genes. This process is referred to as post-integration latency. Latently infected memory CD4 T cells carrying integrated provirus represent a largely stable reservoir with a $t_{1/2}$ of 44 months and are the main barrier to eradication of the virus (18–20). Persistence of HIV-1 infected cells in the body arises through a number of factors. First, memory T cells are long-lived and can survive in the human body for years. HIV-1 proviral DNA is maintained as a part of the host cell genome for the lifetime of that infected cell. In addition, there are several lines of evidence showing that cells harboring integrated HIV-1 proviruses can undergo both homeostatic proliferation and clonal expansion. This expansion may be driven by a response to a particular TCR antigen stimulus or it may be integration-site-driven (14, 15, 21, 22). If these dividing cells harbor replication-competent provirus, this mechanism will contribute to persistent infection.

1.3: Measurements of the reservoir size

Life-long therapy is required to avoid HIV reactivation from long-lived viral reservoirs (23, 24). Currently, there is intense interest in searching for therapeutic interventions that can purge the viral reservoir to achieve complete remission in HIV patients without the need for antiretroviral therapy. Since the viral reservoir in individuals on ART is small, consisting of approximately 1–10 infectious units per million peripheral blood mononuclear cells (PBMC) (18, 19, 25), the evaluation of any intervention relies on our ability to measure accurately and precisely the true size of the reservoir. However, the optimal method of measuring the HIV reservoir size remains controversial, as all current assays have strengths and weaknesses. This problem is reflected in the diversity of reservoir assays evaluated as part of previously completed and current clinical trials (26–29). Overall, there are several categories of HIV reservoir assays, including 1) intracellular HIV DNA, 2) cell-associated HIV RNA, 3) viral outgrowth assays, and 4) inducible HIV RNA assays, amongst others.

1.3.1: HIV DNA assays

Total HIV-1 DNA includes all forms of HIV-1 DNA: circular unintegrated, linear unintegrated and linear integrated. The relative abundance of each species has been reported to be in the following descending order: non-integrated linear DNA > integrated proviral DNA > non-integrated circular DNA (30, 31). Specifically in non-suppressed patients, non-integrated forms make up the vast majority of HIV DNA in the nucleus, which is approximately 100-fold more frequent than the integrated proviral DNA form (32). Separate assays have been developed to quantify each species.

Quantitative real-time PCR (qPCR) or droplet digital PCR (ddPCR) for conserved viral regions can be performed to determine levels of HIV nucleic acid. qPCR monitors the progression

of amplification in each cycle through the use of fluorescent probes, and quantification is performed by measuring the threshold cycle (C_t) at which fluorescence is higher than a certain threshold. While a standard curve is necessary for quantification of copy number by qPCR, it provides a wide dynamic range. Other caveats include susceptibility to primer/probe sequence mismatches that lead to inaccurate quantification and sensitivity challenges in detecting low copy numbers. The former can be tackled using patient-matched primers (33) or calculating the patient-specific mismatch-related quantification errors (MRQE) by comparing the amplification of patient sample with that of a control template without mismatches (34).

1.3.1.1: Total HIV DNA

To determine levels of total HIV DNA, qPCR or ddPCR for conserved viral regions can be performed (35). In both of these platforms, probes for HIV DNA have targeted HIV-1 *gag* (35, 36), *pol* (37) or the long terminal repeat (LTR) region (38–40). When the three different targets were compared side-to-side, targeting the LTR region was shown to be superior and resulted in some cases in a $\log_{10}$-higher number of HIV copies (41). To determine the copy number of HIV-1 DNA per cell, a parallel measurement of a control gene (such as CCR5 (42), β-globin (43) or albumin (35)) is frequently conducted to quantify the number of cells assayed during the HIV DNA measurement. Alternatively, a parallel blood sample, drawn simultaneously, can be stained for CD4 and run for flow cytometric analysis (36).

In patients on suppressive ART, total HIV DNA level is reflective of the total HIV proviral reservoir size and may predict the timing of viral rebound after treatment interruption (44, 45). However, a PCR-based approach for measuring the viral reservoir leads to an over-estimation of the size of the replication-competent reservoir, as the vast majority of viral genomes quantified are

not replication-competent. It has been estimated that measuring total HIV DNA may over-estimate the intact HIV reservoir by greater than 100-fold in those treated during chronic infection and by more than 10-fold in those treated during acute infection (3). It is important to note that unintegrated viral DNA contributes to the total HIV DNA signal, yet possesses limited transcription potential (43, 46). This distinction is especially important when monitoring reservoir size in viremic non-suppressed patients, who have an excess of unintegrated HIV DNA that confounds the interpretation of total DNA levels (47, 48).

1.3.1.2: Circular unintegrated HIV DNA

Circular unintegrated forms include 1-LTR and 2-LTR circular HIV DNA. In non-suppressed patients, non-integrated DNA makes up the majority of total DNA (47). However, in virologically suppressed patients, circular HIV DNA forms represent a minor population. The 2-LTR circles, for example, represent approximately 0.03-5% of total viral DNA during the early stages of viral infection *in vitro* (49, 50). Quantification of 1-LTR circles by qPCR has been technically challenging and unreliable because they lack unique sequence segments to distinguish them from proviral or linear unintegrated DNA (51). The presence of 2-LTR circles can be assayed by using primers specific for the junction between the two LTR ends and performing either qPCR or ddPCR (37). Historically, detection of 2-LTR circles has been considered evidence of recent viral replication, but this association has been called into question (52).

1.3.1.3: Integrated HIV proviral DNA

a) Alu-gag PCR

There are situations where measurement of only integrated proviral HIV DNA is indicated. This issue is especially relevant for participants who are not virologically suppressed, where linear

and circular nonintegrated forms may dominate the total DNA measurement. To quantify integrated DNA alone, a nested PCR, known as Alu-*gag* PCR, can be performed (21, 53). The first PCR utilizes a forward primer that is virus-specific, recognizing the U5 region of the LTR, while the reverse primer binds to Alu repeats in the human genome. This approach results in specific amplification of integrated HIV DNA. Alu elements are abundant ~300 bp-interspersed repeat sequences, distributed at a frequency of 1 Alu element in every 2.5 kb of the human genome (54). Alu-*gag* pre-amplification generates a population of cellular-HIV junction DNA sequences of various lengths. After the initial amplification round, qPCR is used to quantify total copies of integrated provirus (55). Pitfalls of this approach are that only integrated forms of the virus that reside close to Alu repeats will be reliably amplified (56) and the high variability between sample replicates. To address this problem, repetitive sampling has been introduced (53, 56, 57).

b) Gel separation

Agarose gel electrophoresis can be used to separate genomic (approximately 20 kb) high-molecular weight (HMW) DNA from episomal DNA. HMW DNA is then recovered from the gel and subjected to HIV-specific qPCR. This approach has been implemented in some studies and authors have reported that this fractionation procedure eliminates 97-99% of linear HIV-1 DNA and 99% of 2-LTR circles (47, 58–60). This assay is not commonly employed, but can also determine levels of all non-integrated HIV species, where HIV unintegrated DNA equals HIV DNA from total DNA minus integrated HIV DNA from HMW DNA.

c) Fluorescence In-Situ Hybridization (FISH)

FISH can be used to quantify the number of integrated proviral DNA copies (61) and was successfully used on splenocytes from splenectomized HIV patients (62). That study demonstrated that the majority of infected spleen cells in HIV patients harbor more than one proviral copy, with a mean of 3-4 proviruses per infected cell, although work from other groups has shown that >90%

of infected cells in the lymph node harbor only once copy of proviral DNA (63). DNAscope, an optimized *in-situ* hybridization platform that relies on the use of probes spanning the entire length of the viral DNA (vDNA), can detect latently infected cells in lymphoid tissue sections from macaques (64). This technique might represent a sensitive tool to identify sites of latent viral reservoir at the tissue level.

1.3.1.4: Near-Full-Length Single Genome Sequencing (NFL-Seq)

Defective proviruses constitute the vast majority (93-98%) of proviral HIV DNA (3). To better estimate the true size of the intact proviral reservoir, methods to perform full-length single-genome proviral sequencing are becoming increasingly popular. Genomic DNA is extracted from patient cells and subjected to a limiting dilution PCR protocol using primers that span the two LTRs to amplify near-full length HIV proviral DNA from single templates (3, 4, 65–68). Sanger or next-generation sequencing is used to sequence the amplified proviruses. These methods are labor- and cost-intensive, but can provide important details on the types of defective proviral genomes present, in addition to quantifying the number of intact proviruses. Results from these studies have demonstrated that qPCR/ddPCR quantification of HIV proviral DNA significantly overestimates the size of the intact HIV reservoir.

1.3.1.5: Intact Proviral DNA Assay (IPDA)

The intact proviral DNA assay is a newly described assay that separately quantifies intact proviruses by interrogating individual proviruses simultaneously at multiple positions (69). This notion relies on an analysis of 431 near-full-length genome sequences from 28 HIV-1 infected individuals, showing that > 90% of defective proviruses harbor deletions in the packaging signal (psi) and/or *env*. Furthermore, 97% of hypermutated sequences had one or more mutations in a

conserved region within the Rev response element (RRE) harboring a consensus sequence of (TGGG). The IPDA assay categorizes proviruses as intact provided they are positive for both psi and *env* and capable of binding to the intact probe in the RRE. This assay can correctly identify 90% of deleted proviruses as defective.

1.3.2: Cell-associated HIV RNA assays

Within HIV-infected cells, several forms of RNA exist: multiply spliced (ms), incompletely spliced (is) and unspliced (us) (70). Initially, msRNA transcripts are generated, encoding for regulatory proteins, such as Tat and Rev. As the infection proceeds, there is a shift towards isRNA and usRNA, encoding for the full viral genome to be packaged, as well as structural and accessory viral proteins. Assays that measure unspliced HIV RNA have been the most commonly used platform for previous clinical studies, as illustrated by studies determining the effect of HIV latency-reversing agents.

Total HIV RNA transcripts can be isolated and quantified by RT-qPCR or ddPCR, using primers and probes targeting the LTR region (38–40). To assay usRNA species, probe and primers targeting viral *gag*, located downstream of the major 5′ splice donor site (D1), are used. To target the msRNA species, probe and primers targeting *tat* and *rev* are used (71). We have reported that levels of cell-associated (CA)-usRNA are predictive of the timing of viral rebound after treatment interruption (72).

HIV RNA copy numbers are normalized to cellular input, either by running a parallel qPCR for a control gene (such as β-actin [50] or CCR5 [51]) or estimated by total extracted RNA amounts, assuming that 1 ng RNA corresponds to approximately 1000 cells (74). Some groups also report the average transcription per infected cell, calculated as the CA-HIV RNA/DNA ratio

(39). One major limitation of CA-RNA quantification methods is that defective CA-RNA species are also present, similar to HIV DNA (75) and thus RT-qPCR likely overestimates the number of intact HIV transcripts.

1.3.3: Quantitative Viral Outgrowth Assay (QVOA)

While nucleic acid-based measures of HIV reservoir size have some advantages, they are unable to quantify the size of the replication-competent reservoir. QVOA, or the Infectious Units Per Million (IUPM) assay, has historically been the gold standard for detection of the replication-competent HIV reservoir (18, 76). Using a limiting dilution culture format, QVOA measures the number of wells containing detectable HIV-derived p24 antigen released in the supernatant after resting cells are subjected to one round of stimulation (18, 76). Previous reports show that QVOA is relatively robust, and with sufficient cell numbers, HIV-1 can be recovered from the majority of HIV-1 infected participants on suppressive antiretroviral therapy (18, 19, 24, 32). QVOA was used to demonstrate the high stability and low decay rate of the latent virus reservoir in suppressed patients (19), showing generally less than 2-fold variation between longitudinal measurements (20).

The main advantage of this assay is that it detects only the replication-competent virus reservoir. However, QVOA underestimates the reservoir size because at any given time, only a subset of the replication-competent reservoir is activated. Studies have calculated that only 1% of cells harboring HIV provirus release infectious virions after being subjected to maximum *in vitro* activation (4). A large proportion of those non-induced cells harbor defective copies of the integrated HIV provirus, but a subset represents a population of cells with intact virus, which are not activated in any single round of activation. Some reports demonstrated that QVOA did not strongly correlate with the frequency of cells harboring intact proviruses and likely underestimates

the total replication-competent virus reservoir by approximately 25-fold (3, 4). Thus, QVOA should be thought of as the lower-bound estimate of the replication-competent reservoir. QVOA has not been useful in *in vivo* studies measuring the effect of latency reversal agents (LRAs) on the size of the viral reservoir, which highlights its limited sensitivity (27, 29). It has been suggested that more than a 6-fold difference between longitudinal QVOA measurements could be used to reliably detect a change in reservoir size with high confidence (20). Other limitations of QVOA include the requirement of a large sample volume and that it is both time- and resource-intensive. Of note, integrated HIV DNA levels significantly correlate with QVOA (77).

1.3.4: Inducible HIV RNA assays

Quantification of the replication-competent HIV reservoir is challenging due to the overwhelming proportion of infected cells that harbor replication-deficient proviruses and the low frequency of transcriptionally-active cells in those on chronic suppressive ART. Inducible HIV RNA assays seek to bridge the divide between the nucleic acid-based measurements of the HIV reservoir (CA-DNA or CA-RNA) and QVOA. They provide a more accurate reading of the inducible HIV reservoir than the CA-RNA assay alone while potentially providing the frequency of HIV-expressing cells in an assay that is far more rapid and scalable than QVOA. However, replication-defective proviruses may generate RNA transcripts (75) and one limitation of all assays measuring HIV RNA levels is the inability to fully define the replication-competent fraction. The CA-RNA assay measures the copy number of cell-associated viral RNA after stimulation. Briefly, CD4 T cells are stimulated, followed by cell lysis and RNA extraction. Levels of usRNA and msRNA can be measured using RT-qPCR (78, 79). The extent of HIV-1 transcription after activation is based on levels of msRNA, such as those encoding *rev* and *tat*. A limitation of this

assay is the requirement of RNA extraction, where potential loss and degradation of viral RNA may occur.

1.3.5: Protein-based assays

There are few high-throughput and sensitive assays for detecting HIV protein production. Investigators at Merck recently reported the development of an ultra-sensitive immunoassay to quantify p24 and the uncleaved p55 levels in cell lysates and in media from cultured patient cells. It is reported that the assay can detect protein levels down to 14 fg/ml with a dynamic range of > 4 $\log_{10}$, but does require the use of specialized equipment (Quanterix Simoa technology) (80).

1.3.6: Murine Viral Outgrowth Assay (MVOA)

MVOA is a binary end-point assay that uses a mouse model to determine whether patient-derived cells harbor infectious virus (81). In this assay, either whole PBMCs or sorted CD4 T cells are injected into NOD/Prkdc^{scid}/gamma-chain knockout (NSG) mice. Some mice are subjected further to CD8 T cell depletion or T cell stimulation via injection of an anti-CD3 antibody. Over time, HIV RNA from the plasma of xenografted mice is isolated and quantified by RT-qPCR. The assay was successful in recovering virus from patient cells, including an elite controller, who had negative QVOA results (78). It can be used to survey a large number of patient cells, requiring one mouse per 10-50 million CD4 T cells. The assay suffers, however, from drawbacks related to the inherent heterogeneity of human cell engraftment in the murine host and the lack of a quantitative readout.

1.4: Issues surrounding antiretroviral therapy

1.4.1: Persistent low-level viremia

Persistent low-level HIV viremia (LLV) can occur despite continuous antiretroviral treatment. The incidence of LLV on first-line ART has been found to range from 6 – 25% (82–85). In addition, approximately 1 in 5 individuals with LLV have repeated low-level viremia (86). Traditionally, the presence of LLV has been attributed to suboptimal ART adherence (87) or continued viral replication (88, 89). In either scenario, there is potential evidence of viral evolution and emergence of drug resistance mutations (90) and a combination of adherence counseling and ART regimen modification is indicated. However, the presence of viral evolution has not been confirmed in other studies (91) and ART intensification generally has been unsuccessful in suppressing residual viremia clinical trials of individuals with LLV (92, 93). This suggests that for some individuals, persistent LLV may arise due to mechanisms other than persistant virus replication.

1.4.2: Complications of long-term antiretroviral therapy

ART improves the survival and quality of life of HIV-positive individuals, but the life-long use of ART is not without complications. Long-term ART use is associated with cardiovascular, renal, metabolic, hepatic, bone, bone marrow and other complications (94–98). Furthermore, the life-long administration of ART is associated with pill fatigue, stigma and drug-drug interactions. Hence, researchers are searching actively for a cure.

1.5: HIV-1 Cure

With the exception of allogeneic stem cell transplantation (see below), attempts at HIV cure or long-term ART-free remission have been largely unsuccessful. This is in part because the underlying mechanisms that could lead to successful viral control and potential "cure" are poorly characterized. Studying these mechanisms could potentially aid future drug design and vaccine development for HIV cure or remission. Here, we need to differentiate between two forms of "cure": sterilizing vs. functional cure.

1.5.1: Sterilizing cure

Sterilizing cure refers to a situation where no replication-competent HIV-1 remains in an individual who hence is thought to be cured of the virus. There is currently only one confirmed case of HIV cure, Timothy Ray Brown, commonly referred to as the "Berlin patient" (99). The Berlin patient received an allogeneic stem cell transplant from a donor homozygous for the CCR5Δ32 mutation, rendering the donor cells resistant to infection by CCR5-using (R5) virus (99, 100). Prior to the transplantation, he had a plasma viral load of 6.9 X 10^6 copies/mL. Post-transplant, HIV DNA and RNA became undetectable in PBMCs, spinal fluid, lymph nodes and terminal ileum. Importantly, no replication-competent virus could be cultured from PBMCs. Extremely low levels of HIV RNA and DNA were detected by some labs in the plasma and rectum, respectively (101). The circumstances which led to this cure were unique and are attributed to these factors: (1) he received myeloablative chemotherapy and whole body irradiation to deplete the hematopoietic system, 2) he received two allogeneic bone marrow transplants from a donor who was homozygous for CCR5Δ32 mutation, and (3) he exhibited graft-versus-host disease. To this day, the Berlin patient remains free of HIV infection. HIV-1 remission was recently described in two other individuals, who also received bone marrow transplants from donors homozygous for

the CCR5Δ32 mutation, known as the "London patient" and "Düsseldorf patient", presenting with 18 months remission for the former and 3 months remission for the latter (102, 103). However it is still too early to conclusively refer to them as being cured.

1.5.2: Functional cure

1.5.2.1: HIV-1 elite controllers

In contrast to a sterilizing cure, a functional cure represents sustained virologic remission, as in the case of elite controllers (ECs), despite persistence of potentially infectious latent HIV-1 proviruses. Elite controllers are rare individuals who maintain a plasma HIV-1 RNA viral load largely below the limit of quantification by clinical assays and delayed or absent HIV disease progression in the absence of antiretroviral therapy. They comprise 0.5-1% of HIV-1-infected patients in well-described cohorts (104). Elite controllers have been extensively studied (105) and are characterized based on their genetic profile to have favorable HLA class I alleles, including I HLA-B*57 and HLA-B*27 (106, 107). The precise mechanism of viral control in elite controllers is unknown. It has been shown that HIV-specific CD8 T cells from elite controllers produce more pro-inflammatory molecules, like IL-2 and IFN-γ (108) and more cytolytic proteins, like perforin and granzyme B (109, 110). However, it is unlikely that a strong CTL response is the only factor leading to elite control, since elite controllers can maintain viral suppression even in the setting of CTL escape mutations (111).

1.5.2.2: HIV-1 post-treatment controllers

Another group of patients with sustained virologic remission are known as post-treatment controllers (PTCs). These are individuals identified in analytic treatment interruption (ATI) studies. Most patients experience viral rebound within 4 weeks of treatment interruption (112).

PTCs, on the other hand, can control HIV-1 for a prolonged period of time after interruption of antiretroviral therapy; they represent approximately 5-15% of patients who undergo ATI (113). Unlike ECs, favorable HLA alleles are not overrepresented in the PTC population (113).

The first well-described report of post-treatment controllers came from the VISCONTI cohort, short for "Virological and Immunological Sustained CONtrol after Treatment Interruption" study. This cohort comprises 14 individuals who initiated treatment during the early stages of infection and upon ATI, controlled virus for a median of 89 months (113, 114). Eight PTCs had viral loads below the limit of detection at every time point test post-treatment interruption. The remaining six experienced occasional viral blips that were subsequently controlled. Upon initial diagnosis, those PTCs received standard ART. Their viral loads became undetectable and CD4 counts increased within a median of 3 months post-treatment initiation. PTCs had weak HIV-specific CD8 T cell responses, significantly lower than those of elite controllers and low levels of T cell activation. Furthermore, the capacity of CD8 T cells from PTCs to suppress the HIV-1 infection of autologous CD4 T cells *ex vivo* was poor. In the VISCONTI study, PTCs were found to have levels of HIV DNA that were significantly lower than that of ART-treated individuals previously described in the literature, a median 54% of which resided in transitional memory T cells and only 22% in central memory T cells (113).

Our group has recently reported on the CHAMP cohort, short for "The Control of HIV after Antiretroviral Medication Pause" (115). This cohort is comprised of 67 post-treatment controllers identified from 14 completed clinical studies involving a treatment interruption. These PTCs were defined as individuals who underwent treatment interruption and maintained viral loads ≤ 400 copies/mL at two-thirds or more of time points for ≥ 24 weeks. The median duration

of documented viral suppression post-treatment interruption was 89 weeks. Within CHAMP, PTCs were more commonly identified in those treated during early infection (13%) versus chronic infection (4%, $P<0.001$).

A few isolated cases of PTCs have also been described in other studies, including SeaPIP (116), SPARTAC (117), CASCADE (118), PRIMO (119), AIEDRP (120), SALTO (121), the Department of Defense cohort (122), an Italian cohort (123), a Belgian cohort (124, 125), a French pediatric cohort (126), CHER (127), a group in Alabama (128), a female subject in the UK (129), a female subject in Australia (130) and control (unvaccinated) subjects identified in a recent vaccine trial (131). Despite all these described cases, the mechanism behind post-treatment control remains poorly understood.

1.6: Conclusion

The development and evaluation of HIV curative strategies relies upon our ability to accurately and precisely quantify the size of the remaining HIV reservoir. At this time, all HIV reservoir assays have drawbacks such that combinations of assays are generally needed to obtain a comprehensive measure of the HIV reservoir. Techniques that quantify levels of HIV cell-associated DNA are high-throughput, but significantly over-estimate the size of the intact, or true viral reservoir. While the QVOA assay has historically been considered the gold-standard for measuring the size of the replication-competent reservoir, this assay is challenging to perform and is useful only for determining the lower bound for the size of the replication-competent reservoir. Quantifying the number of intact proviruses by sequencing appears to provide the best current estimate of the HIV reservoir's potential true size, but this assay is still relatively new, and is both labor-intensive and expensive, calling into question its scalability in large clinical studies. Newer assays, such as the IPDA assay, single-cell measurement of HIV expression and high-throughput quantification of HIV protein levels represent promising technologies but require additional validation. The development of a rapid, high-throughput assay that can sensitively quantify the levels of the replication-competent HIV reservoir remains the holy grail of HIV reservoir assays and would accelerate discovery of an effective HIV curative strategy. Given the difficulty in scaling up allogeneic stem cell transplants using donors homozygous for the CCR5Δ32 mutation, much interest is currently directed to better understand the mechanisms resulting in long-term virologic control in the hope of replicating this result in HIV-1 non-controllers.

(Page intentionally left blank)

CHAPTER 2

HIV-1 PROVIRAL LANDSCAPES DISTINGUISH POST-TREATMENT CONTROLLERS FROM NON-CONTROLLERS

Radwa Sharaf[1,2], Guinevere Q. Lee[3], Xiaoming Sun[3], Behzad Etemad[1], Layla Aboukhater[1], Zixin Hu[1], Zabrina L. Brumme[4,5], Evgenia Aga[6], Ronald J. Bosch[6], Ying Wen[1], Golnaz Namazi[1], Ce Gao[3], Edward P. Acosta[7], Rajesh T. Gandhi[3,8], Jeffrey M. Jacobson[9], Daniel Skiest[10], David Margolis[11], Ronald Mitsuyasu[12], Paul Volberding[13], Elizabeth Connick[14], Daniel R. Kuritzkes[1], Michael M. Lederman[15], Xu G. Yu[3,7], Mathias Lichterfeld[1,3], Jonathan Z. Li[1]

[1]Brigham and Women's Hospital, Harvard Medical School, Boston, MA [2]Harvard Ph.D. Program in Virology, Division of Medical Sciences, Harvard University, Boston, MA [3]Ragon Institute of MGH, MIT and Harvard, Cambridge, MA [4]Simon Fraser University, Burnaby, BC, Canada [5]British Columbia Centre for Excellence in HIV/AIDS, Vancouver, BC, Canada [6]Harvard T.H. Chan School of Public Health, Boston, MA [7]University of Alabama at Birmingham, Birmingham, AL [8]Massachusetts General Hospital, Harvard Medical School, Boston, MA [9]Temple University, Philadelphia, PA [10]University of Massachusetts Medical School-Baystate, Springfield, MA [11]UNC School of Medicine, Chapel Hill, NC [12]University of California Los Angeles, Los Angeles, CA [13]University of California San Francisco, Gladstone Center for AIDS Research, San Francisco, CA [14]University of Arizona College of Medicine, Tucson, AZ [15]Case Western Reserve University, Cleveland, OH

RS, RTG, ML, XGY and JZL developed the concept and design. RS, BE, LA, ZH, YW, GN, MML, EPA and XS performed the experiments. RS, GQL, CG, ZLB, ML, RJB, EA and JZL were involved in the bioinformatic and statistical analysis. JMJ, DS, DM, RM, PV and EC contributed samples. All
authors were involved in the writing.

Work was published in J Clin Invest. 2018 Aug 31;128(9):4074-4085. doi: 10.1172/JCI120549.

Abstract

HIV post-treatment controllers (PTCs) represent a natural model of sustained HIV remission, but they are rare and little is known about their viral reservoir. We obtained 1450 proviral sequences after near-full-length amplification from 10 PTCs and 16 post-treatment non-controllers (NCs). Before treatment interruption, the median intact and total reservoir size in PTCs was 7-fold lower than in NCs, but the proportion of intact, defective and total clonally-expanded viral genomes was not significantly different between the two groups. Quantification of total, but not intact, proviral genome copies predicted sustained HIV remission as 81% of NCs, but none of the PTCs had a total proviral genome > 4 copies per million PBMCs. The results highlight the restricted intact and defective HIV reservoir in PTCs and suggest that total proviral genome burden could act as the first biomarker for identifying PTCs. Total and defective, but not intact, proviral copy numbers correlated with levels of cell-associated HIV RNA, activated NK cell percentages and both HIV-specific CD4+ and CD8+ responses. These results support the concept that defective HIV genomes can lead to viral antigen production and interact with both the innate and adaptive immune systems.

Introduction

Despite years of suppressive antiretroviral therapy (ART), the vast majority of HIV-infected individuals will experience rapid viral rebound during a treatment interruption (TI) (72). Efforts to achieve an HIV cure were boosted by the case of the Berlin patient, who achieved an apparently sterilizing cure with no detectable virus after a hematopoietic stem cell transplant with donor cells that were naturally resistant to HIV infection (99). However, this approach has limited generalizability given the substantial mortality associated with stem cell transplantation and the rarity of donors with cells resistant to HIV. An alternative approach is a functional cure, or sustained HIV remission, where proviral HIV DNA may still be detectable, but patients maintain viral suppression even after ART discontinuation. These individuals are termed HIV post-treatment controllers (PTCs). The most comprehensive description of PTCs so far has been the VISCONTI cohort of 14 PTCs (113). These individuals were treated during early HIV infection, but unlike HIV elite controllers (ECs), favorable HLA alleles associated with viral control were not overrepresented in these participants. However, PTCs are exceedingly rare and the HIV proviral reservoir determinants of post-treatment control are largely unexplored. We addressed this question using a group of PTCs identified from previously completed AIDS Clinical Trials Group (ACTG) studies (132).

HIV DNA and cell-associated RNA (CA-RNA) were detected pre-ATI in PTCs from both the VISCONTI (113) and ACTG (132) participants. Currently, a smaller HIV reservoir size is thought to be a contributing factor for HIV post-treatment control (133, 134). However, PCR-based methods of HIV reservoir quantification of proviral DNA overestimate the true reservoir size, as most proviral genomes are defective (3–5, 68). We hypothesized that individuals with a smaller intact proviral reservoir prior to treatment interruption are more likely to be post-treatment

controllers. To explore this question, we performed near-full-length sequencing of proviral genomes using next-generation sequencing of single-genome amplicons for a group of PTCs and post-treatment non-controllers (NCs). This approach allows for an in-depth assessment of the intact and defective HIV reservoir, as well as providing evidence of likely clonal expansion. Assessing the types of defective proviruses present (e.g. deleted, hypermutated) provides insight into potential mechanisms underlying post-treatment HIV control. Furthermore, we assessed the relationship between different proviral species, levels of intracellular HIV RNA expression and host immune responses to define the functional capacity of the proviral reservoir and immune correlates of reservoir size.

Materials and Methods

Study population and samples

PTCs were identified from several AIDS Clinical Trials Group (ACTG) analytic treatment interruption studies (135–139). PTCs were defined as individuals who were on suppressive ART and after TI, maintained viral loads ≤400 HIV RNA copies/mL for ≥24 weeks (short term [≤2] viral loads > 400 HIV RNA copies/mL were not exclusionary). Post-TI plasma samples were tested for ART levels and drugs were not detected. NCs were individuals with available stored samples who did not meet the PTC criteria and were selected to match the same study arms. All participants had PBMC samples available immediately before TI (i.e. baseline) for near-full-length proviral sequencing. For a subset of participants with available samples, proviral sequencing was also performed on a post-TI timepoint collected a median of 71 weeks (Q1, Q3: 45, 84 weeks) after ART discontinuation.

Specifically, early-treated participants were stratified by predetermined criteria in the original study protocol to either the acute infection group or the recent infection group (138). Acute infection was defined as having a plasma HIV RNA concentration more than 2000 copies/mL within 14 days of study entry and either a negative ELISA, or a positive ELISA but a negative or indeterminate western blot, or a positive ELISA and western blot in conjunction with either a negative ELISA or a plasma HIV RNA concentration less than 2000 copies/mL in the 30 days prior to entry. The general intention of these criteria was to identify cases in which HIV infection had occurred within the 4 weeks prior to study entry. Recent infection was defined as a positive ELISA and western blot within the 14 days prior to entry but a negative ELISA or plasma HIV RNA concentration less than 2000 copies/mL within the 31–90 days before entry or a positive

ELISA and western blot and a nonreactive detuned ELISA in patients with more than 200 CD4+ cells/μL all within the 21 days before study entry.

Proviral sequencing

Next-generation single-genome sequencing (NG-SGS) utilizes the Illumina deep sequencing platform to efficiently sequence the single-genome near-full-length proviral amplicons. Single-genome sequencing allows the isolation of full-length proviral HIV without the confounding concerns of PCR recombination frequently seen in bulk PCR products. Limiting dilution proviral amplification was performed using a technique adapted from a previously published protocol (65). DNA was extracted from cryopreserved PBMCs using the QIAmp DNA Mini Kit (Qiagen) and used at limiting dilution for nested PCR amplification with Platinum Taq HiFi polymerase (ThermoFisher). The sequences of the primers for the first and second-round PCR reactions were as follows: First round forward primer: 5'-AAATCTCTAGCAGTGGCGCCCGAACAG-3', first round reverse primer: 5'-TGAGGGATCTCTAGTTACCAGAGTC-3'; second round forward primer: 5'-GCGCCCGAACAGGGACYTGAAARCGAAAG-3', second round reverse primer: 5'-GCACTCAAGGCAAGCTTTATTGAGGCTTA-3'. These primers correspond to HXB2 coordinates 623-649, 9662-9686, 638-666 and 9604-9632, respectively. PCR amplicons were sheared and Illumina barcoded libraries were constructed and pooled. Sequencing was performed on the Illumina MiSeq platform and amplicons were assembled using the UltraCycler v1.0. Automated *de novo* sequence assembly generated a continuous fragment of HIV-1 proviral DNA, which was fed into an automated in-house pipeline to determine proviral genome intactness (140), as previously published (66). Briefly, the sequences were aligned to HXB2 to identify sequence defects (e.g. internal deletions, premature stop codons, out-of-frame mutations, internal inversions

and packaging signal defects). The sequences were then run in the Los Alamos HIV Sequence Database Hypermut program to identify hypermutated sequences (141). Proviral sequences that lacked any of the above-mentioned defects were classified as intact. Near-full-length assembled sequences missing one of the PCR primer binding sites, but otherwise meeting the criteria for an intact provirus were labelled "inferred intact". A clonal cluster analysis was also performed to detect genomes that were 100% identical across the entirety of their assembled length. The unit "genomes per million PBMCs" was calculated for total proviral genomes and for each proviral species based on the quantity of DNA assayed.

Additionally, proviral sequences were analyzed in the context of each participant's HLA class I profile for the presence of known HLA-associated polymorphisms in HIV-1 subtype B as defined in a published reference list (142). We also assessed the presence of repeat elements flanking the deletion junctions using a Python script.

Plasma viral sequencing

Plasma viral RNA was extracted using the QIAamp Viral RNA Mini Kits and SGS of HIV-1 *Pro-RT* (HXB2 coordinates 2853-3869) performed as previously published (143, 144). Using ClustalW, the resulting plasma-derived single-genome sequences were aligned with proviral sequences harboring the *Pro-RT* region.

Quantification of HIV DNA and CA-RNA

Cell-associated (CA)-RNA was isolated from cryopreserved PBMCs using the AllPrep DNA/RNA Mini Kit (Qiagen). Unspliced CA-RNA levels were quantified using a real-time PCR approach with primers/probes targeting conserved regions of HIV LTR/*gag* as previously described (72). Cell numbers were quantified by qPCR measurements of CCR5 DNA copy numbers. Measurement of IPO-8 transcripts in total RNA was used as an internal quality control to assess the efficiency of RNA extraction (73).

Immune phenotyping and intracellular cytokine staining

Approximately 10^6 PBMCs each were used for T and NK cell phenotyping. T cells were stained with blue viability dye (Invitrogen) at 37°C for 20 min and then followed with antibodies targeting CD3, CD8, CD4, CD45RO, CD95, HLA-DR, CD38, PD-1 at 4°C for 20 min. NK cells were stained with blue viability dye and antibodies targeting CD3, CD19, CD16, CD56, CD69, CD38, CD57, NKG2D, NKp30 and NKp46.

T cell intracellular cytokine staining (ICS) was performed on PBMCs stimulated with HIV *gag* peptide pool and NK cell ICS was performed with PBMCs stimulated with K562 cells. For T cells, approximately 10^6 cells were stimulated overnight with anti-CD28/49d (0.5μg/mL; BD) and 2 μg/mL of synthetic peptides (overlapping 15- to 20-mer *gag* peptide pools spanning the entire clade B consensus sequence of the HIV-1 *gag* sequence). NK cells were stimulated with K562 cells with an effector-to-target of 10:1 and brefeldin A (1μg/mL; BioLegend), Monesin Solution (1μg/mL; BioLegend) and CD107a antibody were added after a one-hour incubation and cultured for an additional 5 hours. Cells stimulated with PMA (2.5μg/mL) and ionomycin (0.5μg/mL) served as a positive control and R10 medium only served as a negative control. After stimulation, the cells were stained with surface antibodies against CD3, CD19, CD16, CD56 and blue viability

dye at 4°C for 20 min. Subsequently, cells were treated with a fixation and permeabilization solution per the manufacturer's protocol. Cells were stained for 20 min at room temperature with antibodies directed to IFN-γ, IL-2, CD107a and TNF-α. Cells were then fixed by 2% PFA (Affymetrix), acquired on an LSR Fortessa flow cytometer (BD) and analyzed using FlowJo (version v10) software (Tree Star). The proportion of cytokine-secreting cells had to be greater than 0.1% after subtraction to be considered as a positive response.

Soluble markers of inflammation

Soluble markers of inflammation were measured by ELISA. Plasma from all participants was analyzed for levels of IL-6 (HS600B, R&D Systems), sCD14 (DC140, R&D 463 Systems), IFN-γ, IP-10 (DIP100, R&D Systems), sTNFR-I and sTNFR-II (DRT100/200, R&D Systems) and D-dimer (Diagnostica Stago) per the manufacturers' protocols.

Infectivity of recombinant viruses

We generated recombinant virions encoding patient-derived *env* sequences by co-transfecting 293T cells with Δ*env*-NL4-3 plasmid and *env* PCR fragments. Virus was harvested and propagated in U87-CCR5 and U87-CXCR4 cells for 7-10 days. Afterwards, we tested the infectivity of the virus in a TZM-bl infectivity assay. TZM-bl cells (NIH AIDS Reagent Program) are a permissive HeLa cell clone that contains *Tat*–regulated reporter gene for β-galactosidase under the control of the HIV-1 LTR.

Integration site analysis

Integration sites were determined using the integration site loop amplification (ISLA) technique on genomic DNA isolated from PBMCs pre-treatment interruption, as previously published (15).

Viral outgrowth assays

CD4+ T cells were isolated by negative selection and stimulated with PHA (2 μg/mL), rhIL-2 (50 U/mL) and irradiated allogeneic PBMCs from an HIV-negative donor in the lower compartment of a transwell. On day 14 of culture, the supernatant from each well was tested in a TZM-bl infectivity assay. MOLT-4 cells were added to the upper insert of transwells with detectable virus on day 16 and harvested for DNA extraction on day 20, followed by near-full-length proviral amplification and sequencing.

Statistics

Statistical analysis was performed with SAS Studio (Release 3.6, University Edition) and Prism (V7, GraphPad). Wilcoxon rank-sum tests were used to compare reservoir measures between groups. Correlations between reservoir measures and other viral / immune markers were estimated with non-parametric Spearman correlation coefficients. $P<0.05$ was considered significant and denoted as *, $P<0.01$ as ** and $P<0.001$ ***. Data were summarized as individual data plots with lines depicting median values. Where indicated, the size of each data point corresponds to the total number of proviral genomes sequenced for that participant.

Study approval

Participant samples were collected according to protocols approved by the respective Institutional Review Boards. Study participants gave written informed consent in accordance with the Declaration of Helsinki.

Results

Overview of study population and proviral sequencing

Ten PTCs were identified from prior ACTG TI trials, including four PTCs who initiated ART during early HIV infection and six who initiated ART during chronic HIV infection (Figure 2.1). The median duration of documented viral control was 63 weeks for the PTCs. To exclude continued ART use as the cause of HIV control, drug level testing was performed on plasma from all PTCs and no antiretroviral drugs were detectable during the treatment interruption. These ten PTCs were compared to 16 NCs from the same studies and were well matched in their demographic characteristics (Table 2.1 and Table 2.2). Nine individuals (4 PTCs and 5 NCs) were treated during early infection as part of ACTG trial 371 (138), in which participants were treated with ≥ 52 weeks of ART prior to undergoing an ATI. The remaining individuals were treated during chronic infection. A median of 7.4 million PBMCs were sampled from each participant from the pre-treatment interruption time point and 1124 proviral genomes were obtained with a median of 48 proviral genomes per participant (Q1, Q3: 17, 58).

Table 2.1: Demographic characteristics of Post-Treatment Controllers and Non-Controllers.

	PTCs (N=10)	**NCs (N=16)**
Male (%)	8 (80%)	11 (68.8%)
Age, median	42	44
Early-Treated (%)	4 (40%)	5 (31.3%)
Years on ART, median	4.5	4.5
CD4 count, median	894	802
Race		
White (%)	7 (70%)	10 (62.5%)
Black (%)	1 (10%)	3 (18.8%)
Hispanic (%)	2 (20%)	3 (18.8%)

Table 2.2: A list of study participants, along with relevant demographic and clinical history information.

PID	Status	Gender	ART timing	Age *	Race	Source study	Study arm **	VL (pre-ART)	Duration of ART ***	CD4 count (pre-ATI)	HLA Category ****	HLA-A-1	HLA-A-2	HLA-B-1	HLA-B-2	HLA-C-1	HLA-C-2
1A5	PTC	M	Early	36	White Non-Hispanic	A371		334806	1.0349	850	Neutral	02:01	02:01	41:01	44:02	05:01	17:01
1A8	PTC	M	Early	29	White Non-Hispanic	A371		7215	1.0021	1219	Neutral	03:01	03:01	07:02	27:05	02:02	07:02
1A10	PTC	M	Early	44	White Non-Hispanic	A371		71667	0.9993	1056	Neutral	01:01	02:20	08:01	58:01	07:01	07:01
1A11	PTC	M	Early	47	White Non-Hispanic	A371		2790018	1.0048	891	Neutral	03:01	31:01	35:01	35:01	04:01	04:01
1C1	PTC	M	Chronic	50	Black Non-Hispanic	A5068	Placebo + STIs		4.8131	882	Protective	01:02	30:02	58:01	81:01	03:02	08:04
1C2	PTC	M	Chronic	47	Hispanic	A5197	Vaccine	296402	5.9603	988	Neutral	02:06	23:01	48:01	49:01	07:01	08:01
1C4	PTC	M	Chronic	38	White Non-Hispanic	A5170			5.41	1380	Neutral	02:01	32:01	44:02	51:01	05:01	14:02
1C9	PTC	F	Chronic	42	White Non-Hispanic	A5024	Placebo + IL2		4.1916	897	Unfavorable	03:01	32:01	35:02	51:01	04:01	14:02
1C10	PTC	F	Chronic	33	Hispanic	A5170		2488	3.4114	688	Neutral	31:01	33:03	35:01	39:02	04:01	07:02
1C16	PTC	M	Chronic	41	White Non-Hispanic	A5068	Vaccine + no STIs		12.9856	416	Unfavorable	01:01	03:01	08:01	38:01	07:01	12:03
1A105	NC	M	Early	29	White Non-Hispanic	A371		28277	0.9966	1227							
1A108	NC	M	Early	26	Hispanic	A371		15720	1.1718	814	Unfavorable	03:01	26:01	07:02	35:01	04:01	07:02
1A112	NC	M	Early	41	White Non-Hispanic	A371		20388	1.1006	844	Neutral	24:02	68:01	18:01	44:02	07:04	12:03
1A114	NC	F	Early	43	White Non-Hispanic	A371		213720	0.9993	1386	Neutral	01:01	02:01	08:01	27:05	01:02	07:01
1A115	NC	M	Early	28	Hispanic	A371		523881	0.9966	972							
1C101	NC	F	Chronic	39	Hispanic	A5068	Placebo + STIs		9.5852	789	Neutral	30:02	68:01	08:01	52:01	03:04	07:01
1C104	NC	M	Chronic	41	White Non-Hispanic	A5197	Vaccine		3.7837	736	Neutral	02:01	33:01	14:01	18:01	07:01	08:02
1C106	NC	M	Chronic	59	White Non-Hispanic	A5170			6.9213	1488	Unfavorable	23:01	30:02	07:02	08:01	07:01	07:02
1C107	NC	M	Chronic	52	Black Non-Hispanic	A5068	Placebo + STIs		10.694	778	Neutral	02:01	03:01	49:01	52:01	07:01	16:01
1C110	NC	M	Chronic	38	White Non-Hispanic	A5068	Placebo + STIs	17806	5.5578	691	Neutral	11:01	30:01	35:01	49:01	04:01	07:01
1C112	NC	F	Chronic	50	White Non-Hispanic	A5170		4888	5.6619	572	Neutral	01:01	02:01	13:02	40:01	03:04	06:02
1C113	NC	F	Chronic	50	White Non-Hispanic	A5068	Vaccine + no STIs		6.0424	781	Unfavorable	01:01	11:01	35:01	44:03	04:01	04:01
1C114	NC	F	Chronic	44	Black Non-Hispanic	A5068	Placebo + STIs	12000	6.6639	685	Protective	31:01	34:02	27:05	58:02	06:02	15:02
1C116	NC	M	Chronic	44	White Non-Hispanic	A5170		30200	2.3162	903	Neutral	01:01	29:01	08:01	52:01	07:01	12:02
1C117	NC	M	Chronic	45	Black Non-Hispanic	A5068	Vaccine + no STIs	46706	4.5421	1685	Neutral	02:01	68:02	42:02	52:01	07:02	17:01
1C118	NC	M	Chronic	45	White Non-Hispanic	A5024	Vaccine + no STIs		3.2799		Neutral	02:01	03:01	08:01	14:02	07:01	08:02

* At parent study entry
** Placebo denotes the receipt of a placebo therapeutic vaccine. A371 and A5170 had no immunologic interventions.
A5068 participants randomized to STI arm underwent 2 short treatment interruptions lasting 4-6 weeks prior to a longer treatment interruption.
*** In years, from first ART to ATI
**** HLA data is shown for individuals who consented to HLA typing.

ART: Anti-Retroviral Therapy
ATI: Analytic Treatment Interruption
PTC: Post-treatment controller
NC: Post-treatment non-controller
STIs: Structured treatment interruptions

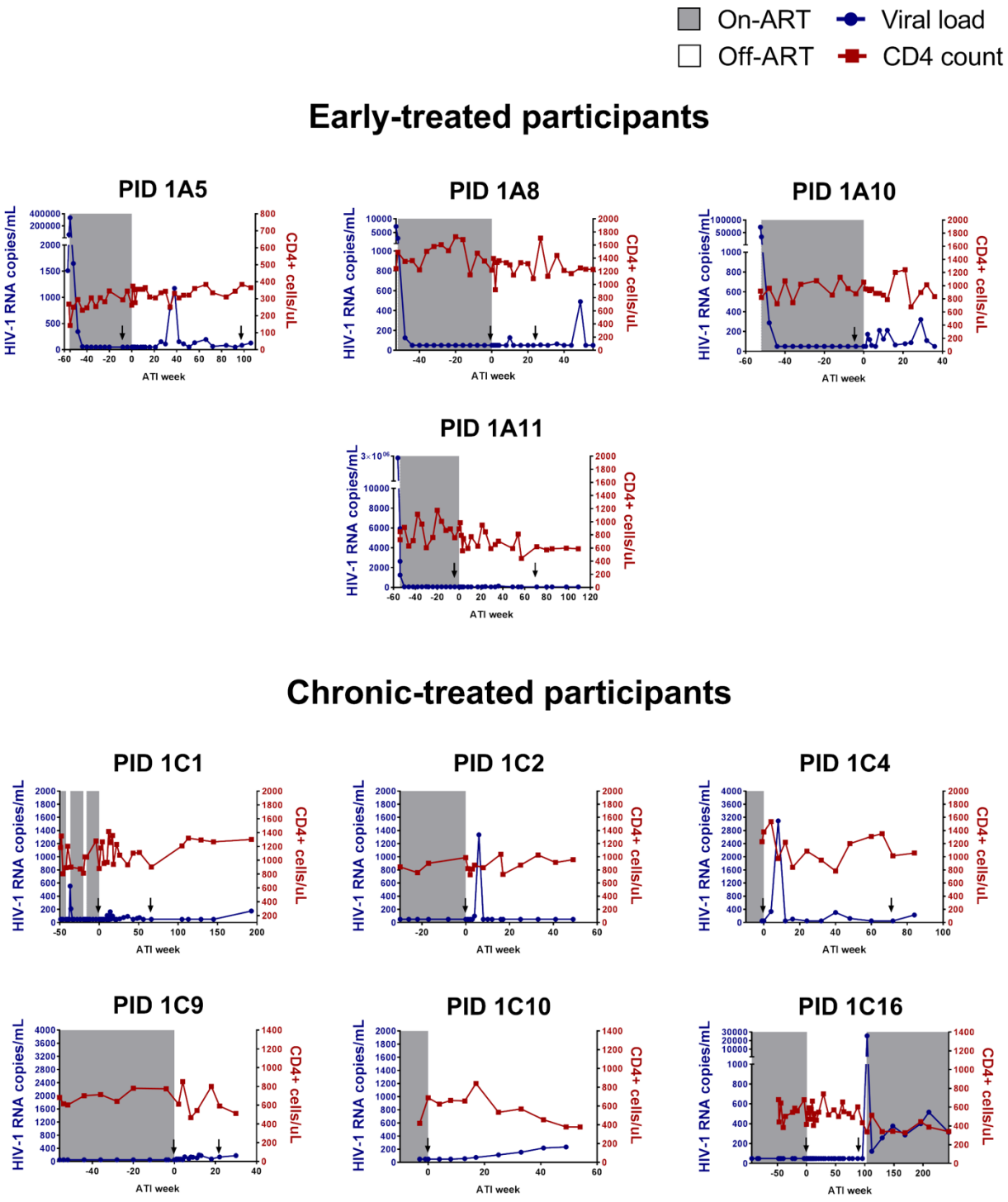

Figure 2.1: Viral loads and CD4 counts for PTCs.
For each of the PTCs, viral loads are graphed in blue and CD4 counts in red. Black arrows represent time points used for proviral genome sequencing at either the pre-ATI or post-ATI timepoint. On-ART period is shaded in grey and the off-ART period shown as white.

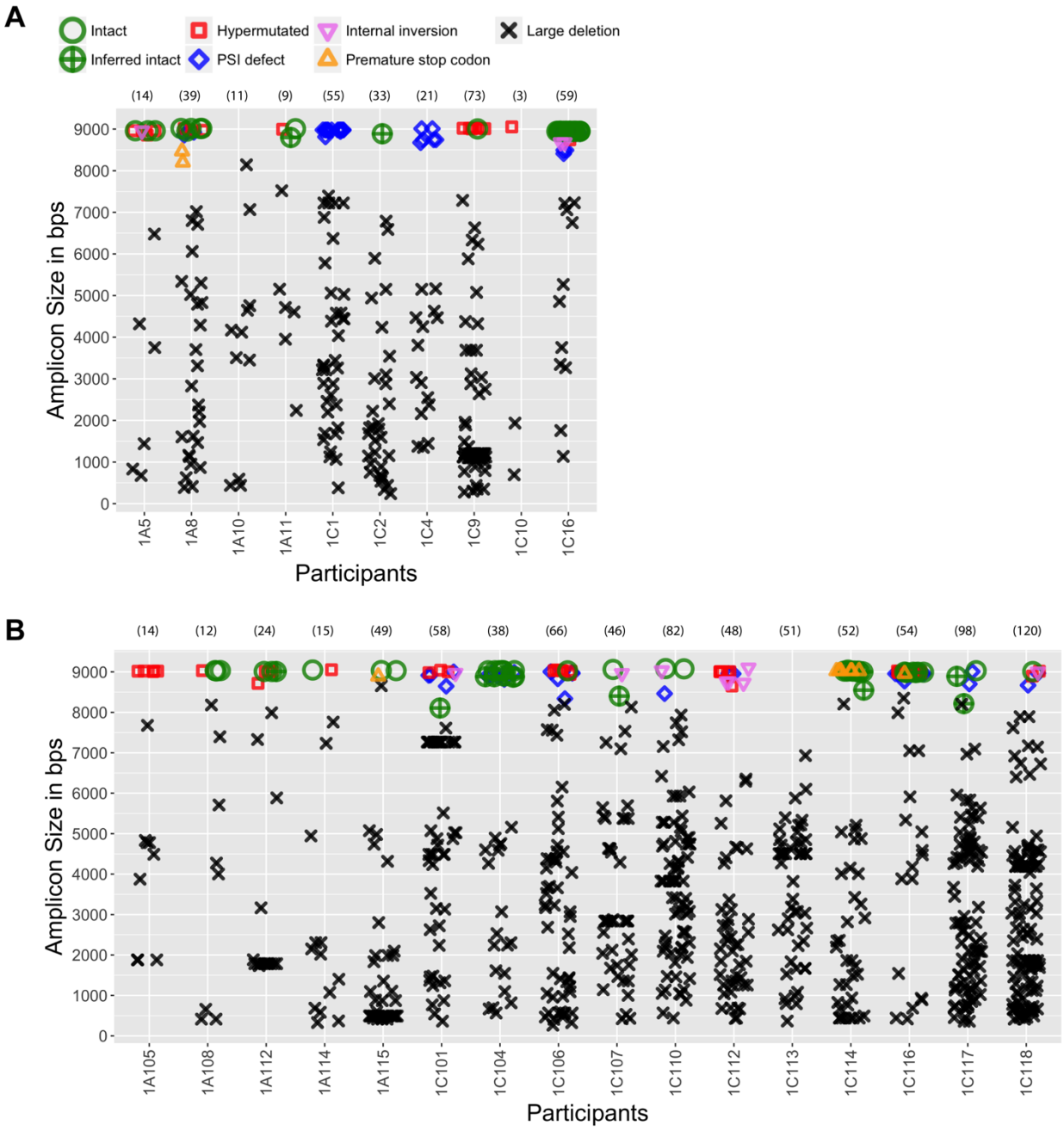

Figure 2.2: Composition of the proviral landscape.
(A and B) For each participant, the amplified proviral sequences are graphed by amplicon size and type of defect and labeled accordingly for PTCs (A) and NCs (B). 303 proviral genomes are shown for PTCs and 821 for NCs. The number of sequences obtained from each participant is shown in parenthesis at the top of the graph. PSI, packaging signal; bps, base pairs.

In addition, we amplified 326 near-full-length proviral sequences from 7 PTCs at a post-treatment interruption time point. All proviral sequences were categorized as either intact or defective. The defects included internal inversions, hypermutations, deletions, premature stop codons and defects in the packaging signal (psi) (Figure 2.2). For each participant, "genomes per million PBMCs" were calculated for total proviral genomes and for each proviral species.

In total, our dataset comprised 137 intact and 1313 defective proviral genomes. Prior to the treatment interruption, defective proviral genomes constituted the vast majority of the HIV reservoir (median 97% of the total proviral genomes), although substantial variation between individuals was observed (Q1, Q3: 87%, 99%) as demonstrated with 4 representative study participants (Figure 2.3A). To ensure that there was no cross-contamination between participant samples, we generated a neighbor joining tree including all the intact sequences obtained for the study and confirmed that all single genome sequences clustered appropriately (Figure 2.3B).

Distinct proviral landscapes in PTCs and NCs

Until now, the intact proviral reservoir has not been described in PTCs. We hypothesized that a smaller intact proviral reservoir size before treatment interruption may be a determinant of post-treatment control. Our results showed that prior to treatment interruption, PTCs had approximately 7-fold lower levels of intact proviral genomes than NCs (IPGs, PTCs vs NCs: median 0.04 vs. 0.28 copies/10^6 PBMCs, $P<0.05$, Figure 2.4A). These intact proviral sequences likely represent the replication-competent reservoir as we detected exact matches with plasma-derived sequences for a subset of participants. We observed lower percentages of intact proviruses in the PTCs compared to NCs, although this difference did not reach statistical significance (median 1.4% vs. 4.1%, P=0.4

Figure 2.3: Near-full-length single-template HIV-1 DNA amplicons
(A) Virograms reflecting the diversity of HIV DNA PCR products amplified from 4 representative participants (2 PTCs and 2 NCs, all treated during chronic infection). Numbers in parentheses indicate absolute frequency of analyzed sequences in each participant. (B) Combined neighbor-joining phylogenetic tree for all 137 intact proviral sequences showing no evidence of cross-participant sequence contamination, with HXB2 as an outgroup. Participants with more than one intact near-full-length proviral sequence are colored and those with only one identified intact sequence are depicted in black. PIDs of each participant are shown to the right of the tree. Asterisks denote clonal sequences detected more than once. PTC, post-treatment controllers; NC, post-treatment non-controllers; PSI, packaging signal.

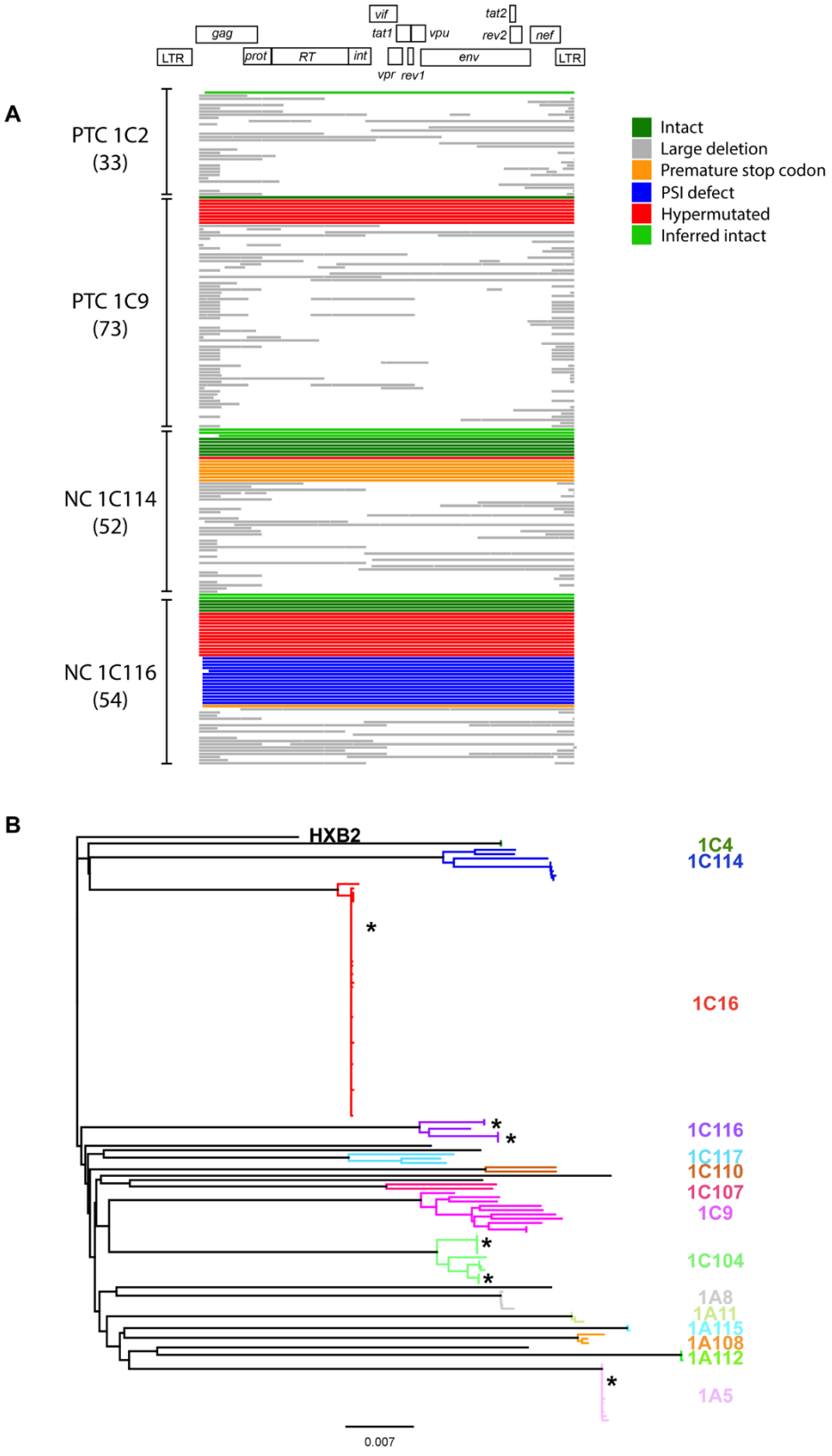

Figure 2.3 (continued)

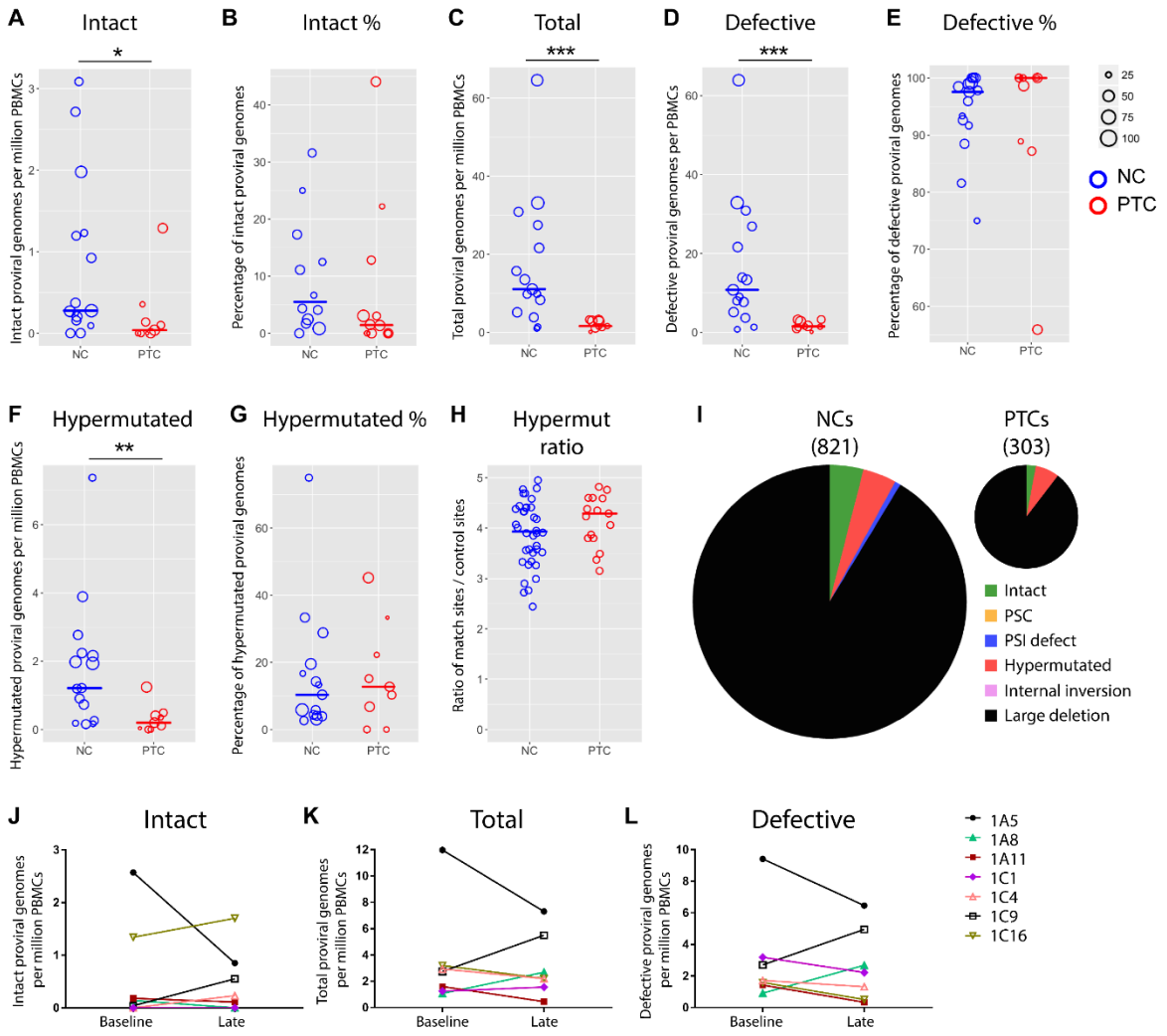

Figure 2.4: Comparison of reservoir measures between PTCs and NCs.
(A) Copy numbers and (B) Percentages of intact proviral genomes within total reservoir are compared between both groups. (C) Copy numbers of total proviral genomes per million PBMCs are compared between groups. (D) Copy numbers and (E) Percentages of defective proviral genomes are depicted for each group. (F) Copy numbers and (G) Percentages of hypermuated proviral genomes are depicted for each group. The size of each data point corresponds to total number of sequences amplified per participant as indicated in the legend in figure A-G. (H) A comparison between PTCs and NCs in the hypermutation rate ratio, calculated as the ratio of the number of match sites out of potential sites to the number of control sites out of potential sites. (I) Pie charts reflecting the median relative contribution of each proviral species for all participants, normalized to 100%. Numbers in parentheses indicate absolute frequency of analyzed sequences in each group. (J-L) Longitudinal analysis of intact (J), total (K) and defective (L) proviral genome copy numbers from the pre- and post-ATI time points for 7 PTCs. Each PTC is shown in a different color. Significance was calculated using a Wilcoxon rank-sum test; $P<0.05$ was considered significant and denoted as *, $P<0.01$ as ** and $P<0.001$ as ***. NCs are depicted in blue and PTCs in red. PTC, post-treatment controllers; NC, post-treatment non-controllers; PSI, packaging signal; PSC, premature stop codon.

Figure 2.4B). Of note, there was a wide variation in the relative proportion of intact proviral genomes, including eight participants whose viral reservoir contained >10% intact proviral genomes, four of which harbored >20% intact proviral genomes.

Interestingly, levels of total proviral genomes (TPGs) were 7-fold lower in PTCs (median 1.6 vs. 11.1 copies/10^6 PBMCs, P<0.001, Figure 2.4C) and were predominantly driven by levels of defective proviral genomes (DPGs, median 1.5 vs. 10.8 copies/10^6 PBMCs, P<0.001, Figure 2.4D). There were no significant differences in the percentages of defective proviruses between PTCs and NCs (median 98.6% vs. 95.9%, Figure 2.4E). Among the readouts examined (IPGs, TPGs and DPGs), levels of TPGs were the best reservoir marker to differentiate between PTCs and NCs, as 81% of NCs vs. 0% of PTCs had TPGs > 4 copies/10^6 PBMCs. No significant correlations between either pre-ATI CD4+ count or duration of ART treatment and any of the reservoir size measurements were detected. As a sensitivity analysis, we also calculated reservoir size per million CD4+ T cells, instead of PBMCs, and observed similar findings.

Next, we assessed whether certain types of defective proviruses were overrepresented in PTCs as they can inform potential mechanisms underlying HIV control. Within the DPGs, PTCs had fewer proviral sequences with large deletions (median 1.1 vs. 10.5 copies/10^6 PBMCs, P<0.001) and fewer hypermutated proviral genomes (HPGs, median 0.2 vs. 1.2 copies/10^6 PBMCs, P<0.01, Figure 2.4F). However, the percentages of proviral sequences with large deletions or hypermutated proviral sequences were not significantly different between PTCs and NCs (Figure 2.4G). Furthermore, there was no difference between PTCs and NCs in the extent of APOBEC-induced hypermutations relative to control (non-APOBEC) mutations (Figure 2.4H). The median proportions of each proviral species in the PTCs and NCs are shown in Figure 2.4I.

In addition, we were interested in exploring whether treatment during early vs. chronic infection changed the proportion of the different subsets of proviruses. In comparing the early and chronic-treated participants, chronic-treated NCs had higher levels of TPGs (median 15.7 vs. 2.6 copies/10^6 PBMCs, $P<0.05$) and DPGs (median 13.3 vs. 2.5 copies/10^6 PBMCs, $P<0.05$) compared to early-treated NCs but no significant differences in percentages of any proviral subset or in the copy numbers of IPGs or HPGs.

To confirm that the proviral sequences we characterized as intact were replication competent, we isolated CD4+ T cells from 2 study participants, 1A8 (PTC) and 1C114 (NC), for whom large numbers of PBMCs were available. The cells were activated and co-cultured with MOLT-4 cells in a viral outgrowth assay using a trans-well system. MOLT-4 cells from wells where virus was detected in the supernatant were subjected to near-full-length proviral

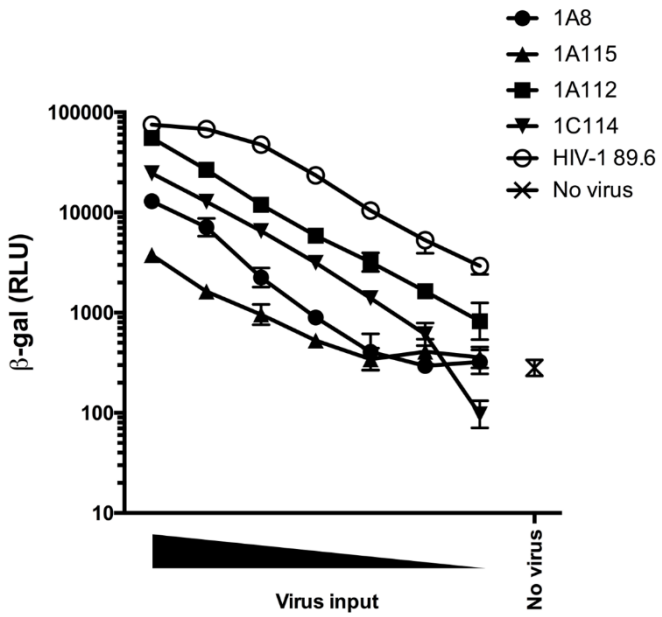

Figure 2.5: Infectivity assay on TZM-bl cells.
Infectivity of recombinant virions generated using *env* PCR fragments from intact proviral genomes was tested in a TZM-bl assay. RLU, relative luminescence units.

amp

the intact provirus, differing by only 4 and 5 nucleotides out of 9,020 nucleotides, respectively. These few nucleotide differences likely represent the expected variation arising during the 3-week culture period used to obtain each isolate (145, 146) and translated to 1 amino acid change in *env* for 1A8 and 2 changes in *env* for 1C114. To confirm that our bioinformatic calls of intact *env* reflect true functionality, we separately tested the functionality of *env* by co-transfecting *env* PCR fragments with a Δ*env*-NL4-3 plasmid and determined the infectivity of the produced virus in a TZM-bl assay. Figure 2.5 shows the infectivity titer for four recombinant viral constructs harboring intact proviral *env* from these participants, indicating that they are functional.

Stability of the intact HIV reservoir after treatment interruption in PTCs

Upon treatment interruption, levels of HIV DNA increase dramatically in most HIV patients (147). We wanted to investigate whether this increase also occurred in PTCs post-ATI, especially within the intact proviral reservoir. Levels of IPGs, TPGs and DPGs were assayed for 7 PTCs with available samples at a late timepoint, a median of 71 weeks post-treatment interruption. Unlike previously reported NCs (147), we detected no consistent increases in levels of IPGs, TPGs and DPGs between the pre- and post-treatment interruption timepoints (Figure 2.4J-L). The median ratio of pre:post-TI genomes per million PBMCs was 0.9 for IPGs, 1.3 for TPGs and 1.4 for DPGs. No new HIV drug resistance mutations were detected in any of these individuals after treatment interruption compared to the pre-interruption time point (148, 149).

No differences between PTCs and NCs in the clonal expansion of cells harboring intact proviral sequences

As illustrated in Figure 2.3B, our dataset included several participants with a significant number of identical intact proviral sequences and likely represent clonally-expanded sequences.

Thus, we assessed whether the smaller intact proviral reservoir detected in PTCs is caused by differential rates of clonal expansion. To investigate this, we assessed the percentage of identical proviral sequences detected more than once and found no significant differences between PTCs and NCs in the proportion of clonally-expanded proviral genomes. This was true regardless of whether the clonally-expanded populations harbored intact (PTCs vs. NCs: median 0% in both cases) or defective proviral sequences (median 14% vs. 17%, Figure 2.6A). Likewise, the absolute number of IPGs detected more than once was not significantly different between PTCs vs NCs, although PTCs did have a smaller number of DPGs detected more than once (median 0.2 vs. 2.7 copies/10^6 PBMCs, $P<0.01$, Figure 2.6B). A sensitivity analysis limited to participants who initiated ART during chronic infection yielded similar results. Of note, there were 4 participants who harbored a high percentage of clonal intact proviruses, 3 of whom initiated ART during chronic infection (31% for PID 1C16, 26% for PID 1C104 and 9% for PID 1C116, Figure 2.6C) and 1 treated during early infection (21% for PID 1A5). These intact sequences could be grouped into a few clusters of identical sequences with the largest two clusters comprising ≥50% of all expanded intact sequences. We confirmed that the detection of identical near-full-length single-genome sequences represented clonal expansion by performing integration site analysis for these same four participants. Our results confirmed that clonality estimates calculated by identical near-full-length proviral genomes were similar to those calculated from integration site analysis (Figure 2.6D). The frequency of clonally-expanded proviruses determined by near-full-length sequence analysis was on average 75% (Q1, Q3: 61, 82%) of the frequency determined by integration site analysis.

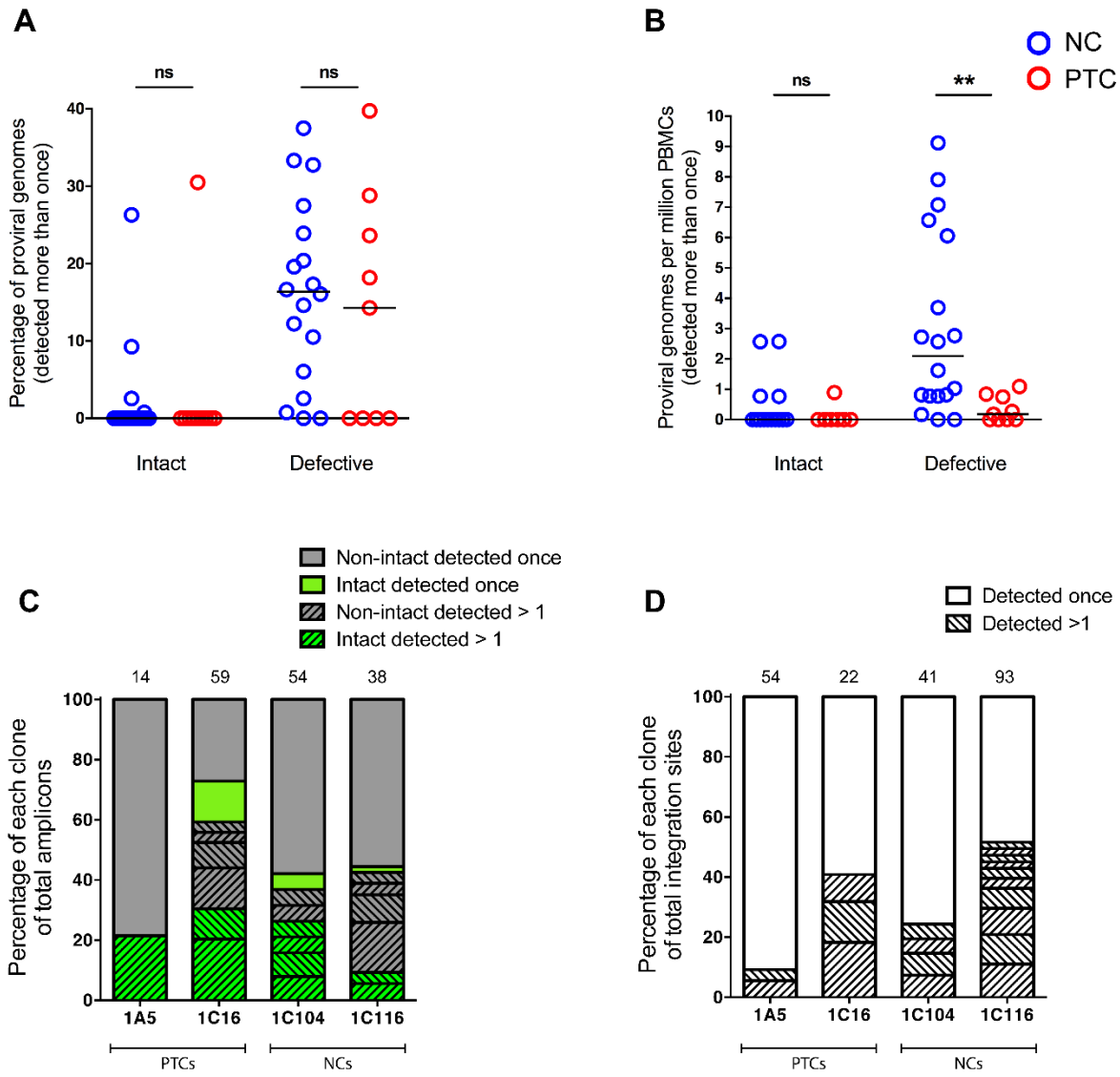

Figure 2.6: Contribution of clonal sequences to the proviral reservoir
(A) No difference between PTCs and NCs in percentages of either intact or defective proviral genome copies detected more than once. (B) PTCs have lower numbers of defective proviruses detected more than once, but no difference in intact copy numbers. Significance was calculated using a Wilcoxon rank-sum test; P<0.01 is denoted as **; ns, not significant. (C) Analysis of four participants who harbored a high percentage of intact proviruses detected more than once. Different stripe patterns depict different clones. Total number of amplicons is shown above each bar. (D) Integration site analysis of the same four participants in (C). Different stripe patterns depict different clones. Total number of integration sites is shown above each bar. PTC, post-treatment controllers; NC, post-treatment non-controllers.

A possible driver of clonally-expanded cells harboring intact proviruses could be T cell activation, given that it induces cellular proliferation and clonal expansion. However, we observed

no significant correlation between percentages of HLA-DR+ CD38+ CD4+ or CD8+ T cells and either the proportion or absolute numbers of clonally-expanded IPGs and DPGs.

HLA typing and HLA-associated escape polymorphisms

In order to examine the role of protective HLA alleles in post-treatment control, we analyzed available HLA typing for 6 of the PTCs and 11 of the NCs treated during chronic infection. Overall, protective HLA alleles were rare and found in only 1 participant of each group. We next surveyed for evidence of immune pressure on the proviral reservoir by examining inferred HLA-associated escape mutations within *gag*, *pol* and *nef* in the context of each participant's HLA class I profile (142). Inferred escape mutations matching the participants' HLA allele(s) were present at a median of 25% of possible amino acid sites in *gag*, 17.4% in *pol* and 25.8% in *nef* across all participants. There were no significant differences between PTCs and NCs in the extent of mutations detected. We also analyzed the proportion of inferred HLA escape mutations after treatment interruption in four PTCs and observed a modest increase in the percentage of HLA escape sites for at least one gene in three of the four individuals.

Defective proviral genome copies are associated with levels of CA-RNA and timing to viral rebound

Levels of intracellular HIV RNA expression have been shown to predict the timing of viral rebound after treatment interruption (72, 131). Thus, we assessed whether levels of intact provirus correlated with both levels of CA-RNA, as well as timing to viral rebound. Contrary to our expectations, the number of pre-interruption IPGs was not significantly associated with unspliced CA-RNA levels as quantified by qPCR. However, the number of TPGs and DPGs were associated with levels of CA-RNA (r=0.50, P<0.05, Figure 2.7A). In addition, the number of TPGs and DPGs,

but not IPGs, predicted the timing of subsequent viral rebound post-ATI (Figure 2.7B). Individuals with late viral rebound (≥400 HIV-1 RNA copies/mL) were found to have the lowest TPG and DPG numbers (viral rebound >16 vs. 4-16 vs. <4 weeks: median DPGs 1.5 vs. 9.1 vs. 13.0). There

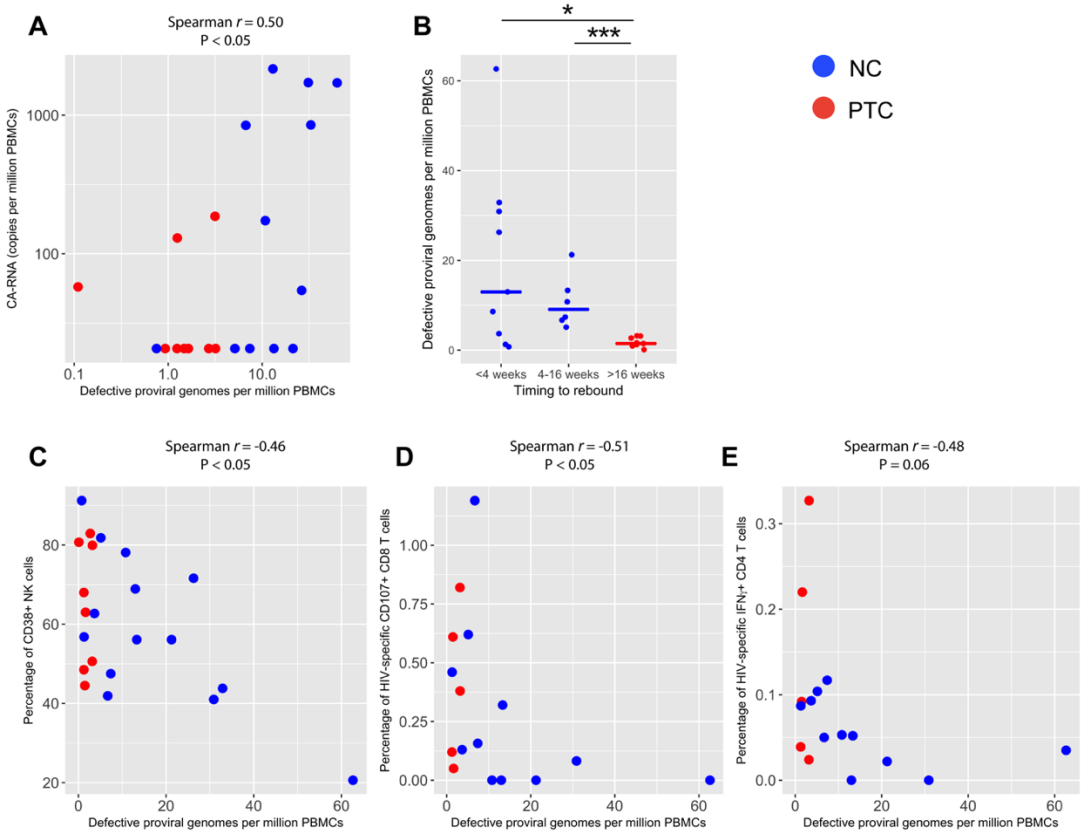

Figure 2.7: Relationship between defective proviral genome copy numbers versus viral and immune markers.
(A) Correlation between levels of cell-associated HIV RNA and copy numbers of defective proviral genomes. (B) Individuals with delayed viral rebound had lower levels of defective proviral genomes. Significance was calculated using a Wilcoxon rank-sum test; P<0.05 was considered significant and denoted as * and P<0.001 as ***. (C) Correlation between percentage of CD38+ NK cells and copy numbers of defective proviral genomes. (D) Correlation between percentage of HIV-specific CD107+ CD8 T cells and copy numbers of defective proviral genomes. (E) Correlation between percentage of HIV-specific IFNγ+ CD4 T cells and copy numbers of defective proviral genomes. NCs are depicted in blue and PTCs in red. Correlations between reservoir measures were estimated with non-parametric Spearman correlation coefficients. PTC, post-treatment controllers; NC, post-treatment non-controllers.

was no association between the levels of any specific type of defective sequences and either levels of CA-RNA or timing to viral rebound.

Association of defective proviral genomes with both innate and adaptive immune responses

Next, we hypothesized that the intact proviral reservoir size is dictated by levels of immune activation and the strength of the HIV-specific cellular immune response. Immune phenotyping was performed for CD4+/CD8+ T cells and NK cells for markers of activation and cellular exhaustion prior to treatment interruption. The extent of NK cell function and HIV *gag*-specific T cell responses were assessed by intracellular cytokine staining. Amongst all participants, none of the NK cell phenotypes or T cell responses were associated with levels of IPGs. However, higher CD38+ NK cell percentages were associated with lower numbers of DPGs (r=-0.46, P<0.05, Figure 2.7C). Similarly, higher levels of HIV-specific CD8+ cells expressing CD107a and HIV-specific IFN-γ-secreting CD4+ cells were both associated with lower DPGs (CD8+ CD107a+ r=-0.51, P<0.05 and CD4+ IFN-γ+ r=-0.48, P=0.06, Figure 2.7D-E). Given that the vast majority of the proviruses are defective, all the trends described are also true for TPGs. There was no association between the levels of specific types of defect and any of the innate or adaptive immune responses. Furthermore, there were no significant associations between TPGs, DPGs or IPGs and levels of soluble inflammatory markers D-dimer, IL-6, IP10, sCD14, sCD163 or CRP.

Common motifs present at proviral deletion junctions

Given the high frequency of proviruses with large deletions, we assessed the presence of common motifs at the site of proviral deletions and found that repeat elements were detected at the deletion junction in 11% of the proviral genomes with large deletions (Figure 2.8A). These repeat elements ranged in size from 3 to 20 nucleotides (Figure 2.8B). Interestingly, one specific repeat

element residing at HXB2 coordinates 4781-4800 (TTTTAAAAGAAAAGGGGGGA) flanked the deletion junctions in 16 different proviral sequences originating from 8 study participants (2 PTCs and 6 NCs, Figure 2.8C). This element maps to both the polypurine tract located in *pol* (cPPT), as well as in *nef*/U3 (3'PPT) and likely represents a hotspot for deletion. This sequence functions as a primer site for plus strand DNA synthesis and has been previously studied for its role in HIV replication (150–152).

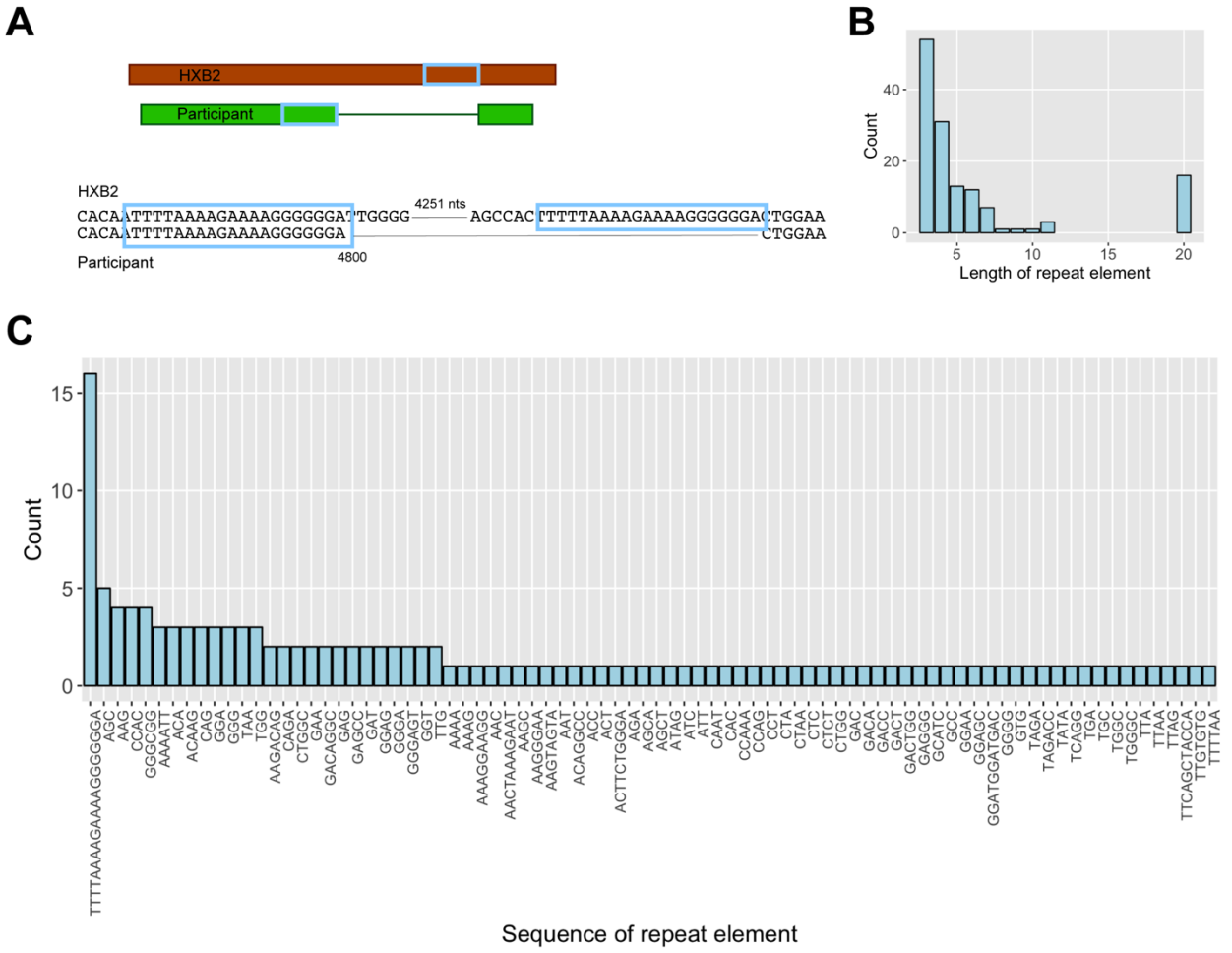

Figure 2.8: Detection of repeat elements at HIV proviral deletion junctions.
(A) Illustration of a common pattern present flanking both ends of the deletion junction. (B) Histogram of number of proviral genomes detected with repeat elements of varying lengths. One specific 20 base nucleotide repeat is over-represented. (C) Histogram of the number of times each repeat was detected. nts, nucleotides.

Discussion

Up until now, the best studied PTCs have been the VISCONTI cohort (113, 114), but other isolated cases of PTCs have also been described (116–121, 123, 124, 126, 131, 153). In the VISCONTI study, 14 acutely-treated participants were found to have levels of HIV DNA that were significantly lower than that of ART-treated individuals previously described in the literature (113). However, it is clear that the vast majority of the HIV DNA reservoir is comprised of replication defective proviruses (3–5, 66, 68) and an in-depth analysis of the proviral reservoir, including the frequency of intact proviruses, has yet to be performed for any of these PTCs. In this study, we provide the first detailed survey of the proviral genomic landscape in a PTC cohort and contrast it with that of NCs.

Our results show that prior to treatment interruption, the DNA reservoir size, defined as either total or intact proviral genomes, was a median 7-fold lower in PTCs than in NCs. Specifically, 81% of NCs had > 4 total proviral genome copies/10^6 PBMCs, while none of the PTCs had a total reservoir size that reached this threshold. Low levels of total HIV DNA are associated with short-term delays in viral rebound timing (45, 121), as exemplified by the report of two Boston patients who underwent allogeneic hematopoietic stem cell transplantation with susceptible donor cells. In both patients, proviral DNA was reduced to undetectable levels post transplantation and viral rebound was delayed until 12 and 32 weeks post-TI despite an immune system that was functionally naïve to HIV (154). This observation led some to predict that at least a 3-4 $\log_{10}$ reduction in the HIV reservoir may be needed to achieve sustained HIV remission (155, 156). Our finding of a substantial difference in time to rebound between post-treatment controllers and non-controllers despite relatively modest (7-fold) differences in total and intact proviral genomes suggests that factors other than reservoir size must play an important role in determining

time to rebound. Such factors could include differences in viral replication rate and/or robust anti-HIV immune responses. This interpretation is underscored by the finding that despite prolonged treatment interruption, levels of total and intact proviral reservoir did not significantly increase in PTCs, similar to results from the VISCONTI study. This finding contrasts with the pattern reported for other HIV-infected subjects, where the HIV DNA burden significantly increases upon treatment interruption due to viral replication (147, 157, 158).

Given the rarity of PTCs and safety concerns involving treatment interruption studies, future HIV cure trials would benefit from a set of biomarkers that could predict which participants are more likely to be PTCs prior to treatment interruption. Our finding that the majority of NCs, but none of the PTCs, had > 4 total proviral genomes/10^6 PBMCs prior to treatment interruption suggests that quantification of total proviral genome copy numbers could contribute to the prediction of sustained HIV remission. PTCs had a greater variation in the number of intact proviral genomes that hindered use of this parameter in differentiating between the two groups. In particular, > 40% of the total proviral reservoir for PTC 1C16 was intact, including two large clonal populations. This observation highlights that the size of the intact proviral reservoir has limited predictive ability for viral rebound timing and additional analysis of the integration sites and viral replication fitness are needed.

Similar to previously published reports (3–5, 66, 68), we found that the vast majority of proviral genomes amplified from participant-derived DNA were defective and only a small proportion had intact open reading frames. This was true both for participants treated in either the early or the chronic stage of HIV infection. We were intrigued to find that for PTCs, the proportion of intact proviruses was almost 3 times lower (1.4%) than in NCs (4.1%), although this comparison

did not reach statistical significance and the characterization of additional participants is needed to further explore this finding. We also found no significant differences in the frequency of any particular defective proviral species between PTCs and NCs. Of note, our analysis of defective proviral genomes revealed the proportionally higher prevalence of a specific proviral deletion, represented in 8 distinct participants and reported previously in two other cohorts (4, 5). This pattern comprises a 20 nucleotide repeat sequence flanking the deletion junction, representative of the polypurine tract and appears to be a hotspot for proviral deletions.

HIV integration site analysis suggests that clonal proliferation of HIV-infected cells plays an important role in the proliferation and persistence of HIV infected cells (14, 15). Other groups have shown that clonally-expanded populations of HIV-infected cells can harbor intact, replication-competent proviruses (66, 145, 159). A recent report provided definitive evidence that reactivatable latent cells can arise by clonal expansion *in vivo* by determining that the cells harbored identical TCR sequences through scRNA-seq (160). Thus, we evaluated whether clonal expansion of intact proviruses could be playing a role in the reservoir size differences between NCs and PTCs by assessing the number and frequency of identical proviral sequences detected more than once. We observed no difference between PTCs and NCs in the proportion of identical intact proviral sequences detected more than once. This finding suggests that the clonal expansion rate of cells harboring intact proviruses is similar between PTCs and NCs and therefore does not explain the smaller reservoir size in PTCs nor their ability to maintain viral suppression.

We also evaluated the relationship between the proviral landscape and 1) levels of viral transcription and 2) immune activity. The level of unspliced CA-RNA during suppressive ART has been shown in several studies to be predictive of the timing of viral rebound after ART

discontinuation (72, 131), which suggested that CA-RNA may largely reflect transcription of the intact provirus. Surprisingly, we found that the level of total and defective, but not intact, proviral genomes, was significantly associated with CA-RNA levels. These results reinforce a recent finding that defective proviruses express intracellular HIV RNA (161) and that the bulk of the CA-RNA quantified is likely defective given that the vast majority of proviruses are replication-incompetent (4, 5, 162). Any relationship between the size of the intact proviral reservoir and CA-RNA levels is likely obscured by the overwhelming number of defective proviruses also expressing HIV RNA.

In addition, we found an association between higher levels of NK cell activation and HIV-specific T cell activity with lower levels of total and defective proviral genomes. This observation suggests that a more robust HIV-specific immune response can identify and effectively eliminate HIV-infected cells, even those harboring defective proviruses. Combined with the CA-RNA results, these findings support the concept that defective HIV genomes can lead to viral RNA transcription and antigen production (5, 162), which leads to interactions between cells harboring defective HIV genomes with both the innate and adaptive immune system. Further studies are needed to explore this finding.

We also found that the level of defective, but not intact, proviral genomes was associated with the timing of viral rebound after ART interruption. The reason behind this counter-intuitive result is unclear, but possible explanations include 1) The size of the defective proviral genome within the peripheral blood reflects the overall true reservoir size within the body, including within anatomic sites; 2) Given the low frequency of intact proviruses, a larger sample may be needed to detect a relationship with the timing of viral rebound.

The limitations of this study should also be acknowledged. First, there were individuals with extremely small reservoir sizes and relatively few amplified proviral sequences. This factor may affect the accuracy of the estimated frequency of different proviral species. However, the results were largely unchanged if the analysis was restricted to only participants with > 20 proviral sequences. Second, *in vitro* reconstitution of the reported full-length intact proviruses is needed to confirm that they are indeed replication-competent (4), although we were able to detect identical matches between intact proviral and plasma-derived sequences and obtained highly similar sequences in viral outgrowth assays.

In this report, we provide the most comprehensive survey to date of the proviral landscape in both PTCs and NCs prior to treatment interruption. The results highlight the restricted intact and defective HIV reservoir in PTCs and suggest that total proviral genome burden could act as the first biomarker for identifying PTCs. Additional studies are needed to confirm these findings and to explore whether inefficient viral replication and/or robust anti-HIV immune responses are also present in these individuals. We also found that the size of the defective proviral reservoir was associated with levels of CA-RNA and several NK and T cell markers. Until recently, the defective proviral reservoir appears to have been under-appreciated, but these results support the concept that defective proviruses are far from quiescent (162) and are likely playing key roles in immune activation, shaping anti-HIV immune responses and may be a marker of the timing of plasma viral emergence after ART discontinuation.

(Page intentionally left blank)

CHAPTER 3

EFFECT OF SHORT-TERM ART INTERRUPTION ON LEVELS OF INTEGRATED HIV-1 DNA

Zachary Strongin*[1], Radwa Sharaf*[1], D. Jake VanBelzen[2], Jeffrey M. Jacobson[3], Elizabeth Connick[4], Paul Volberding[5], Daniel J. Skiest[6], Rajesh T. Gandhi[7], Daniel R. Kuritzkes[1], Una O'Doherty[2], Jonathan Z. Li[1]

[1]Brigham and Women's Hospital, Harvard Medical School, Boston, MA [2]University of Pennsylvania, Philadelphia, PA [3]Temple University, Philadelphia, PA [4]University of Arizona, Tucson, AZ [5]University of California, San Francisco, San Francisco, CA, [6]Tufts University, Boston, MA [7]Massachusetts General Hospital, Boston, MA

ZS, RS and JZL developed the concept and design. ZS, RS, DJV and UO performed the experiments. JMJ, EC, PV, DS, RTG and DRK contributed samples. All authors were involved in the writing.

**Authors contributed equally*

Work was published in J Virol. 2018 May 29;92(12). pii: e00285-18. doi: 10.1128/JVI.00285-18.

Abstract

Analytic treatment interruption (ATI) studies are required to evaluate strategies aimed at achieving ART-free HIV remission, but the impact of ATI on the viral reservoir remains unclear. We validated a DNA size selection-based assay for measuring levels of integrated HIV DNA and applied it to assess the effects of short-term ATI on the HIV reservoir. Samples from participants from four AIDS Clinical Trials Group (ACTG) ATI studies were assayed for integrated HIV DNA levels. Cryopreserved PBMCs were obtained for 12 participants with available samples pre-ATI and approximately 6 months after ART resumption. Four participants also had samples available during the ATI. The median duration of ATI was 12 weeks. Validation of the HIV Integrated DNA size-Exclusion (HIDE) assay was performed using samples spiked with unintegrated HIV DNA, HIV-infected cell lines, and participant PBMCs. The HIDE assay eliminated 99% of unintegrated HIV DNA species and strongly correlated with the established Alu-*gag* assay. For the majority of individuals, integrated DNA levels increased during ATI and subsequently declined upon ART resumption. There was no significant difference in levels of integrated HIV DNA between the pre- and post-ATI time points, with the median ratio of post:pre-ATI HIV DNA levels of 0.95. Using a new integrated HIV DNA assay, we found minimal change in the levels of integrated HIV DNA in participants who underwent an ATI followed by 6 months of ART. This suggests that short-term ATI can be conducted without a significant impact on levels of integrated proviral DNA in the peripheral blood.

Introduction

Antiretroviral therapy (ART) is effective in maintaining viral suppression, but cannot eradicate the viral reservoir (23, 24). After ART initiation, the decline in the HIV reservoir is most dramatic during the first year of treatment, but subsequently slows with largely stable HIV DNA levels despite more than a decade of ART (48, 163). Consequently, the cessation of ART generally results in rapid viral rebound (72).

Strategies aimed at achieving sustained ART-free remission will ultimately require efficacy testing using analytic treatment interruption (ATI) studies. However, there are a number of safety concerns associated with ATI trials. One recent study suggested that ATI can be associated with the irreversible increase in the viral reservoir, as reflected by levels of integrated HIV DNA (164). However, this conclusion was reached by the evaluation of participants who underwent 48 weeks of ATI, an extended duration that is substantially longer than the duration of modern ATI trials.

The assessment of the HIV reservoir changes in treatment interruption trials would benefit from a scalable assay that can quantify levels of integrated HIV DNA, especially as non-integrated forms of HIV DNA comprise a major proportion of total HIV DNA during ATI and for a period after ART reinitiation (47). However, the traditional Alu-*gag* integrated HIV DNA assay is challenging to perform and dependent on the presence of Alu elements in close proximity to the HIV integration sites (53, 56, 165). For these reasons, we validated a novel assay for measuring HIV integrated DNA levels that avoids these drawbacks by relying on size-selecting genomic DNA to eliminate non-integrated HIV DNA, followed by quantitative PCR (qPCR) measurements of integrated DNA levels based on a previously proposed method (166). We termed this the HIV

Integrated DNA size-Exclusion (HIDE) assay and employed it to assess changes in levels of integrated HIV DNA in participants of AIDS Clinical Trials Group (ACTG) ATI trials.

Materials and Methods

Study Participants

Cryopreserved peripheral blood mononuclear cells (PBMCs) were obtained for 12 participants with available samples from previously completed ACTG ATI trials (A5197 (135), A5068 (139), A371 (138), A5170 (136)). All participants were on an ART regimen for at least 1 year prior to ATI, experienced viral rebound within 5 weeks of treatment interruption and subsequently achieved viral suppression upon ART resumption. The median [Q1, Q3] length of the ATI was 12 [7,17] weeks. Samples were obtained at a time point immediately prior to ATI and a median [Q1, Q3] of 27 [24,33] weeks after ART reinitiation. Four participants had samples available during the ATI.

HIV Integrated DNA size-Exclusion (HIDE) Assay

DNA was extracted from cryopreserved PBMCs using the QIAmp DNA Mini Kit, loaded into a 0.75% gel cassette with an external S1 marker, and size-selected using a 20kb High-Pass protocol on the BluePippin Pulsed-Field Gel Electrophoresis System (Sage Science) to remove non-integrated viral DNA species. HIV DNA levels were quantified by qPCR with primers/probe targeting HIV LTR/*gag* and normalized to cellular input by qPCR targeting the CCR5 gene (42). The limit of detection (LOD) for each sample was calculated based on a 2 HIV DNA copies/well value adjusted to cellular input.

HIDE Assay Validation

To confirm the removal of non-integrated HIV DNA by the HIDE assay, we spiked HIV-negative DNA with either linear near-full-length HIV amplicons or a 12kb HIV-encoding plasmid at varying quantities. To ensure that measurements of integrated DNA did not change due to the

size-selection process, we also measured HIV DNA levels before and after size selection in three HIV infected cell lines with integrated replication-defective HIV provirus. These included J-Lat cells (clone 9.2) containing an *env* defective proviral copy, 8E5 cells containing an *RT* defective proviral copy, and CEM cells infected with pseudotyped Δ*env* HIV virions allowing only one round of replication and propagated *in vitro* for 4 weeks (57). Prior to size selection and quantification, DNA extracted from the HIV-infected cell lines was diluted in HIV-negative DNA to approximate *in vivo* integrated HIV DNA levels. Integrated DNA levels in these cell lines and in cells from one participant were also assayed by the Alu-*gag* method (56, 165).

Statistical Analysis

Data analysis was performed using GraphPad Prism 6 (GraphPad, La Jolla, CA). Wilcoxon matched-pairs signed rank test was used in analysis of pre- and post-size selection values as well as in analysis of pre- and post-ATI integrated DNA levels. The ratio of post:pre-ATI integrated DNA levels was compared to the ratio of 1.0 by the Wilcoxon signed-rank test. The LOD value was used in the analysis for samples quantified below the LOD.

Ethics Statement

Written informed consent was provided by all study participants for use of stored samples in HIV-related research. This study was approved by the Partners Institutional Review Board.

Results

HIDE Assay Validation

On average, 27% of input DNA was recovered post size-selection for DNA fragments larger than 20kb. The HIDE assay eliminated approximately 99% of linear and circular non-integrated HIV DNA species at either high or low levels of non-integrated DNA (Figure 3.1A). We performed the HIDE assay on three cell lines containing integrated, replication-incompetent HIV DNA. The mean ratio of HIV DNA levels before and after size-selection was 1.02, demonstrating that the assay did not selectively eliminate integrated HIV DNA. We also assessed levels of HIV DNA pre- and post-size selection for one participant. On long-term suppressive

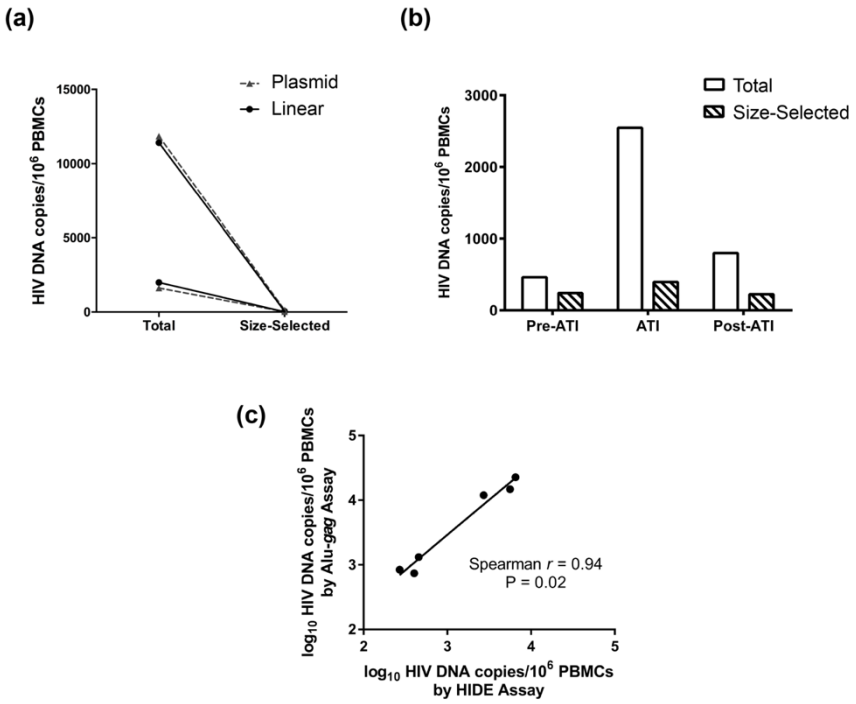

Figure 3.1: HIDE assay validation.
(A) HIV DNA levels for uninfected DNA spiked with linear or circular HIV DNA before and after genomic DNA size-selection. (B) Levels of total and size-selected HIV DNA in participant PBMCs at a pre-ATI (39 months on ART), during treatment interruption and post-ATI (6 months after ART restart) timepoint. (C) Correlation between integrated HIV DNA levels measured by the HIDE assay and by the Alu-*gag* assay for three HIV-infected cell lines and for the three samples shown in part b.

ART, we observed little difference in HIV DNA with and without size selection (Figure 3.1B), but during the ATI, we observed an increase in total HIV DNA while the size-selected HIV DNA levels did not change, reflecting the expected increase in non-integrated DNA after ART interruption (47). In addition, the integrated HIV DNA levels measured by the HIDE assay correlated strongly with integrated DNA measurements by the Alu-*gag* method (Spearman r=0.94, P=0.02, Figure 3.1C).

Effect of Short-Term ATI on Integrated HIV DNA Levels

The 12 ACTG ATI participants had been on ART for a median of 3.9 years with a median CD4 count of 852 cells/mm^3. Four participants had available samples during ATI at a median of 12 weeks after ART discontinuation and with a median plasma viral load of 51,664 copies/mL. These participants were found to have a median increase in integrated HIV DNA levels during ATI of +94 HIV DNA copies/10^6 PBMCs and levels subsequently declined after ≥24 weeks of ART at a median of -109 HIV DNA copies/10^6 PBMCs (Figure 3.2A). Amongst all 12 participants, there was no significant difference between the pre- and post-ATI time points in levels of HIV integrated DNA (median difference -15 copies/10^6 PBMCs, Wilcoxon Signed Rank P=0.34, Figure 3.2B). The median ratio of post:pre-ATI HIV DNA levels was 0.95 (Q1, Q3: 0.8, 1.6, Figure 3.2C), which was not significantly different than a ratio of 1.0 (P=0.79). Within the 42% of individuals that had higher HIV DNA levels post-ATI, the increase in integrated DNA levels was generally small, with a median change of 11 HIV DNA copies/10^6 PBMCs (Q1, Q3: 7, 20 HIV DNA copies/10^6 PBMCs). There was no significant correlation between duration of ATI and the ratio of post:pre-ATI reservoir size.

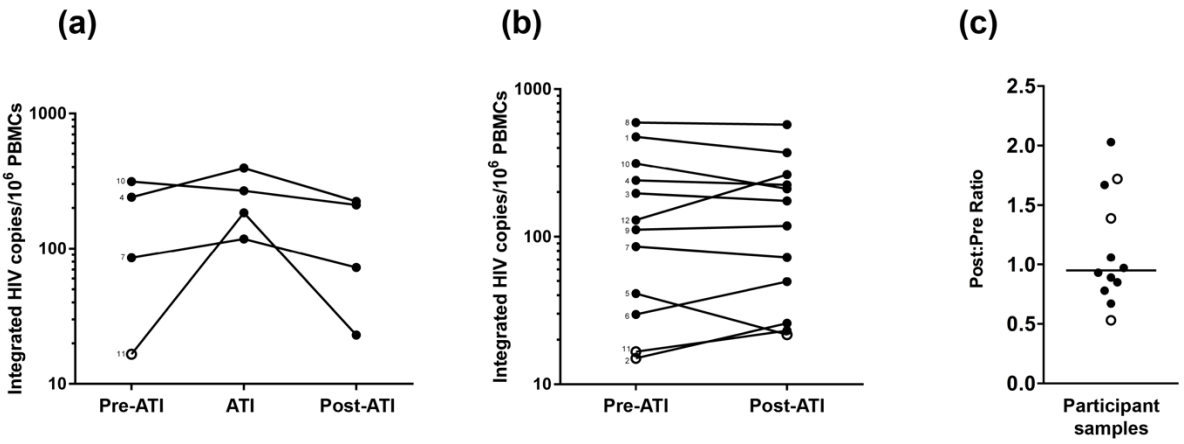

Figure 3.2: Treatment interruption had minimal effect on levels of integrated HIV DNA in PBMCs.
(A) Levels of integrated HIV DNA pre-ATI, during treatment interruption and post-ATI in 4 ACTG participants. (B) Pre- and post-ATI levels of integrated HIV DNA for 12 participants. For samples that are below the limit of detection (LOD), the LOD for that sample is used (open circle). (C) Ratio of post:pre-ATI levels of integrated HIV DNA. Open circle represents if either the pre- or post-ATI time point was below the LOD. Line represents median value.

Discussion

In this study, we validated a new technique for quantifying levels of integrated HIV DNA, termed the HIDE assay, that is less sample- and labor-intensive than the currently used Alu-*gag* assay. We used this assay to assess the impact of short-term ATI on changes in the integrated HIV DNA. The HIDE assay eliminated approximately 99% of non-integrated HIV DNA species, did not affect levels of integrated HIV DNA, and showed high correlation with the standard Alu-*gag* assay. We also found minimal change in levels of integrated HIV DNA after short-term ATI, followed by approximately 6 months of ART.

While quantifying intact full-length proviral numbers and the viral outgrowth assay are the gold-standards for measuring the HIV reservoir, these assays are costly, labor/time-intensive, dependent on large sample volumes, and challenging to implement for large-scale clinical studies (18, 77, 167). In non-suppressed individuals, it is difficult to interpret total HIV DNA levels given the presence of non-integrated forms of HIV DNA (47). In addition, non-integrated HIV DNA species can persist despite long-term ART, suggesting that measuring total HIV DNA, even in patients on long-term ART, may over-estimate integrated HIV DNA levels (168, 169). While assays for integrated HIV DNA do not differentiate between replication-competent and incompetent virus, levels of integrated HIV DNA have been shown to strongly correlate with QVOA, suggesting that integrated HIV DNA can provide a valuable surrogate for the true reservoir size (77, 170). The HIDE assay overcomes two key hurdles intrinsic to the conventional Alu-*gag* assay, including the need for integrated DNA standards that are challenging to create and the reliance on the proximity of random Alu elements to the HIV provirus, requiring high numbers of replicates to account for the varying amplification efficiency (165, 171). By eliminating non-integrated DNA species and using only conserved HIV specific primers, this assay, while using

fewer replicates, can effectively measure both widely diverse and highly clonal proviral populations (42).

ATI trials remain an indispensable tool in the evaluation of strategies for HIV remission. However, there remains a concern amongst both potential participants and physicians about the potential reseeding or expansion of the HIV reservoir due to the ATI. This question remains controversial as some studies have shown a return to baseline reservoir levels after ART reinitiation (45, 147, 158), while another study reported an increase in HIV integrated DNA levels after ATI that was not reversible with ART reinitiation (164). However, the latter study included participants with prolonged treatment interruption that is not reflective of the short-term ATI studies that are being performed in the modern era (172). Using the HIDE assay, we found that in general, short-term ATI did not have a significant impact on levels of integrated HIV DNA after ART resumption. Despite an increase in integrated DNA levels during the ATI, the viral reservoir subsequently reduced to pre-ATI levels after approximately 6 months of ART, possibly suggesting that most newly infected cells during the ATI have relatively limited life-spans. These findings suggest that short-term ATI studies can be conducted without an irreversible increase in integrated HIV DNA levels. However, additional studies will be needed to confirm these findings within the intact proviral reservoir and amongst the tissue reservoirs of HIV.

In summary, this study validated the HIDE assay, a size-selection-based method to quantify levels of integrated HIV DNA. The HIDE assay showed that short-term ATI had minimal impact on levels of integrated HIV DNA after ART resumption. The HIDE assay could be a useful technique for evaluating the impact of strategies aimed at reducing the HIV reservoir and the

results provide a measure of reassurance on the impact of short-term ATI on reseeding of the HIV reservoir.

(Page intentionally left blank)

CHAPTER 4

PERSISTENT HIV-1 LOW-LEVEL VIREMIA CAN ARISE FROM TRANSCRIPTIONALLY-ACTIVE HIV-INFECTED CELLULAR CLONES

Radwa Sharaf[1*], Xin Zhang[1,2*], Behzad Etemad[1], Ce Gao[3], Xiaoming Sun[3], Kevin Einkauf[3], Sigal Yawetz[1], Barbara Turk[4], Guinevere Q. Lee[3], Stephane Hua[3], Jackson Lau[1], Zixin Hu[1], Colline Wong[1], Jesse Fajnzylber[1], Alexandra Rosenthal[1], Daniel R. Kuritzkes[1], Xu G. Yu[1,3], Athe Tsibris[1], Mathias Lichterfeld[1,3], Jonathan Z. Li[1]

[1]Division of Infectious Diseases, Brigham and Women's Hospital, Harvard Medical School, Boston, MA [2]Beijing Pinggu Hospital, Beijing, China [3]Ragon Institute of MGH, MIT and Harvard, Cambridge, MA, [4]Atrius Health, Boston, MA

RS, DRK, AT, ML, and JZL developed the concept and design. RS, XZ, BE, XS, SH, KE, SY, BT, JL, ZH, AR, AT, CW, and JF were involved in the sample/data collection and performed the experiments. RS, CG, GQL, ML, XY, and JZL were involved in the bioinformatic analysis. All authors were involved in the writing of the manuscript.

**Authors contributed equally*

Work is currently under review.

Abstract

Persistent low-level HIV viremia (LLV) can occur despite continuous antiretroviral treatment, but the mechanism remains unclear. Here, we describe an individual with persistent LLV for > 4 years despite detectable plasma ARV levels and ≥2 active ARVs by resistance genotyping. We performed HIV single-genome sequencing and a novel assay combining near-full length PBMC proviral sequencing and integration site identification. In total, 2 clonal populations comprised 95% of plasma RNA sequences, with the largest comprising 86% of plasma sequences and harboring no ARV resistance. This majority plasma clone matched 6% of all intact proviruses, which were integrated into the CD200R1 gene. The second largest plasma population comprised 9% of plasma HIV, but matched 54% of intact proviruses, with an integration site in the cell division-associated STAG2 gene. This finding highlights that persistent LLV can arise from a clonally-expanded cellular population without viral evolution and viral suppression will require targeting of this transcriptionally-active reservoir.

Introduction

The introduction of antiretroviral therapy (ART) has led to viral suppression in the majority of people living with HIV (PLWH), resulting in a dramatic decrease in HIV-related morbidity and mortality. However, detectable low-level viremia is commonly found in a subset of patients despite the use of ART. The incidence of low-level viremia (LLV) on first-line ART has been found to range from 6 – 25% (82–85). In addition, approximately 1 in 5 individuals with LLV have repeated low-level viremia (86). In studies with long-term follow-up, the persistent LLV can last for a year or longer, even in individuals who undergo ART modification (173). Persistent low-level viremia remains an area of clinical concern given its clinical consequences as it has been found to increase the risk of subsequent virologic failure (86, 173–176) and increase the risk of HIV transmission (177, 178).

Traditionally, the presence of LLV has been attributed to suboptimal ART adherence (179) or continued viral replication in tissue reservoirs with incomplete ART penetration (88, 89). In either scenario, there is potential evidence of viral evolution and emergence of drug resistance mutations (90), thus a combination of adherence counseling and ART regimen modification is indicated. However, the presence of viral evolution has not been confirmed in other studies (91) and ART intensification has not generally been successful in clinical trials of individuals with LLV or residual viremia (92, 93). This suggests that for some individuals, persistent LLV may arise due to alternative mechanisms.

In this study, we describe an individual living with HIV for >20 years with persistent LLV over 4.5 years despite high levels of self-reported ART adherence and multiple changes to the ART regimen. Commercial drug level testing and HIV resistance genotyping were obtained. We

assessed the presence of viral evolution and the mechanisms behind the persistent LLV by performing plasma HIV single-genome sequencing at multiple time points and employing a novel assay to obtain near-full-length PBMC proviral sequences with their matched integration sites in the host genome. Furthermore, we performed RNA transcriptomic analysis to define the potential influence of host gene activity on levels of proviral transcription.

Materials and Methods

HIV Eradication and Latency (HEAL) cohort

The HEAL cohort is a Boston-based longitudinal cohort of participants with HIV who are receiving, or initiating antiretroviral therapy. The study was approved by the Partners Institutional Review Board and began in 2016, investigating HIV latency and reservoir dynamics in the study participants. Approximately ninety participants have been enrolled thus far with one participant manifesting persistent low-level viremia.

ART resistance genotyping and plasma drug level testing

Commercial resistance genotyping for NRTI, NNRTI and PI mutations was performed using the Viroseq HIV-1 Genotyping System kit. HIV-1 integrase genotype testing was performed by Quest Diagnostics. ARV drug level testing was performed by the infectious disease pharmacokinetics lab at the University of Florida. Testing was performed for darunavir and dolutegravir by liquid chromatography with tandem mass spectrometry.

Plasma single-genome sequencing

Plasma viral RNA was extracted using the single-copy assay protocol (180) and cDNA synthesized using Superscript IV (Invitrogen) and p9017 primer (HXB2 coordinates 9038-9017). Nested amplification of the *Pol-Env* region (HXB2 coordinates 2090-8796) or the *Pro-RT* region (HXB2 coordinates 2853-3869) was performed at limiting dilution. Using ClustalW, the resulting plasma-derived single-genome sequences were aligned with proviral sequences and neighbor-joining phylogenetic trees were generated.

HIV near-full-length proviral sequencing

DNA was isolated from peripheral blood mononuclear cells (PBMCs) using the QIAamp DNA Mini Kit (Qiagen) and subjected to HIV-1 near-full-length amplification and Illumina MiSeq sequencing as previously described (67). The resulting short reads were *de novo* assembled using Ultracycler v1.0. Sequences were aligned to HXB2 to identify large deletions, out-of-frame indels, premature stop codons, internal inversions, or packaging signal defects using an automated in-house pipeline (66). Hypermutated sequences were identified using Los Alamos HIV Sequence Database Hypermut 2.0 (141). Viral sequences that lacked all mutations listed above were classified as genome-intact.

Matched Integration site and Proviral Sequencing (MIP-Seq)

MIP-Seq is a method to identify the integration sites of intact proviruses (181). Extracted DNA was diluted to single viral genome levels and subjected to multiple displacement amplification (MDA) using the REPLI-g Single Cell Kit (Qiagen). After whole genome amplification, DNA from each well was split and separately subjected to near-full-length proviral amplification and integration site analysis. HIV-1 near-full-length amplification (HXB2 coordinates 638-9610) was performed using a 5-amplicon approach (182). All near-full-length 5-amplicon positive products were subjected to Illumina MiSeq sequencing and the resulting short reads were *de novo* assembled using Ultracycler v1.0 as described above. Integration sites associated with each viral sequence were obtained using integration site loop amplification (15). MiSeq paired end FASTQ files were demultiplexed and analyzed through an in-house bioinformatics pipeline. A subset of integration sites was confirmed by nested PCR amplification using integration-site-specific primers on one end and HIV primers on the other end, as outlined in table 4.1.

Infectivity of recombinant viruses

We generated recombinant virions encoding participant-derived sequences by co-transfecting 293T cells with Δ*pol*-NL4-3 plasmid and *pol* PCR fragments or Δ*env*-NL4-3 plasmid and *env* PCR fragments. Virus was harvested and propagated in U87-CCR5 and U87-CXCR4 cells for 7-10 days. Afterwards, we tested the infectivity of the virus in a TZM-bl infectivity assay. TZM-bl cells (NIH AIDS Reagent Program) are a permissive HeLa cell clone that contain *Tat*–regulated reporter gene for β-galactosidase under the control of the HIV-1 LTR.

RNA-Seq

Total RNA was extracted from memory CD4 T cells using a PicoPure RNA Isolation Kit. RNA-Seq libraries were generated as previously described (183), followed by sequencing on an Illumina NextSeq 500 Instrument. The quantification of transcript abundance was conducted using RSEM software (v1.2.22) supported by STAR aligner software (STAR 2.5.1b) and aligned to the hg38 human genome. Transcripts per million (TPM) values were then normalized among all samples using the upper quantile normalization method. Host gene transcriptional interference was assessed in the top 10 percentile of highly expressed genes that overlap with other genes as compiled in OvergeneDB (184). Spearman correlation was used to determine the expression levels of one gene (gene 1) with the overlapping gene (gene 2) present in the reverse orientation.

Table 4.1. Primer sequences used to confirm the integration sites of clone 1 and clone 2.

Integration-site-specific primers		**hg38 coordinates**
CIS_h22_F1	AGACTATGCCACTGTACTCCAGCCTG	chrX 124031402-124031427
CIS_h22_F2	AAAACACAGCACAAAAGTCTTATATATG	chrX 124031284-124031311
CIS_h22_R1	CCAAACCGAATGAATGGTCATCACCAAC	chrX 124031036-124031063
CIS_h22_R2	GAAGTTGTTAAAATGGGCAAGAGTGCTAT	chrX 124031093-124031121
ISL76_F1	TCAACCAGGGTTGGATGAAGAATTAATAAATTTCA	chr3 112921938-112921972
ISL76_F2	TGTCTATTGTGAACATTGCTTGGTAATATTTATA	chr3 112921988-112922021
ISL76_R1	AACATAAGTCTATTTGCTCCATAGCAGAAA	chr3 112922288-112922317
ISL76_R2	CAATCATACCATCTGAGATTTTTAAGACAGCT	chr3 112922200-112922231
HIV-specific primers		**HXB2 coordinates**
RT3.1	GCTCCTACTATGGGTTCTTTCTCTAACTGG	3830-3859
RT3798R	CAAACTCCCACTCAGGAATCCA	3798-3777
GP41Fo	TTCAGACCTGGAGGAGGAGATAT	7626-7648
GP41Fi	GGACAATTGGAGAAGTGAATTAT	7652-7674

Results

Clinical summary

The patient is a male individual diagnosed with HIV-1 in 1990. He had a long history of antiretroviral treatment (ART), including nucleoside reverse transcriptase inhibitor (NRTI) zidovudine monotherapy, zidovudine and lamivudine dual therapy, as well as subsequent treatment with both protease inhibitors (PIs) and non-nucleoside reverse transcriptase inhibitors (NNRTIs) with documented viral suppression between 2000-2004. In consultation with his physician, the patient discontinued ART for approximately 3 years and in 2007, he had a plasma HIV-1 RNA level of 12,842 copies/mL and was started on a regimen of co-formulated tenofovir disoproxil fumarate and emtricitabine (TDF/FTC) with ritonavir-boosted atazanavir (ATV/r). He achieved virologic suppression with a viral load <75 HIV-1 RNA copies/mL (Year 0 in Figure 1). At 3.7 years after viral suppression, the patient had a low-level viremia of 224 HIV-1 RNA copies/mL with virologic re-suppression documented 2 months later and continuing through 5.9 years. At that time, the patient had plasma HIV-1 RNA levels of 150 copies/mL and over the subsequent 4.5 years, he has had 18 consecutive viral load measurements ranging between 150-810 HIV-1 RNA copies/mL. This low-level viremia persisted despite a stable CD4 T cell count and ART intensification first with co-formulated rilpivirine (RPV)/TDF/FTC plus the integrase strand-transfer inhibitor (INSTI) dolutegravir (DTG), and subsequently with co-formulated tenofovir alafenamide plus emtricitabine (TAF/FTC) with ritonavir-boosted darunavir (DRV/r), and DTG. Levels of HIV-1 DNA were tested at the timepoints sampled and were determined to be 210 and 250 copies/million PBMCs at timepoints 1 and 2, respectively.

Commercial antiretroviral medication (ARV) resistance and plasma drug level testing

Commercial ARV resistance genotyping for NRTI, NNRTI and PI at 7.1 and 7.5 years after recent viral suppression demonstrated no ARV resistance mutations, despite viral loads of 590 and 430 HIV-1 RNA copies/mL, respectively. A subsequent resistance genotyping test at 7.9 years when plasma viral load was 413 HIV-1 RNA copies/mL showed the presence of the following thymidine analog resistance mutations (TAM): D67N, K70R, K219Q, with no resistance to either the PIs or INSTIs. Random plasma ARV levels were obtained at 7.6 and 7.9 years with viral loads of 260 and 413 HIV-1 RNA copies/mL (Figure 4.1). Peak plasma darunavir concentrations of 5-8 mcg/ml occur 2.5-4 hours post-dose, while trough concentrations generally

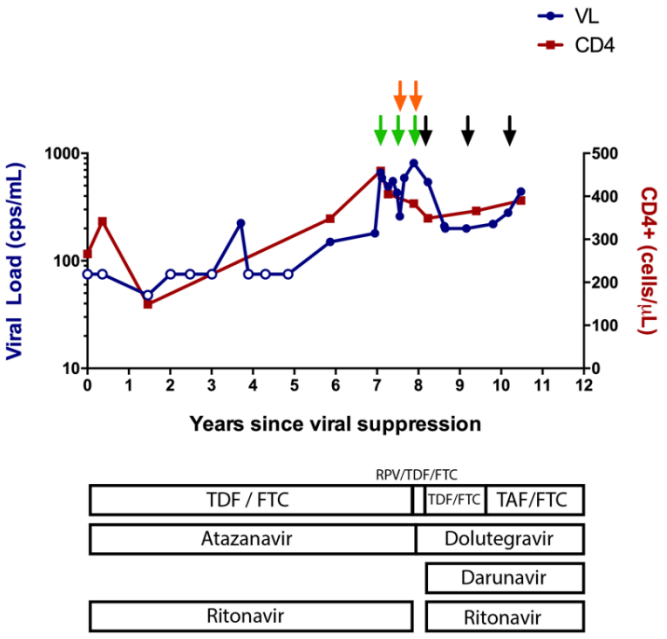

Time	Resistance
7.1 yrs	None
7.5 yrs	None
7.9 yrs	D67N, K70R, K219Q

Time	Drug	Concentration (mcg/mL)
7.6 yrs	DTG	0.29
	DRV	1.52
7.9 yrs	DTG	2.88
	DRV	7.21

Sampling time	Time point
8.2 yrs	1st timepoint
9.2 yrs	2nd timepoint
10.2 yrs	3rd timepoint

Figure 4.1: Plasma viral loads and CD4 counts.
At each timepoint, the viral load is graphed in blue and CD4 count in red. Open blue circles denote viral load levels below limit of detection. The drug regimens are depicted below the graph, according to the timescale on the x-axis. Green arrows represent timepoints used for genotype resistance testing and orange arrows represent timepoints used for drug level testing. Black arrows indicate the timepoints used for plasma and proviral sequencing. Years depicted on the x-axis represent years since the most recent viral suppression. TDF, tenofovir disproxil fumarate; FTC, emtricitabine; RPV, rilpivirine; TAF, tenofovir alafenambide; DTG, dolutegravir; DRV, darunavir; yrs, years; cps, copies.

the concentration was measured at 7.21 mcg/ml 2 hours after the last dose. At steady state, dolutegravir peak concentrations typically are 3.3 mcg/ml approximately 2 hours post-dose (186) and steady-state trough concentrations are generally <1 mcg/ml. At the 7.6 years timepoint, the dolutegravir concentration was measured at 0.29 mcg/ml 11 hours after the last dose. At the 7.9 years timepoint, the concentration was measured at 2.88 mcg/ml 2 hours after the last dose. Overall, these results are consistent with high levels of self-reported ART adherence.

Persistent plasma LLV is comprised primarily of two clonal populations

Single-genome sequencing of plasma HIV *pol* RNA was performed at 3 timepoints 1 year apart (at 8.2, 9.2, and 10.2 years, Figure 4.1). In total, 2 clonal populations, hereafter identified as clone 1 and clone 2, made up 95% of all single-genome plasma *pol* sequences across all the time points (Figure 4.2). The largest plasma viral clone, clone 2, comprised 86% of all plasma sequences (range 67% - 100% at each time point). This clone harbored no known drug-resistance mutations. The other clonal population (clone 1) comprised 9% of all plasma sequences, although it was detected only at the first sampling time point (8.2 years). All clone 1 plasma sequences harbored the same D67N, K70R, and K219Q mutations identified on commercial HIV resistance genotyping at 7.9 years. No evidence of viral evolution was seen by phylogenetic analysis and emergence of new drug resistance mutations were not detected in plasma HIV sequences over the 3-year sampling period.

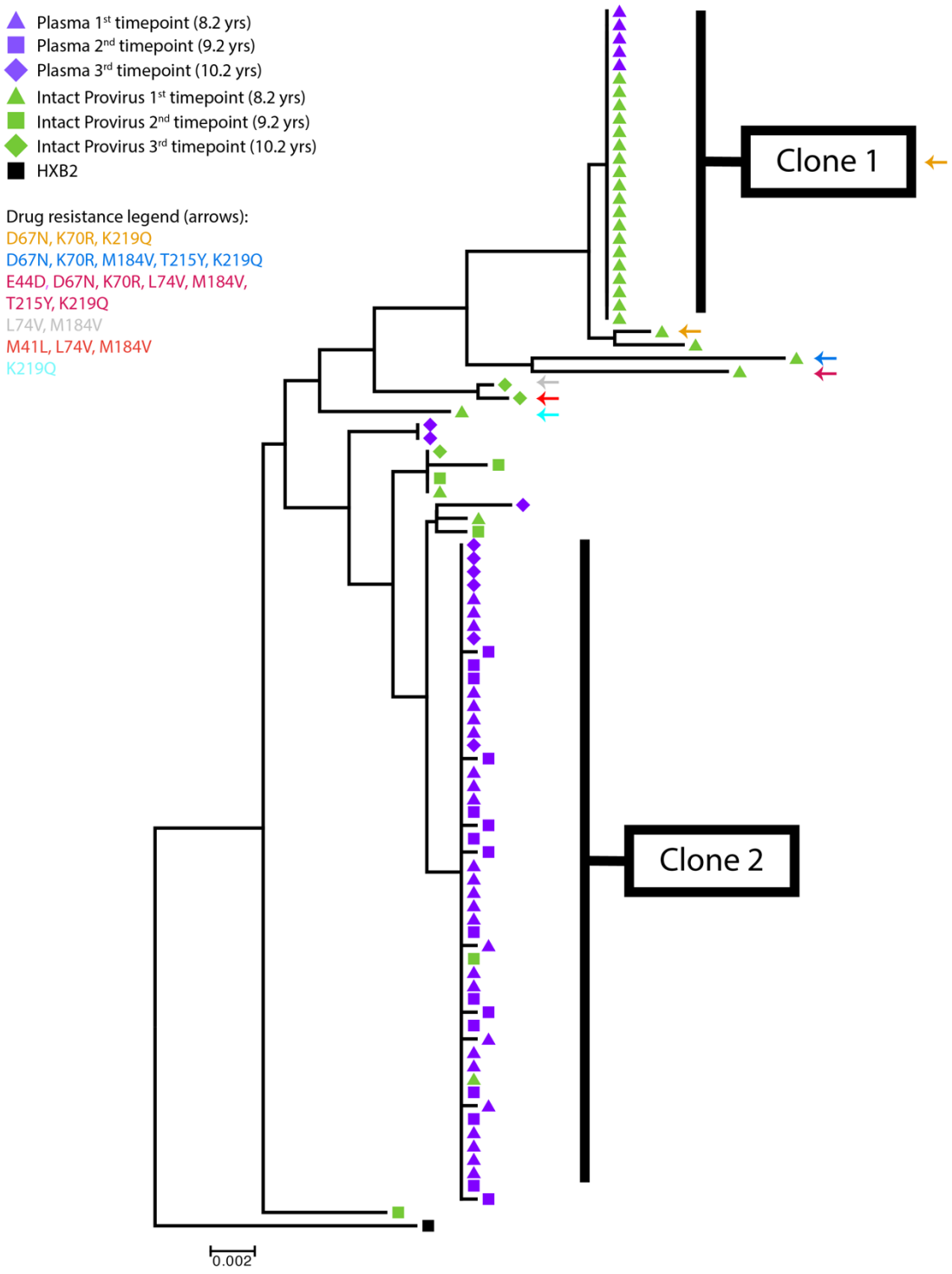

Figure 4.2: Neighbor-joining tree of the *Pro-RT* region in both proviral and plasma-derived sequences.
This figure depicts a phylogenetic tree of sequences obtained from the LLV participant rooted to HXB2. Sequences were obtained from plasma (shown in purple) or PBMCs (shown in green) at one of three different timepoint. The adjacent arrows illustrated the drug resistance mutations present in each sequence as detailed in the legend.

To confirm the results from the plasma sequencing of HIV *pol*, we also performed single-genome HIV sequencing of a nearly 7 kb region from the plasma virus spanning *pol* to *env*. The *pol-env* sequence confirmed the clonality of these two populations (Figure 4.3). No integrase drug resistance mutations were identified in these plasma sequences.

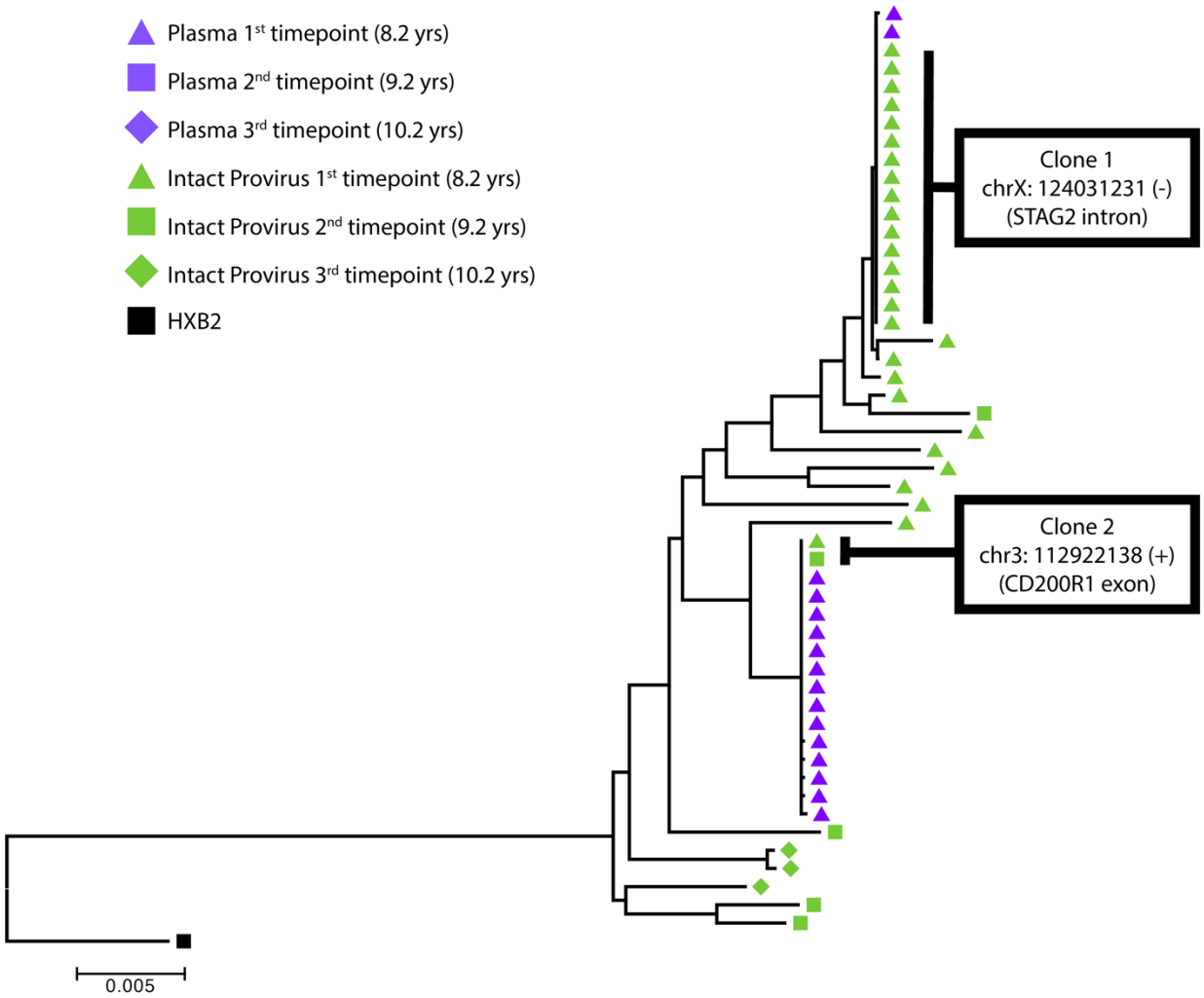

Figure 4.3: Neighbor-joining tree of the near-full-length sequences derived from both provirus and plasma.
This figure depicts a phylogenetic tree of sequences obtained from the LLV participant rooted to HXB2. Sequences spanning a ~ 7 kb region of HIV were obtained from plasma (shown in purple) or PBMCs (shown in green) at one of three different timepoint. Clone 1 and 2 are indicated with the bold black line, along with their associated integration site, annotated by chromosome number, location and strand.

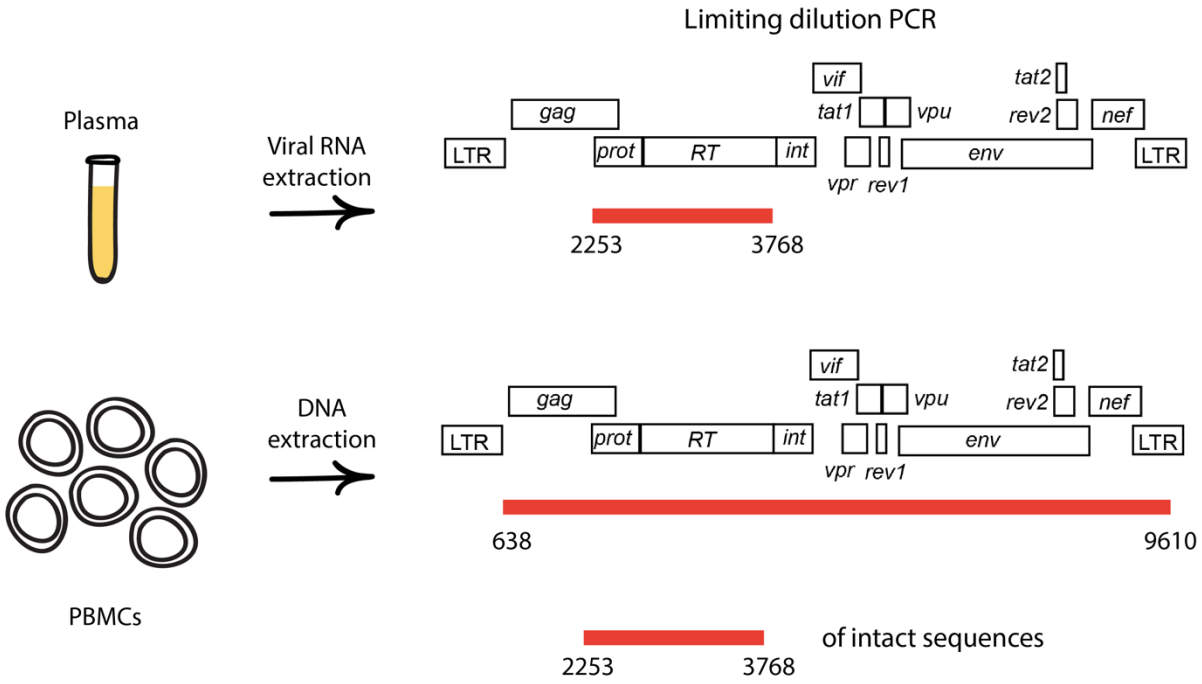

Figure 4.4: Flowchart for obtaining *Pro-RT* sequences from intact proviral sequences and plasma viral RNA. Numbers are based on HXB2 coordinates.

The persistent low-level HIV viremia arose from clonally-expanded HIV-infected cellular populations

At the 3 sampling time points, near-full-length sequencing of an approximately 9 kb region of the HIV-1 proviral genome was performed using DNA extracted from PBMCs as depicted in Figure 4.4. In total, we obtained 623 proviral genomes, of which 9.1% were categorized as intact (Figure 4.5). Intact proviruses that exactly matched the largest plasma clonal variant, clone 2, were identified both at the 1st and 2nd time points (8.2 and 9.2 years), but comprised only 6% of all intact proviruses (Figure 4.2). Interestingly, the majority of intact proviruses consisted of one clonal proviral sequence, comprising 54% of all intact proviruses and matching the clone 1 plasma variants present at 9% of the plasma HIV RNA population (Figures 4.2 and 4.3). The proviral sequences within this clone also harbored the D67N, K70R, and K219Q NRTI resistance

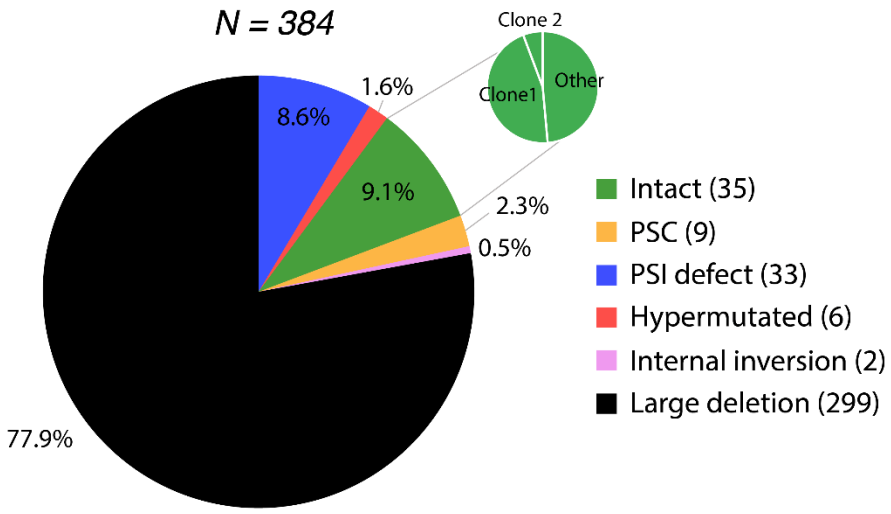

Figure 4.5: Pie chart reflecting the relative contribution of each proviral species across all three timepoints. The makeup of the intact proviral reservoir is represented in the smaller pie chart. PSC, premature stop codon; PSI, packaging signal.

mutations. Additional ARV resistance mutations were identified within the proviral reservoir that were not detected in plasma, including one proviral variant harboring the following resistance mutations: D67N, K70R, L74V, M184V, T215Y, and K219Q. No PI or INSTI resistance mutations were detected in any provirus. Infectivity of recombinant virions generated using *pol* and *env* PCR fragments from both clone 1 and clone 2 intact proviruses was confirmed in a TZM-bl assay (Figure 4.6).

The proviral clone matching the major plasma variant is integrated in a silent gene

Next, we sought to determine the integration site locations of intact proviruses by using a recently-described assay termed the Matched Integration site and Proviral sequencing (MIP-Seq) assay (181). This technique is based on an initial step of whole genome amplification (WGA) under limiting dilution conditions to generate sufficient material for both near-full-length proviral

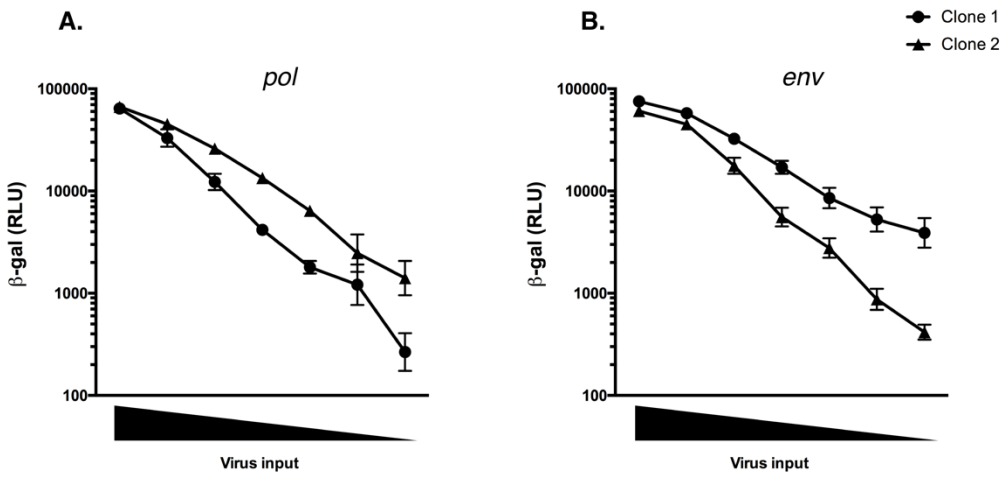

Figure 4.6: Infectivity assay on TZM-bl cells.
Infectivity of recombinant virions generated using (A) *pol* or (B) *env* PCR fragments from intact proviral genome of clone 1 and 2 was tested in a TZM-bl assay. RLU, relative luminescence units.

amplification and integration site analysis (Figure 4.7). Using this assay, we confirmed that identical near-full-length proviruses were integrated into the same loci and identified the integration sites for the intact proviruses comprising both clone 1 and 2 populations. The largest population of clonally-expanded intact provirus (clone 1) was found to be integrated into chrX:124031231(-), corresponding to the intron of the STAG2 gene in chromosome X. The STAG2 protein is part of the cohesin complex regulating chromosome structure and cell division (187). HIV proviruses responsible for the largest plasma viral population (clone 2) were integrated into chr3:112922138(+), which corresponds to exon 7 of the CD200R1 gene in chromosome 3. The CD200R1 gene encodes a transmembrane receptor that regulates the expression of pro-inflammatory molecules, but is not generally expressed at high levels in CD4 cells except in the setting of chronic immune stimulation (188, 189). Both proviral clones were integrated in an opposite direction relative to the gene.

Finally, we performed RNA-Seq on total memory CD4 T cells from all three timepoints to assess the transcriptional activity of the genes into which these two HIV proviral sequences were integrated: 1) STAG2 gene for clone 1 and 2) CD200R1 gene for clone 2, which comprises the majority of plasma variants. STAG2 was expressed at a median 161.5 transcripts per million (TPM), placing it in the top 10% of all expressed genes. This level of expression is substantially higher than the median TPM for all expressed transcripts (11.8 TPM) and higher than housekeeping genes like GAPDH (Figure 4.8A). In contrast, no CD200R1 transcripts were

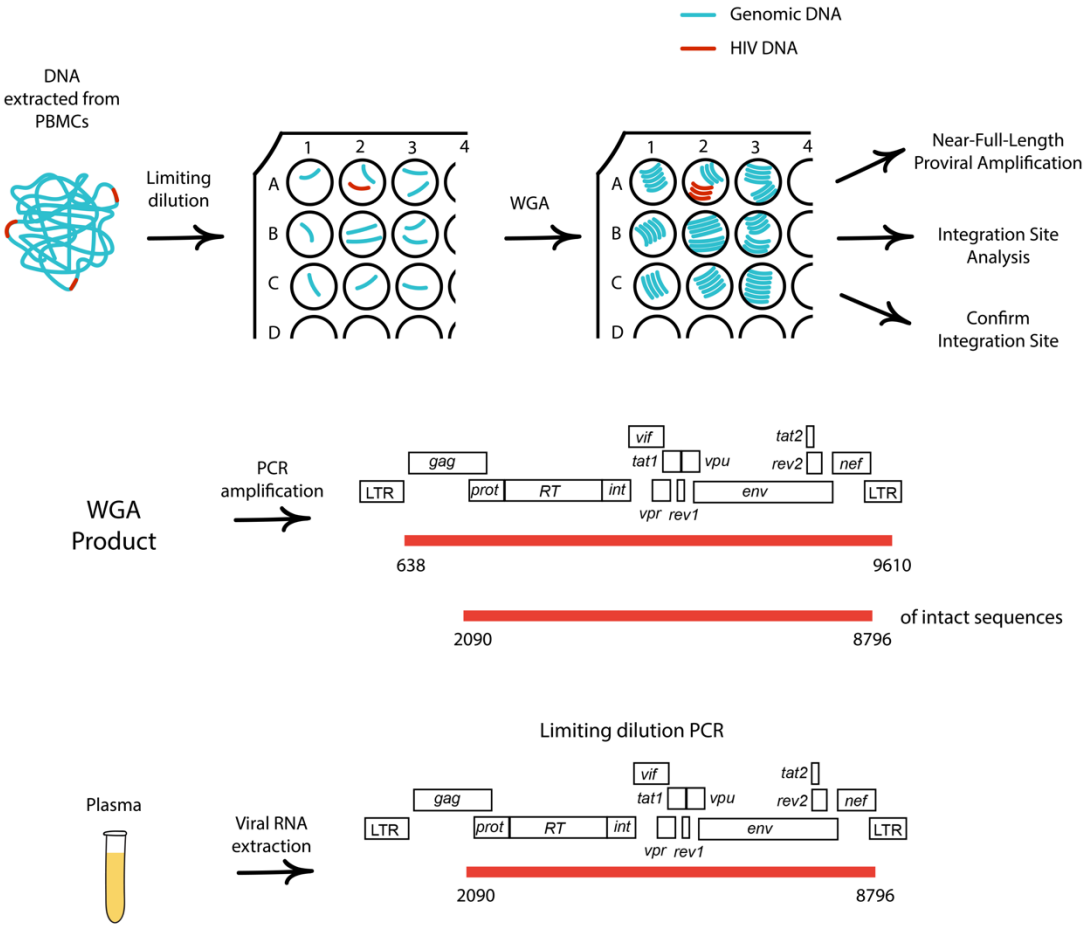

Figure 4.7: Flowchart for obtaining near-full-length plasma and proviral sequences with the associated integration site via Matched Integration site and Proviral sequencing (MIP-Seq) assay. WGA, whole-genome amplification. Numbers are based on HXB2 coordinates.

detected in any of the three timepoints across two biological replicates. These results suggest that higher levels of host gene transcription could negatively impact levels of proviral transcription, especially in the setting of proviral clones integrated in the opposite direction of the host gene. If this hypothesis is true, we should see evidence of transcriptional interference between overlapping host genes located in opposite orientation to each other. Using a database comprised of overlapping gene pairs (184), we tested the correlation between expression levels of the top 10% of highly expressed genes and that of their overlapping gene, residing in the opposite orientation. In 95 gene pairs, we found a strong negative correlation between the expression of one gene and its overlapping neighboring gene (Spearman correlation, $P < 0.0001$, Figure 4.8B), providing additional evidence of host gene transcriptional interference as a regulator of proviral gene expression.

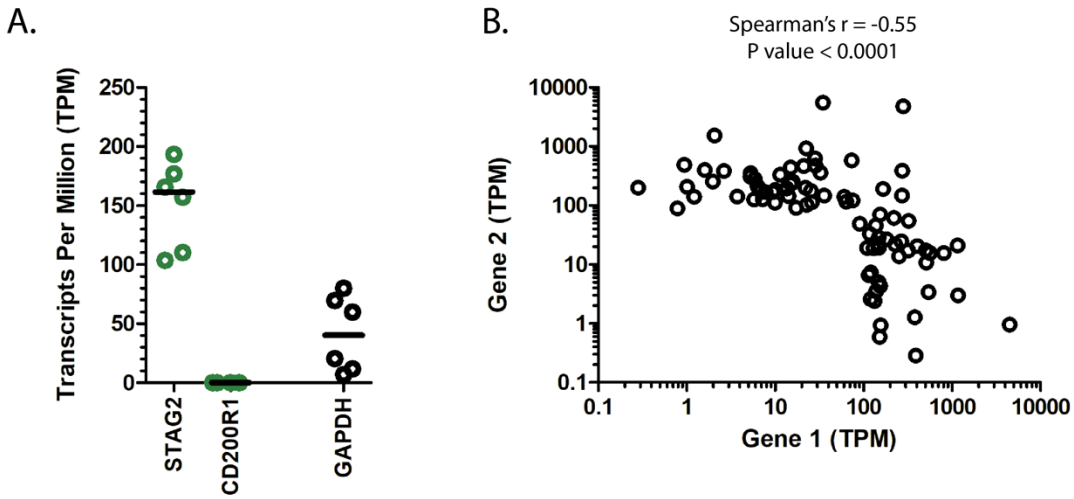

Figure 4.8: RNA-Seq results.
(A) TPM counts from an RNA-Seq experiment performed on total memory CD4 T cells showing values for STAG2 for clone 1 and CD200R1 for clone 2. Green circles denote counts for the two genes where intact proviruses were integrated. Black circles denote counts for GAPDH. (B) Correlation between the expression of overlapping genes positioned in opposite orientation to each other.

In this report, we describe an individual with stable LLV over > 4 years. Using intensive single-genome sequencing of the plasma RNA and PBMC DNA, we show that 95% of the plasma RNA sequences were comprised of just 2 clonal populations, with the largest clonal population stable over 3 years and harboring no HIV drug resistance mutations. Using the MIP-Seq technique, we found that these plasma clonal variants arose from clonally-expanded populations of intact proviruses integrated into genes that modulate CD4 cell function or regulate cellular division. Transcriptomic analysis further suggest that host gene transcriptional activity may play a role in regulating levels of proviral expression.

The presence of LLV despite ART has become an area of increasing concern as recent reports have highlighted the clinical significance of LLV and persistent LLV as a risk factor for subsequent treatment failure (86, 176, 190). For individuals on ART, the cause of LLV has historically been attributed to suboptimal ART adherence and/or the acquisition of HIV drug resistance (179, 191–194). Previous studies supporting the presence of active viral replication have shown that ART resistance mutations can accumulate when viremia levels persist in the low but detectable range (195, 196). While these factors represent an important cause of persistent LLV, controversy remained as evidence also showed that persistent LLV can be maintained for long periods of time without leading to high-level virologic failure or the development of new resistance mutations (91, 173, 191, 197–199). The participant described here reported high levels of ART adherence, which was corroborated by several additional pieces of evidence suggesting that suboptimal ART adherence and/or active viral replication were not likely causes of the persistent LLV. This evidence includes: 1) the stability of the LLV over > 4 years despite multiple ART changes and intensification, 2) plasma ARV levels in the expected range at the time of the LLV, and 3) the lack of viral evolution or drug resistance accumulation over time.

There have been previous reports of clonally-expanded plasma viral populations in perinatally-infected children with persistent LLV (193) as well as in an adult with persistent LLV in the setting of metastatic squamous cell carcinoma, radiation and chemotherapy (22). Through intensive single-genome sampling of the plasma RNA and proviral DNA, we show for the first time that in an adult without concurrent malignancy, persistent LLV can be composed of primarily oligoclonal variants produced by a few large clonally expanded HIV-infected cellular populations. The largest of these plasma clones harbored no HIV drug resistance and the frequency of this clone was stable over three years. These results describe a mechanism of persistent low-level viremia that has not been well appreciated up to now and offer an alternative explanation for the disparate outcomes of adults with persistent low-level viremia in prior clinical studies. Despite the presence of persistent low-level viremia, our results do not support the presence of ongoing viral replication and suggest that ART intensification is unlikely to be of clinical benefit in this setting. The investigation of interventions targeting these clonally-expanded HIV-infected cells is warranted, especially as LLV has been associated with a higher risk of virologic failure (86, 176, 190) and other adverse consequences, including immune activation (200), microbial translocation (201), systemic inflammation (199) and cases of HIV transmission (177, 178).

Identifying the HIV integration site of intact proviruses has represented a major technical hurdle in the field as 1) there remains some doubt as to whether some identical proviruses may arise not only from clonal expansion of HIV-infected cells, but also from early seeding of multiple cellular reservoirs during a time of limited viral diversity and 2) it has not been possible to explore the hypothesis that the integration site may influence HIV transcriptional activity of intact proviruses and thus contribute to the presence of low-level viremia. We utilized a recently-

developed technique, termed MIP-Seq, that allowed us to identify the matched integration sites of intact proviruses (181). This approach enabled us to confirm that identical intact proviral sequences from this participant indeed arose from clonally-expanded populations of HIV-infected cells and to investigate the host integration sites of the proviral populations that led to the persistent low-level viremia.

We found that the largest proviral clone (clone 1) was integrated into the intron of the STAG2 gene in the X chromosome in the opposite orientation relative to the gene. STAG2 is part of the cohesin complex with a critical function in the regulation of chromosome structure and cellular division (202–204). STAG2 enhances HIV LTR promoters, as well as the activity of TNFα (205). In addition, STAG2 interacts with the viral transactivator *tat* and promotes *tat*-mediated activation of the LTR (205). It is unknown whether HIV integration into this intronic region disrupts RNA splicing for this gene, which may be especially relevant as only one copy of this gene is present in this male (XY) participant. On the other hand, the proviral clone producing the majority of the plasma viremia was found to be integrated in the reverse orientation into exon 7 of the CD200R1 gene. This gene encodes for an immunomodulatory transmembrane receptor on myeloid and CD4 cells, although not generally expressed at high levels except in the setting of chronic immune stimulation (189, 206, 207).

Interestingly, transcriptomic analysis of memory CD4+ cells in this individual showed that STAG2 was consistently expressed at high levels while CD200R1 expression was undetectable throughout. These results raise the intriguing possibility that host transcriptional interference, whereby host RNA pol II complexes may induce premature termination of HIV-1 transcription, could be responsible for reduced transcription levels from proviral clone 1, leading to its low

frequency in the plasma despite the abundance of a clonally-expanded cellular population harboring this provirus (Figure 4.9). In contrast, the absence of host transcriptional interference in the CD200R1 gene could contribute to the relatively high expression levels of proviral clone 2 and thus persistent LLV (Figure 4.9). This hypothesis is supported by evidence of transcriptional interference of host genes present in overlapping and reverse orientations. In addition, transcriptional host gene interference with HIV-1 proviral gene expression was previously described in *in vitro* HIV-1 models and was shown to effectively inhibit gene expression of proviruses (208–211). The fact that cells from clone 2 are the source of the major plasma variant, yet persist over time, suggests that these cells are escaping both immune surveillance, as well as viral protein-mediated cytotoxicity. This finding is puzzling. However, previous reports have shown that host factors can promote the persistence of HIV-1 infected CD4 T cells by activating cellular survival programs (212, 213) and that cells harboring replication-competent HIV may be resistant to clearance by CD8+ T cells (214). Additional studies will be needed to assess mechanisms by which these transcriptionally-active HIV reservoirs can maintain the LLV in the face of these selective pressures.

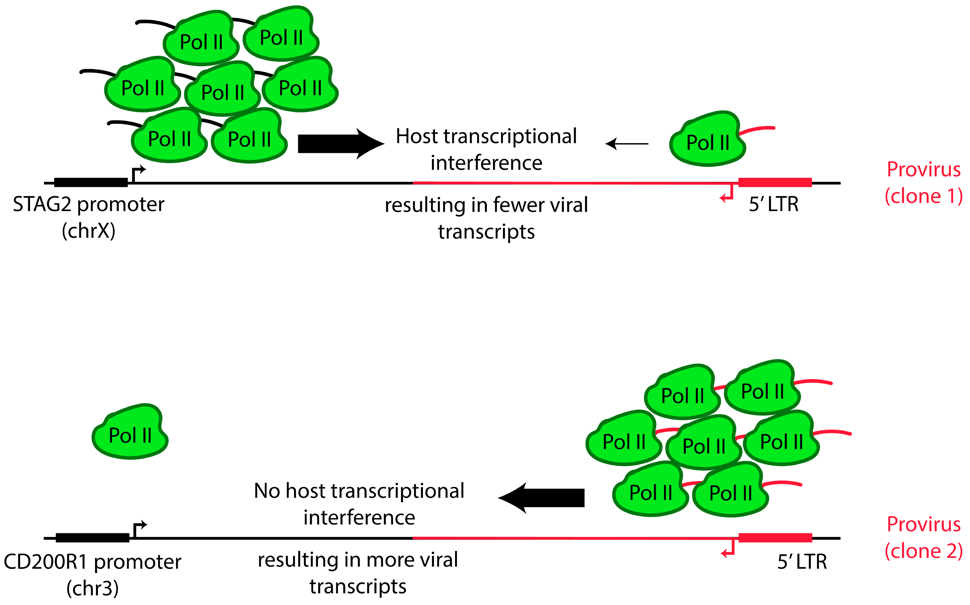

Figure 4.9: Model for transcriptional interference in clone 1 and 2.

It has been demonstrated that different chromatin environments can impose different degrees of transcriptional regulation on the integrated HIV proviral genome, with reactivatable latent HIV residing in more transcriptionally active regions of the genome (215, 216). Our results highlight that the orientation of the integrated intact provirus relative to the host gene, as well as the transcriptional activity of that gene, may be of additional value as both pieces of information may influence which clones will be impacted by convergent transcription. Recent published work from our group also showed that among intact proviruses integrated in genes, a higher proportion was integrated in an opposite orientation to the host gene (181). This finding was observed in two patients on prolonged antiretroviral therapy and suggested that intact proviruses located in an opposite orientation to host genes were preferentially selected for.

Of note, the TAM mutations present in clone 1 were detected by commercial HIV resistance testing at year 7.9 and by single-genome plasma and proviral sequencing at year 8.2. In

addition, the proviral clone 1 represented the major proviral population detected at year 8.2. However, these mutations were not detected on commercial resistance testing at years 7.1 and 7.5, and neither plasma nor proviral single-genome sequences harboring these mutations were identified at years 9.2 and 10.2. The dramatic fluctuations in the frequency of proviral clone 1 is consistent with reports that clonally expanded populations of HIV-infected cells wax and wane over time (217). Whether this fluctuation is in response to antigenic stimulation and/or influenced by proviral integration into host genes remains an area of uncertainty. The HIV resistance genotyping at years 7.1 and 7.5 was performed by Sanger sequencing, which offers limited sensitivity as only mutations above ~20% frequency can be reliably detected. Thus, it is likely that clone 1 sequences were present at a low frequency at years 7.1 and 7.5, below the limit of detection of the commercial resistance testing.

Our study has a few notable limitations. First, technical barriers in amplifying single-genome plasma RNA from low-level viremia samples limited us to analyzing a ~ 7 kb region of plasma HIV *pol-env* sequence. We believe that these plasma clones arose from matching proviral clones as 1) we did not identify any proviral sequences containing exact matches in this 7 kb region, but harbored mismatches outside of that region, and 2) the clonal prediction score calculator estimates that amplifying this 7 kb region should identify clonal proviral sequences with 100% accuracy (218). Another limitation of this study is that the RNA-Seq was performed on total memory CD4 T cells as it remains technically challenging to perform transcriptomic analysis of HIV-expressing cells given their rarity, even in this participant. Finally, this work represents an intensive study of a single case and larger studies are needed to determine the relative contribution of clonally-expanded reservoir versus active viral replication as the underlying mechanism amongst the general population of patients with persistent LLV.

In summary, this report demonstrates that persistent LLV can arise from the integration of HIV into a clonally-expanded CD4 population without evidence of ongoing viral replication or concurrent malignancy. These results also highlight the likely influence of host transcriptional interference on viral gene expression. Interventions that specifically target transcriptionally-active HIV-infected cells or reduces antigenic stimulation may be needed to achieve viral suppression in patients with persistent LLV.

(Page intentionally left blank)

CHAPTER 5

CONCLUSIONS AND SIGNIFICANCE

Any evaluation of interventions aimed at functional cure will require a treatment interruption. However, concerns still remain among clinicians regarding the stopping of treatment including patient safety, higher risk of transmission and selection for drug resistant viruses. Previous studies have shown that treatment interruption leads to a transient increase in the HIV reservoir size (58, 147). However, recent data suggests that the risks associated with treatment interruption can be attenuated and may be outweighed by the potential benefits of assessing the efficacy of new interventions for HIV remission.

Despite the risk associated with a transient increase in the reservoir, we and others have shown that upon treatment re-initiation, the reservoir size returns to its pre-treatment interruption values (58, 147, 219), as detailed in chapter 3 of this thesis. Furthermore, it has been demonstrated that the viral decay kinetics upon treatment resumption are similar to those in drug-naïve individuals (112, 220, 221). Similarly, several studies have shown that drug-resistant viral variants are usually not selected during the ATI (137, 221). The risk of developing drug resistance may be particularly higher in the context of repeated treatment interruptions (222) and in cases when drugs with prolonged half-lives, such as non-nucleoside reverse transcriptase inhibitors (NNTRIs) are used (223). This limitation can be overcome by switching participants to agents other than NNRTIs before the treatment interruption phase and conducting drug resistance testing before resuming treatment.

Most individuals will exhibit viral rebound after treatment is interrupted as shown in figure 5.1. Previous studies have shown that measurements of HIV-1 DNA were predictive of the time to plasma virus rebound (45, 121, 224) and may help identify individuals who could safely interrupt ART in future treatment interruption trials. In certain individuals, particularly those with

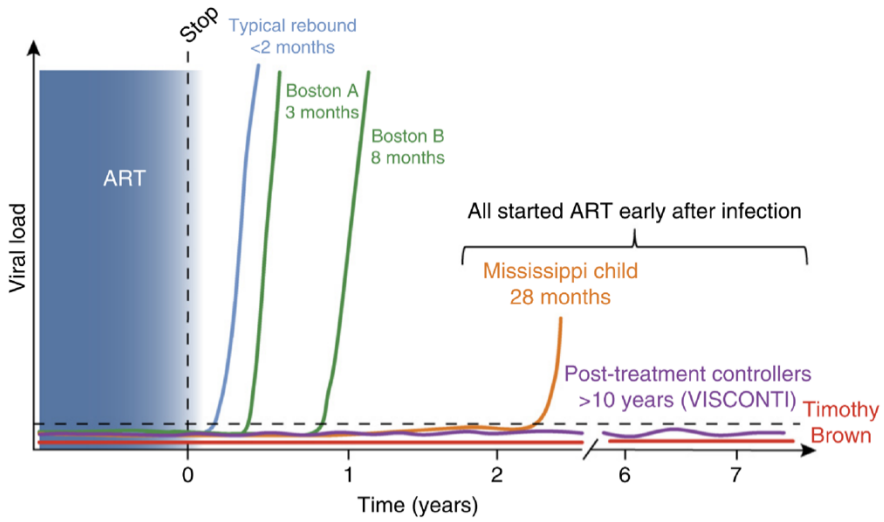

Figure 5.1: HIV remission cases off ART.
From Deeks et al, Nature medicine, 2016

an ultralow reservoir size, viral rebound may be delayed as compared to individuals with a larger reservoir size (158). Furthermore, timing of treatment initiation influences the median time to viral rebound, which is significantly longer in patients treated during early/acute HIV infection (8 weeks) versus those treated during chronic infection (4 weeks) (225, 226). This observation is likely a result of a smaller reservoir in HIV-infected individuals who start treatment early after HIV infection compared to those who start treatment later in infection (21, 227–231). This association between early treatment initiation and a smaller reservoir size has been reported by multiple groups using different assays to measure the reservoir size, including measures of total HIV DNA (228–231), integrated HIV-1 DNA (21, 231), QVOA (227, 230, 231) and total near-full-length proviral genomes (67).

The term “post-treatment controllers” (PTCs) was coined to identify a group of HIV-1-infected individuals who interrupt treatment, yet maintain viral control, as displayed in figure 5.1 (113). PTCs were identified at a higher frequency (13-15%) within individuals treated during early

infection compared to chronic infection (4%) (113, 115, 122–125, 130). There are reasons to believe that treatment altered the course of natural infection in PTCs, suggesting that therapy delivered at the right time to the right people may be "curative". These individuals are likely a heterogeneous group with multiple potential mechanisms of control, providing a unique opportunity to better understand viral persistence and host control. Because of new WHO guidelines released in 2015 that recommend treating all HIV-infected individuals as early as possible regardless of their CD4 count (232), it is likely that more individuals with favorable conditions to control infection after treatment interruption will appear over time. In this context, the priority is to identify markers that will allow the identification of patients who are more likely to become PTCs and in whom ART could be safely interrupted. As detailed in the second chapter of this thesis, we have found that levels of total proviral genomes (TPGs) can serve as a biomarker differentiating between PTCs and post-treatment non-controllers (NCs), given that prior to treatment interruption, 81% of NCs vs. 0% of PTCs had TPGs > 4 copies per million PBMCs.

Mechanisms underlying post-treatment control are still poorly understood. These factors can be grouped into two categories: host-related or virus-related. In this thesis, we have explored a few of these viral factors. Throughout chapter 2, we explored differences in the proviral landscape between PTCs and NCs, particularly within the intact reservoir, showing that PTCs harbor a ~7-fold smaller intact reservoir size. On the other hand, as outlined in chapter 2, we found no evidence to suggest that levels of clonal expansion within cells harboring intact proviruses differ between PTCs and NCs. Other factors that can be studied in future work include differences in integration sites of intact proviruses and viral replication fitness, the latter being of particular relevance given prior reports showing that the *ex vivo* cultivation of virus from CD4 T cells of a PTC consistently failed and showed delayed kinetics in three other PTCs (124). *In vitro* replication

studies of viruses from these three PTCs showed low to absent growth in two cases and a virus with normal fitness in the third case (124). In addition, the field would benefit from a comparison of host genetic variants, susceptibility of CD4 T cells for infection and expression levels of host restriction factors between the two groups.

Furthermore, a comprehensive analysis of the host antiviral immune response within PTCs is still needed, both cellular and humoral. Previous work from our group demonstrated that PTCs possess higher levels of baseline HIV-specific IFNγ-producing CD4 T cells compared to non-controllers (132). This is in contrast to reports from the VISCONTI (113, 233) and Belgian cohorts (124) demonstrating no differences in the frequency and cytokine production ability of HIV-specific CD4 and CD8 T cells within PTCs compared to patients on continuous ART. In addition to cytokine production, functional assays such as viral inhibition, target cell killing and T cell proliferation would be highly informative. There is evidence suggesting that T cells from PTCs have higher proliferative responses towards *gag* and *pol* peptides (124). In addition, it was reported that CD8 T cells sampled after 10 years of post-treatment control can suppress HIV-1 replication *in vivo* (129). With regards to the humoral immune response, little work has been performed in understanding the antibody-mediated immune response within PTCs. The only published evidence to date comes from the Belgian cohort showing that PTCs possess high levels of autologous neutralizing antibodies (124). In other cases, HIV-specific antibodies were undetectable (127).

One of the concerns regarding the study of PTCs is whether PTCs may, in fact, represent elite controllers who received ART during early infection, before they were able to demonstrate spontaneous virologic control. Multiple lines of evidence argue against this theory. First, within some of these individuals, viral loads were measured prior to treatment initiation and were found

to be persistently high (67), suggesting that it is unlikely they would have been able to spontaneously control HIV-1. Second, both in our cohort, as well as in the VISCONTI cohort, PTCs expressed lower levels of T-cell activation markers and weaker HIV-specific CD8 T cell responses, compared to HIV-1 controllers (108, 113, 132). Third, protective HLA alleles such as class I HLA-B*57 and HLA-B*27 alleles are highly enriched in elite controllers (106, 107), but no such enrichment exists within the PTCs studied to date (67, 113). Fourth, elite controllers represent 0.5-1% of well-described cohorts of HIV patients (104). PTCs, on the other hand, are identified at much higher frequencies, ranging between 4-15% (113, 115). Finally, there is a case report of an individual who was unable to control HIV-1 after the first treatment interruption, resumed treatment and after a second treatment interruption successfully controlled HIV-1 for 9 years (120). This case provides further evidence arguing against the idea that PTCs are predisposed to naturally control HIV-1 in the absence of treatment.

In addition to our studies of PTCs, studies performed for this dissertation include detailed analysis of a subject presenting with persistent low-level viremia, where viral load measurements over more than three years fluctuated between 200-800 copies/mL. This viremia persisted despite high levels of self-reported ART adherence, detectable plasma drug levels, an active ART regimen by virus resistance testing and multiple rounds of ART intensification. Our results showed that 95% of all the plasma *Pro-RT* sequences within this study participant were comprised of 2 clonal populations. These plasma clones were exact matches to intact proviral sequences amplified from the participant's PBMCs. Thus, we concluded that a persistent clone harboring intact provirus is constantly releasing virions without signs of active viral replication and that further ART intensification is unlikely to be effective in fully suppressing the viremia.

Given that this individual is currently on a protease inhibitor, these released virions would likely be immature and thus defective, yet they would still be quantified by plasma viral load testing and contribute to the measurable low-level viremia. It is unclear whether this viremia poses any transmission threat to sexual partners. Recently, another group similarly reported that in 4 out of 9 patients presenting with persistent low-level viremia, large cell clones carrying intact proviruses were identical in the *Pro-pol* region to the plasma virus (234). The mechanisms involved in clonal expansion and persistence of these cells harboring intact proviruses need to be understood to effectively target the HIV reservoir in these patients.

In chapter 4 of this thesis, we describe a novel assay, termed MIP-Seq, which stands for Matched Integration Site and Proviral Sequencing. The MIP-Seq methodology represents the first report to assess combined HIV integration sites of near-full-length proviral sequences in the setting of persistent LLV. Identifying the HIV integration site of intact proviruses has represented a major technical hurdle in the field. This knowledge is particularly crucial to a better understanding of the viral reservoir as there remains some doubt as to whether some identical proviruses arise not only from clonal expansion of HIV-infected cells, but also from early seeding of multiple cellular reservoirs during a time of limited viral diversity. Prior to our work, it was not been possible to explore the hypothesis that the integration site may influence HIV transcriptional activity of intact proviruses and thus contribute to the presence of low-level viremia. Recently, another group described an assay based on the same principles as MIP-Seq, interrogating both the near-full-length sequence, as well as integration site of the provirus (235).

Performing MIP-Seq on samples from this LLV participant showed that the largest cellular clone, which contributed a minor population of plasma virus, harbored an intact provirus integrated

in the opposite orientation relative to a highly transcribed gene. On the other hand, one of the small cellular clones contributed the majority of the plasma virus. This intact provirus was integrated in the opposite orientation relative to a host gene that was found to be transcriptionally silent. These results strongly suggest that transcriptional interference plays a role in the differential expression levels of proviral HIV-1 DNA in patients presenting with persistent low-level viremia. This hypothesis is supported by our identification of transcriptional interference of host genes that are also present in overlapping and reverse orientations.

It is important to note some of the limitations of our work. Most of the studies conducted thus far in the HIV field, including ones discussed in this thesis, have focused on cells isolated from peripheral blood. Little is known about reservoirs present in tissues, particularly the major anatomical HIV reservoirs such as the gut and lymph nodes, mainly attributed to the difficulty of obtaining these samples. There are conflicting data as to whether compartmentalization exists between virus isolated from the blood and that residing in tissues such as lymph nodes. Some studies report differences between lymph nodes and blood in the viral sequences (88, 236, 237), while other studies have shown a lack of compartmentalization of the HIV sequences between blood and lymphoid tissues (238–241). Another drawback concerns the limited number of participants included in our studies. Given that the PTC phenotype is rare, it is difficult to assemble a large cohort of individuals. Our group has recently published on the CHAMP cohort, the largest cohort to-date comprising 67 PTCs from 14 different treatment interruption studies (115). These larger cohorts of PTCs will enable future work to include a larger sample size of individuals.

In summary, within this thesis, we have described the proviral landscape in post-treatment controllers and determined that levels of total, as well as intact, proviral genomes are significantly

lower in post-treatment controllers, compared to non-controllers. We have shown that a short treatment interruption leads to an increase in the viral reservoir, but this increase is reversible upon treatment resumption. Finally, we demonstrated that plasma virus in an individual with persistent low-level viremia is largely clonal and may be influenced by transcriptional interference from the host gene into which the provirus is integrated.

References

1. Cuevas JM, Geller R, Garijo R, López-Aldeguer J, Sanjuán R. Extremely High Mutation Rate of HIV-1 In Vivo. *PLoS Biol*. 2015;13(9):1–19.

2. Abram ME, Ferris AL, Shao W, Alvord WG, Hughes SH. Nature, position, and frequency of mutations made in a single cycle of HIV-1 replication. *J Virol*. 2010;84(19):9864–9878.

3. Bruner KM, et al. Defective proviruses rapidly accumulate during acute HIV-1 infection. *Nat Med*. 2016;22(9):1043–1049.

4. Ho Y-C, et al. Replication-competent noninduced proviruses in the latent reservoir increase barrier to HIV-1 cure. *Cell*. 2013;155(3):540–51.

5. Imamichi H, et al. Defective HIV-1 proviruses produce novel protein-coding RNA species in HIV-infected patients on combination antiretroviral therapy. *Proc Natl Acad Sci*. 2016;113(31):8783–8788.

6. Cherepanov P, et al. HIV-1 integrase forms stable tetramers and associates with LEDGF/p75 protein in human cells. *J Biol Chem*. 2003;278(1):372–81.

7. Maertens G, et al. LEDGF/p75 is essential for nuclear and chromosomal targeting of HIV-1 integrase in human cells. *J Biol Chem*. 2003;278(35):33528–39.

8. Llano M, et al. LEDGF/p75 determines cellular trafficking of diverse lentiviral but not murine oncoretroviral integrase proteins and is a component of functional lentiviral preintegration complexes. *J Virol*. 2004;78(17):9524–37.

9. Ciuffi A, et al. A role for LEDGF/p75 in targeting HIV DNA integration. *Nat Med*. 2005;11(12):1287–9.

10. Sowd GA, et al. A critical role for alternative polyadenylation factor CPSF6 in targeting HIV-1 integration to transcriptionally active chromatin. *Proc Natl Acad Sci U S A*. 2016;113(8):E1054-63.

11. Bejarano DA, et al. HIV-1 nuclear import in macrophages is regulated by CPSF6-capsid interactions at the nuclear pore complex. *Elife*. 2019;8. doi:10.7554/eLife.41800.

12. Chin CR, et al. Direct Visualization of HIV-1 Replication Intermediates Shows that Capsid and CPSF6 Modulate HIV-1 Intra-nuclear Invasion and Integration. *Cell Rep*. 2015;13(8):1717–1731.

13. Schröder ARW, et al. HIV-1 integration in the human genome favors active genes and local hotspots. *Cell*. 2002;110(4):521–9.

14. Maldarelli F, et al. Specific HIV integration sites are linked to clonal expansion and persistence of infected cells. *Science*. 2014;345(6193):179–83.

15. Wagner TA, et al. Proliferation of cells with HIV integrated into cancer genes contributes to persistent infection. *Science*. 2014;345(6196):570–3.

16. Wu X, Burgess SM. Integration target site selection for retroviruses and transposable elements. *Cell Mol Life Sci*. 2004;61(19–20):2588–96.

17. Holman AG, Coffin JM. Symmetrical base preferences surrounding HIV-1, avian sarcoma/leukosis virus, and murine leukemia virus integration sites. *Proc Natl Acad Sci U S A*. 2005;102(17):6103–7.

18. Finzi D, et al. Identification of a reservoir for HIV-1 in patients on highly active antiretroviral therapy. *Science*. 1997;278(5341):1295–300.

19. Siliciano JD, et al. Long-term follow-up studies confirm the stability of the latent reservoir for HIV-1 in resting CD4+ T cells. *Nat Med*. 2003;9(6):727–728.

20. Crooks AM, et al. Precise quantitation of the latent HIV-1 reservoir: Implications for eradication strategies. *J Infect Dis*. 2015;212(9):1361–1365.

21. Chomont N, et al. HIV reservoir size and persistence are driven by T cell survival and homeostatic proliferation. *Nat Med*. 2009;15(8):893–900.

22. Simonetti FR, et al. Clonally expanded CD4+ T cells can produce infectious HIV-1 in vivo. *Proc Natl Acad Sci U S A*. 2016;113(7):1883–1888.

23. Chun TW, Fauci a S. Latent reservoirs of HIV: obstacles to the eradication of virus. *Proc Natl Acad Sci U S A*. 1999;96(September):10958–10961.

24. Finzi D, et al. Latent infection of CD4+ T cells provides a mechanism for lifelong persistence of HIV-1, even in patients on effective combination therapy. *Nat Med*. 1999;5(5):512–517.

25. Bailey JR, et al. Residual human immunodeficiency virus type 1 viremia in some patients on antiretroviral therapy is dominated by a small number of invariant clones rarely found in circulating CD4+ T cells. *J Virol*. 2006;80(13):6441–57.

26. Archin NM, et al. Administration of vorinostat disrupts HIV-1 latency in patients on antiretroviral therapy. *Nature*. 2012;487(7408):482–5.

27. Søgaard OS, et al. The Depsipeptide Romidepsin Reverses HIV-1 Latency In Vivo. *PLoS Pathog*. 2015;11(9):e1005142.

28. Delagrèverie HM, Delaugerre C, Lewin SR, Deeks SG, Li JZ. Ongoing Clinical Trials of Human Immunodeficiency Virus Latency-Reversing and Immunomodulatory Agents. *Open Forum Infect Dis*. 2016;3(4):ofw189.

29. Rasmussen TA, et al. Panobinostat, a histone deacetylase inhibitor, for latent virus

reactivation in HIV-infected patients on suppressive antiretroviral therapy: A phase 1/2, single group, clinical trial. *Lancet HIV*. 2014;1(1):e13–e21.

30. Vandegraaff N, Kumar R, Burrell CJ. Kinetics of Human Immunodeficiency Virus Type 1 (HIV) DNA Integration in Acutely Infected Cells as Determined Using a Novel Assay for Detection of Integrated HIV DNA. *J Virol*. 2001;1(22):11253–11260.

31. Butler SL, Hansen MS, Bushman FD. A quantitative assay for HIV DNA integration in vivo. *Nat Med*. 2001;7(5):631–634.

32. Chun TW, et al. Quantification of latent tissue reservoirs and total body viral load in HIV-1 infection. *Nature*. 1997;387(6629):183–8.

33. Kaiser P, et al. Productive human immunodeficiency virus type 1 infection in peripheral blood predominantly takes place in CD4/CD8 double-negative T lymphocytes. *J Virol*. 2007;81(18):9693–706.

34. Pasternak AO, et al. Cellular levels of HIV unspliced RNA from patients on combination antiretroviral therapy with undetectable plasma viremia predict the therapy outcome. *PLoS One*. 2009;4(12):e8490.

35. Klatt NR, et al. Limited HIV infection of central memory and stem cell memory CD4+ T cells is associated with lack of progression in viremic individuals. *PLoS Pathog*. 2014;10(8):e1004345.

36. Nottet HSLM, et al. HIV-1 can persist in aged memory CD4+ T lymphocytes with minimal signs of evolution after 8.3 years of effective highly active antiretroviral therapy. *J Acquir Immune Defic Syndr*. 2009;50(4):345–353.

37. Strain MC, et al. Highly precise measurement of HIV DNA by droplet digital PCR. *PLoS One*. 2013;8(4):e55943.

38. Yukl SA, et al. A comparison of methods for measuring rectal HIV levels suggests that HIV DNA resides in cells other than CD4+ T cells, including myeloid cells. *AIDS*. 2014;28(3):439–42.

39. Yukl SA, et al. The distribution of HIV DNA and RNA in cell subsets differs in gut and blood of HIV-positive patients on ART: implications for viral persistence. *J Infect Dis*. 2013;208(8):1212–20.

40. Hatano H, et al. Comparison of HIV DNA and RNA in gut-associated lymphoid tissue of HIV-infected controllers and noncontrollers. *AIDS*. 2013;27(14):2255–60.

41. Rozera G, et al. Comparison of real-time PCR methods for measurement of HIV-1 proviral DNA. *J Virol Methods*. 2010;164(1–2):135–138.

42. Malnati MS, et al. A universal real-time PCR assay for the quantification of group-M HIV-1 proviral load. *Nat Protoc*. 2008;3(7):1240–1248.

43. Brussel A, Sonigo P. Evidence for Gene Expression by Unintegrated Human Immunodeficiency Virus Type 1 DNA Species. *J Virol*. 2004;78(20):11263–11271.

44. Yerly S, et al. Proviral HIV-DNA predicts viral rebound and viral setpoint after structured treatment interruptions. *Aids*. 2004;18(0269–9370 (Print)):1951–1953.

45. Williams JP, et al. HIV-1 DNA predicts disease progression and post-treatment virological control. *Elife*. 2014;3:e03821.

46. Wu Y, Marsh JW. Gene transcription in HIV infection. *Microbes Infect*. 2003;5(11):1023–1027.

47. Koelsch KK, et al. Dynamics of total, linear nonintegrated, and integrated HIV-1 DNA in vivo and in vitro. *J Infect Dis*. 2008;197(3):411–9.

48. Besson GJ, et al. HIV-1 DNA decay dynamics in blood during more than a decade of suppressive antiretroviral therapy. *Clin Infect Dis*. 2014;59(9):1312–1321.

49. Iyer SR, Yu D, Biancotto A, Margolis LB, Wu Y. Measurement of human immunodeficiency virus type 1 preintegration transcription by using Rev-dependent Rev-CEM cells reveals a sizable transcribing DNA population comparable to that from proviral templates. *J Virol*. 2009;83(17):8662–73.

50. Wu Y, Marsh JW. Early transcription from nonintegrated DNA in human immunodeficiency virus infection. *J Virol*. 2003;77(19):10376–82.

51. Yoder KE, Fishel R. PCR-based detection is unable to consistently distinguish HIV 1LTR circles. *J Virol Methods*. 2006;138(1–2):201–6.

52. Pace MJ, Graf EH, O'Doherty U. HIV 2-long terminal repeat circular DNA is stable in primary CD4+T Cells. *Virology*. 2013;441(1):18–21.

53. De Spiegelaere W, et al. Quantification of integrated HIV DNA by repetitive-sampling Alu-HIV PCR on the basis of poisson statistics. *Clin Chem*. 2014;60(6):886–895.

54. Grover D, et al. Alu repeat analysis in the complete human genome: Trends and variations with respect to genomic composition. *Bioinformatics*. 2004;20(6):813–817.

55. Mbisa JL, Delviks-Frankenberry KA, Thomas JA, Gorelick RJ, Pathak VK. Real-time PCR analysis of HIV-1 replication post-entry events. *Methods Mol Biol*. 2009;485:55–72.

56. Agosto LM, et al. HIV-1 integrates into resting CD4+ T cells even at low inoculums as demonstrated with an improved assay for HIV-1 integration. *Virology*. 2007;368(1):60–72.

57. Liszewski MK, Yu JJ, O'Doherty U. Detecting HIV-1 integration by repetitive-sampling Alu-gag PCR. *Methods*. 2009;47(4):254–260.

58. Strongin Z, et al. Effect of Short-Term Antiretroviral Therapy Interruption on Levels of

Integrated HIV DNA. *J Virol*. 2018;92(12). doi:10.1128/JVI.00285-18.

59. Lada SM, et al. Quantitation of Integrated HIV Provirus by Pulsed-Field Gel Electrophoresis and Droplet Digital PCR. *J Clin Microbiol*. 2018;56(12):631–4.

60. Lehrman G, et al. Depletion of latent HIV-1 infection in vivo: a proof-of-concept study. *Lancet*. 2005;366(9485):549–55.

61. Suspène R, Meyerhans A. Quantification of unintegrated HIV-1 DNA at the single cell level in vivo. *PLoS One*. 2012;7(5):e36246.

62. Jung A, et al. Recombination: Multiply infected spleen cells in HIV patients. *Nature*. 2002;418(6894):144.

63. Josefsson L, et al. Single Cell Analysis of Lymph Node Tissue from HIV-1 Infected Patients Reveals that the Majority of CD4+ T-cells Contain One HIV-1 DNA Molecule. *PLoS Pathog*. 2013;9(6). doi:10.1371/journal.ppat.1003432.

64. Deleage C, et al. Defining HIV and SIV Reservoirs in Lymphoid Tissues. *Pathog Immun*. 2016;1(1):68–106.

65. Li B, et al. Rapid reversion of sequence polymorphisms dominates early human immunodeficiency virus type 1 evolution. *J Virol*. 2007;81(1):193–201.

66. Lee GQ, et al. Clonal expansion of genome-intact HIV-1 in functionally-polarized Th1 CD4 T cells. *J Clin Invest*. 2017;127(7):2689–2696.

67. Sharaf R, et al. HIV-1 proviral landscapes distinguish posttreatment controllers from noncontrollers. *J Clin Invest*. 2018;128(9):4074–4085.

68. Hiener B, et al. Identification of Genetically Intact HIV-1 Proviruses in Specific CD4 + T Cells from Effectively Treated Participants. *Cell Rep*. 2017;21(3):813–822.

69. Bruner KM, et al. A quantitative approach for measuring the reservoir of latent HIV-1 proviruses. *Nature*. 2019; doi:10.1038/s41586-019-0898-8.

70. Purcell DF, Martin MA. Alternative splicing of human immunodeficiency virus type 1 mRNA modulates viral protein expression, replication, and infectivity. *J Virol*. 1993;67(11):6365–78.

71. Pasternak AO, et al. Highly sensitive methods based on seminested real-time reverse transcription-PCR for quantitation of human immunodeficiency virus type 1 unspliced and multiply spliced RNA and proviral DNA. *J Clin Microbiol*. 2008;46(7):2206–2211.

72. Li JZ, et al. The size of the expressed HIV reservoir predicts timing of viral rebound after treatment interruption. *AIDS*. 2016;30(3):343–53.

73. Ledderose C, Heyn J, Limbeck E, Kreth S. Selection of reliable reference genes for

quantitative real-time PCR in human T cells and neutrophils. *BMC Res Notes*. 2011;4(1):427.

74. Gutiérrez C, et al. Bryostatin-1 for latent virus reactivation in HIV-infected patients on antiretroviral therapy. *AIDS*. 2016;30(9):1385–92.

75. Kearney MF, et al. Origin of Rebound Plasma HIV Includes Cells with Identical Proviruses That Are Transcriptionally Active before Stopping of Antiretroviral Therapy. *J Virol*. 2016;90(3):1369–1376.

76. Siliciano JD, Siliciano RF. Enhanced Culture Assay for Detection and Quantitation of Latently Infected, Resting Virus in HIV-1-Infected Individuals. *Methods Mol Biol*. 2005;304(3):3–15.

77. Eriksson S, et al. Comparative analysis of measures of viral reservoirs in HIV-1 eradication studies. *PLoS Pathog*. 2013;9(2):e1003174.

78. Hermankova M, et al. Analysis of human immunodeficiency virus type 1 gene expression in latently infected resting CD4+ T lymphocytes in vivo. *J Virol*. 2003;77(13):7383–92.

79. Wei DG, et al. Histone deacetylase inhibitor romidepsin induces HIV expression in CD4 T cells from patients on suppressive antiretroviral therapy at concentrations achieved by clinical dosing. *PLoS Pathog*. 2014;10(4):e1004071.

80. Howell B, et al. Developing and applying ultrasensitive p24 protein immunoassay for HIV lateny. *J Virus Erad*. 2015;Suppl 1(1):1–18 Oral Presentation 3.1.

81. Metcalf Pate KA, et al. A murine viral outgrowth assay to detect residual HIV type 1 in patients with undetectable viral loads. *J Infect Dis*. 2015;212(9):1387–1396.

82. Antiretroviral Therapy Cohort Collaboration (ART-CC), et al. Impact of low-level viremia on clinical and virological outcomes in treated HIV-1-infected patients. *AIDS*. 2015;29(3):373–83.

83. Bernal E, et al. Low-Level Viremia Is Associated With Clinical Progression in HIV-Infected Patients Receiving Antiretroviral Treatment. *JAIDS J Acquir Immune Defic Syndr*. 2018;78(3):329–337.

84. Geretti AM, et al. Determinants of virological failure after successful viral load suppression in first-line highly active antiretroviral therapy. *Antivir Ther*. 2008;13(7):927–936.

85. Ryscavage P, Kelly S, Li JZ, Richard Harrigan P, Taiwo B. Significance and clinical management of persistent low-level viremia and very-low-level viremia in HIV-1-infected patients. *Antimicrob Agents Chemother*. 2014;58(7):3585–3598.

86. Hermans LE, et al. Effect of HIV-1 low-level viraemia during antiretroviral therapy on treatment outcomes in WHO-guided South African treatment programmes: a multicentre

cohort study. *Lancet Infect Dis*. 2018;18(2):188–197.

87. Konstantopoulos C, Ribaudo H, Ragland K, Bangsberg DR, Li JZ. Antiretroviral Regimen and Suboptimal Medication Adherence Are Associated With Low-Level Human Immunodeficiency Virus Viremia. *Open Forum Infect Dis*. 2015;2(1):ofu119-ofu119.

88. Lorenzo-Redondo R, et al. Persistent HIV-1 replication maintains the tissue reservoir during therapy. *Nature*. 2016;530(7588):51–56.

89. Fletcher C V., et al. Persistent HIV-1 replication is associated with lower antiretroviral drug concentrations in lymphatic tissues. *Proc Natl Acad Sci U S A*. 2014;111(6):2307–12.

90. Li JZ, et al. Prevalence and significance of HIV-1 drug resistance mutations among patients on antiretroviral therapy with detectable low-level Viremia. *Antimicrob Agents Chemother*. 2012;56(11):5998–6000.

91. Vancoillie L, et al. Longitudinal sequencing of HIV-1 infected patients with low-level viremia for years while on ART shows no indications for genetic evolution of the virus. *Virology*. 2017;510(July):185–193.

92. Dinoso JB, et al. Treatment intensification does not reduce residual HIV-1 viremia in patients on highly active antiretroviral therapy. *Proc Natl Acad Sci U S A*. 2009;106(23):9403–8.

93. Gandhi RT, et al. The Effect of Raltegravir Intensification on Low-level Residual Viremia in HIV-Infected Patients on Antiretroviral Therapy: A Randomized Controlled Trial. *PLoS Med*. 2010;7(8):e1000321.

94. Haugaard SB. Toxic metabolic syndrome associated with HAART. *Expert Opin Drug Metab Toxicol*. 2006;2(3):429–45.

95. Hofman P, Nelson AM. The pathology induced by highly active antiretroviral therapy against human immunodeficiency virus: an update. *Curr Med Chem*. 2006;13(26):3121–32.

96. Bradbury RA, Samaras K. Antiretroviral therapy and the human immunodeficiency virus - improved survival but at what cost? *Diabetes Obes Metab*. 2008;10(6):441–50.

97. Montessori V, Press N, Harris M, Akagi L, Montaner JSG. Adverse effects of antiretroviral therapy for HIV infection. *CMAJ*. 2004;170(2):229–38.

98. Herman JS, Easterbrook PJ. The metabolic toxicities of antiretroviral therapy. *Int J STD AIDS*. 2001;12(9):555-62; quiz 563–4.

99. Hütter G, et al. Long-Term Control of HIV by CCR5 Delta32/Delta32 Stem-Cell Transplantation. *N Engl J Med*. 2009;360(7):692–698.

100. Allers K, et al. Evidence for the cure of HIV infection by CCR5Δ32/Δ32 stem cell transplantation. *Blood*. 2011;117(10):2791–2799.

101. Yukl SA, et al. Challenges in detecting HIV persistence during potentially curative interventions: a study of the Berlin patient. *PLoS Pathog*. 2013;9(5):e1003347.

102. Gupta RK, et al. HIV-1 remission following CCR5Δ32/Δ32 haematopoietic stem-cell transplantation. *Nature*. 2019; doi:10.1038/s41586-019-1027-4.

103. Jensen B-E, et al. Analytic treatment interruption (ATI) after allogeneic CCR5-D32 HSCT for AML in 2013. *(CROI abstract 394, 2019)*.

104. Okulicz JF, Lambotte O. Epidemiology and clinical characteristics of elite controllers. *Curr Opin HIV AIDS*. 2011;6(3):163–8.

105. Deeks SG, Walker BD. Human Immunodeficiency Virus Controllers: Mechanisms of Durable Virus Control in the Absence of Antiretroviral Therapy. *Immunity*. 2007;27(3):406–416.

106. International HIV Controllers Study, et al. The Major Genetic Determinants of HIV-1 Control Affect HLA Class I Peptide Presentation. *Science (80-)*. 2010;330(6010):1551–1557.

107. Migueles SA, et al. HLA B*5701 is highly associated with restriction of virus replication in a subgroup of HIV-infected long term nonprogressors. *Proc Natl Acad Sci U S A*. 2000;97(6):2709–14.

108. Lobritz MA, Lassen KG, Arts EJ. HIV-1 replicative fitness in elite controllers. *Curr Opin HIV AIDS*. 2011;6(3):214–20.

109. Migueles SA, et al. Lytic Granule Loading of CD8+ T Cells Is Required for HIV-Infected Cell Elimination Associated with Immune Control. *Immunity*. 2008;29(6):1009–1021.

110. Hersperger AR, et al. Perforin expression directly ex vivo by HIV-specific CD8+T-cells is a correlate of HIV elite control. *PLoS Pathog*. 2010;6(5):1–13.

111. Bailey JR, Williams TM, Siliciano RF, Blankson JN. Maintenance of viral suppression in HIV-1–infected HLA-B*57 $^{+}$ elite suppressors despite CTL escape mutations. *J Exp Med*. 2006;203(5):1357–1369.

112. Ruiz L, et al. Structured treatment interruption in chronically HIV-1 infected patients after long-term viral suppression. *AIDS*. 2000;14(4):397–403.

113. Sáez-Cirión A, et al. Post-treatment HIV-1 controllers with a long-term virological remission after the interruption of early initiated antiretroviral therapy ANRS VISCONTI Study. *PLoS Pathog*. 2013;9(3):e1003211.

114. Hocqueloux L, et al. Long-term immunovirologic control following antiretroviral therapy interruption in patients treated at the time of primary HIV-1 infection. *AIDS*.

2010;24(10):1598–601.

115. Namazi G, et al. The Control of HIV after Antiretroviral Medication Pause (CHAMP) study: post-treatment controllers identified from 14 clinical studies. *J Infect Dis*. 2018;218. doi:10.1093/infdis/jiy479.

116. Maenza J, et al. How often does treatment of primary HIV lead to post-treatment control? *Antivir Ther*. 2015;20(8):855–863.

117. Stöhr W, et al. Duration of HIV-1 Viral Suppression on Cessation of Antiretroviral Therapy in Primary Infection Correlates with Time on Therapy. *PLoS One*. 2013;8(10):8–13.

118. Lodi S, et al. Immunovirologic Control 24 Months After Interruption of Antiretroviral Therapy Initiated Close to HIV Seroconversion. *Arch Intern Med*. 2012;172(16):1252.

119. Goujard C, et al. HIV-1 control after transient antiretroviral treatment initiated in primary infection: role of patient characteristics and effect of therapy. *Antivir Ther*. 2012;17(6):1001–9.

120. Salgado M, et al. Prolonged control of replication-competent dual- tropic human immunodeficiency virus-1 following cessation of highly active antiretroviral therapy. *Retrovirology*. 2011;8(1):97.

121. Assoumou L, et al. A low HIV-DNA level in peripheral blood mononuclear cells at antiretroviral treatment interruption predicts a higher probability of maintaining viral control. *AIDS*. 2015;29(15):2003–7.

122. Perkins MJ, et al. Brief Report: Prevalence of Posttreatment Controller Phenotype Is Rare in HIV-Infected Persons After Stopping Antiretroviral Therapy. *J Acquir Immune Defic Syndr*. 2017;75(3):364–369.

123. Maggiolo F, Di Filippo E, Comi L, Callegaro A. Post-treatment controllers after treatment interruption in chronically HIV-infected patients. *AIDS*. 2018;32(5):623–628.

124. Van Gulck E, et al. Immune and viral correlates of "secondary viral control" after treatment interruption in chronically HIV-1 infected patients. *PLoS One*. 2012;7(5):e37792.

125. Van Gulck E, et al. Control of viral replication after cessation of HAART. *AIDS Res Ther*. 2011;8:4–8.

126. Frange P, et al. HIV-1 virological remission lasting more than 12 years after interruption of early antiretroviral therapy in a perinatally infected teenager enrolled in the French ANRS EPF-CO10 paediatric cohort: a case report. *Lancet HIV*. 2016;3(1):e49–e54.

127. Violari A, et al. A child with perinatal HIV infection and long-term sustained virological control following antiretroviral treatment cessation. *Nat Commun*. 2019;10(1):412.

128. Bedimo R, et al. Sustained HIV viral suppression following treatment interruption: an observational study. *AIDS Res Hum Retroviruses*. 2006;22(1):40–4.

129. Kinloch-de Loes S, et al. Aviremia 10 Years Postdiscontinuation of Antiretroviral Therapy Initiated During Primary Human Immunodeficiency Virus-1 Infection and Association With Gag-Specific T-Cell Responses. *Open forum Infect Dis*. 2015;2(4):ofv144.

130. McMahon JH, et al. Post-treatment control in an adult with perinatally acquired HIV following cessation of antiretroviral therapy. *AIDS*. 2017;31(9):1344–1346.

131. Sneller MC, et al. A randomized controlled safety/efficacy trial of therapeutic vaccination in HIV-infected individuals who initiated antiretroviral therapy early in infection. *Sci Transl Med*. 2017;9(419):eaan8848.

132. Etemad B, et al. Viral and immune characteristics of HIV post-treatment controllers in ACTG studies *(CROI abstract 347, 2016)*.

133. Conway JM, Perelson AS. Post-treatment control of HIV infection. *Proc Natl Acad Sci*. 2015;112(17):5467–5472.

134. Cockerham LR, Hatano H, Deeks SG. Post-Treatment Controllers: Role in HIV "Cure" Research. *Curr HIV/AIDS Rep*. 2016;13(1):1–9.

135. Schooley RT, et al. AIDS clinical trials group 5197: a placebo-controlled trial of immunization of HIV-1-infected persons with a replication-deficient adenovirus type 5 vaccine expressing the HIV-1 core protein. *J Infect Dis*. 2010;202(5):705–16.

136. Skiest DJ, et al. Interruption of Antiretroviral Treatment in HIV-Infected Patients with Preserved Immune Function Is Associated with a Low Rate of Clinical Progression: A Prospective Study by AIDS Clinical Trials Group 5170. *J Infect Dis*. 2007;195(10):1426–1436.

137. Kilby JM, et al. A randomized, partially blinded phase 2 trial of antiretroviral therapy, HIV-specific immunizations, and interleukin-2 cycles to promote efficient control of viral replication (ACTG A5024). *J Infect Dis*. 2006;194(12):1672–6.

138. Volberding P, et al. Antiretroviral therapy in acute and recent HIV infection: a prospective multicenter stratified trial of intentionally interrupted treatment. *AIDS*. 2009;23(15):1987–95.

139. Jacobson JM, et al. Evidence that intermittent structured treatment interruption, but not immunization with ALVAC-HIV vCP1452, promotes host control of HIV replication: the results of AIDS Clinical Trials Group 5068. *J Infect Dis*. 2006;194(5):623–632.

140. R Core Team. R: A language and environment for statistical computing. R Foundation for Statistical Computing, Vienna, Austria. URL: http://www.R-project.org/.

141. Rose PP, Korber BT. Detecting hypermutations in viral sequences with an emphasis on G → A hypermutation. *Bioinformatics*. 2000;16(4):400–401.

142. Carlson JM, et al. Correlates of protective cellular immunity revealed by analysis of population-level immune escape pathways in HIV-1. *J Virol*. 2012;86(24):13202–16.

143. Palmer S, et al. Multiple, linked human immunodeficiency virus type 1 drug resistance mutations in treatment-experienced patients are missed by standard genotype analysis. *J Clin Microbiol*. 2005;43(1):406–13.

144. Kearney M, et al. Frequent polymorphism at drug resistance sites in HIV-1 protease and reverse transcriptase. *AIDS*. 2008;22(4):497–501.

145. Hosmane NN, et al. Proliferation of latently infected CD4 + T cells carrying replication-competent HIV-1: Potential role in latent reservoir dynamics. *J Exp Med*. 2017;214(4):959–972.

146. Mansky LM, Temin HM. Lower in vivo mutation rate of human immunodeficiency virus type 1 than that predicted from the fidelity of purified reverse transcriptase. *J Virol*. 1995;69(8):5087–94.

147. Clarridge KE, et al. Effect of analytical treatment interruption and reinitiation of antiretroviral therapy on HIV reservoirs and immunologic parameters in infected individuals. *PLoS Pathog*. 2018;14(1):e1006792.

148. Rhee S-Y, et al. Human immunodeficiency virus reverse transcriptase and protease sequence database. *Nucleic Acids Res*. 2003;31(1):298–303.

149. Shafer RW. Rationale and Uses of a Public HIV Drug-Resistance Database. *J Infect Dis*. 2006;194(s1):S51–S58.

150. Miles LR, et al. Effect of polypurine tract (PPT) mutations on human immunodeficiency virus type 1 replication: a virus with a completely randomized PPT retains low infectivity. *J Virol*. 2005;79(11):6859–67.

151. Charneau P, Alizon M, Clavel F. A second origin of DNA plus-strand synthesis is required for optimal human A Second Origin of DNA Plus-Strand Synthesis Is Required for Optimal Human Immunodeficiency Virus Replication. *J Virol*. 1992;66(5):2814–2820.

152. Schultz SJ, Zhang M, Kelleher CD, Champoux JJ. Analysis of plus-strand primer selection, removal, and reutilization by retroviral reverse transcriptases. *J Biol Chem*. 2000;275(41):32299–32309.

153. Perkins M, et al. Post-Treatment Control of HIV Infection in an Early Diagnosed Well Characterized Military Cohort of Chronically HIV-1-Infected Subjects. *Open Forum Infect Dis*. 2015;2(suppl_1):1072.

154. Henrich TJ, et al. Antiretroviral-Free HIV-1 Remission and Viral Rebound After

Allogeneic Stem Cell Transplantation. *Ann Intern Med*. 2014;161(5):319.

155. Hill AL, Rosenbloom DIS, Fu F, Nowak MA, Siliciano RF. Predicting the outcomes of treatment to eradicate the latent reservoir for HIV-1. *Proc Natl Acad Sci*. 2014;111(37):13475–13480.

156. Hill AL, et al. Real-Time Predictions of Reservoir Size and Rebound Time during Antiretroviral Therapy Interruption Trials for HIV. *PLoS Pathog*. 2016;12(4):1–26.

157. Garbuglia AR, et al. HIV-1 DNA burden dynamics in CD4 T cells and monocytes in patients undergoing a transient therapy interruption. *J Med Virol*. 2004;74(3):373–381.

158. Calin R, et al. Treatment interruption in chronically HIV-infected patients with an ultralow HIV reservoir. *AIDS*. 2016;30(5):761–9.

159. Bui JK, et al. Proviruses with identical sequences comprise a large fraction of the replication-competent HIV reservoir. *PLoS Pathog*. 2017;13(3):e1006283.

160. Cohn LB, et al. Clonal CD4 + T cells in the HIV-1 latent reservoir display a distinct gene profile upon reactivation. *Nat Med*. 2018; doi:10.1038/s41591-018-0017-7.

161. Wiegand A, et al. Single-cell analysis of HIV-1 transcriptional activity reveals expression of proviruses in expanded clones during ART. *Proc Natl Acad Sci*. 2017;114(18):E3659–E3668.

162. Pollack RA, et al. Defective HIV-1 Proviruses Are Expressed and Can Be Recognized by Cytotoxic T Lymphocytes, which Shape the Proviral Landscape. *Cell Host Microbe*. 2017;21(4):494–506.e4.

163. Gandhi RT, et al. Levels of HIV-1 persistence on antiretroviral therapy are not associated with markers of inflammation or activation. *PLoS Pathog*. 2017;13(4):1–21.

164. Montserrat M, et al. Impact of long-term antiretroviral therapy interruption and resumption on viral reservoir in HIV-1 infected patients. *AIDS*. 2017;31(13):1895–1897.

165. O'Doherty U, Swiggard WJ, Jeyakumar D, McGain D, Malim MH. A sensitive, quantitative assay for human immunodeficiency virus type 1 integration. *J Virol*. 2002;76(21):10942–50.

166. Lada S, et al. Novel Assay to Measure Integrated HIV DNA in PBMC from ART-Suppressed Persons *(CROI abstract 300, 2017)*.

167. Sharaf RR, Li JZ. The Alphabet Soup of HIV Reservoir Markers. *Curr HIV/AIDS Rep*. 2017;14(2). doi:10.1007/s11904-017-0355-y.

168. Murray JM, et al. HIV DNA Subspecies Persist in both Activated and Resting Memory CD4+ T Cells during Antiretroviral Therapy. *J Virol*. 2014;88(6):3516–3526.

169. Agosto LM, et al. Patients on HAART often have an excess of unintegrated HIV DNA:

Implications for monitoring reservoirs. *Virology*. 2011;409(1):46–53.

170. Kiselinova M, et al. Integrated and Total HIV-1 DNA Predict Ex Vivo Viral Outgrowth. *PLoS Pathog*. 2016;12(3). doi:10.1371/journal.ppat.1005472.

171. Yu JJ, et al. A more precise HIV integration assay designed to detect small differences finds lower levels of integrated DNA in HAART treated patients. *Virology*. 2008;379(1):78–86.

172. Li JZ, Smith DM, Mellors JW. The need for treatment interruption studies and biomarker identification in the search for an HIV cure. *AIDS*. 2015;29(12):1429–32.

173. Boillat-Blanco N, et al. Virological outcome and management of persistent low-level viraemia in HIV-1-infected patients: 11 years of the Swiss HIV Cohort Study. *Antivir Ther*. 2015;20(2):165–75.

174. Hofstra LM, et al. Residual viremia is preceding viral blips and persistent low-level viremia in treated HIV-1 patients. *PLoS One*. 2014;9(10):e110749.

175. Laprise C, de Pokomandy A, Baril J-G, Dufresne S, Trottier H. Virologic failure following persistent low-level viremia in a cohort of HIV-positive patients: results from 12 years of observation. *Clin Infect Dis*. 2013;57(10):1489–96.

176. Esber A, et al. Persistent low level viremia predicts subsequent virologic failure. Is it time to change the 3rd 90? *Clin Infect Dis*. 2018;(July 2018):23–27.

177. Cohen MS, et al. Antiretroviral Therapy for the Prevention of HIV-1 Transmission. *N Engl J Med*. 2016;375(9):830–839.

178. Attia S, Egger M, Müller M, Zwahlen M, Low N. Sexual transmission of HIV according to viral load and antiretroviral therapy: systematic review and meta-analysis. *AIDS*. 2009;23(11):1397–404.

179. Konstantopoulos C, Ribaudo H, Ragland K, Bangsberg DR, Li JZ. Antiretroviral regimen and suboptimal medication adherence are associated with low-level human immunodeficiency virus viremia. *Open forum Infect Dis*. 2015;2(1):ofu119.

180. Cillo AR, et al. Improved single-copy assays for quantification of persistent HIV-1 viremia in patients on suppressive antiretroviral therapy. *J Clin Microbiol*. 2014;52(11):3944–3951.

181. Einkauf KB, et al. Intact HIV-1 proviruses accumulate at distinct chromosomal positions during prolonged antiretroviral therapy. *J Clin Invest*. 2019;129(2). doi:10.1172/JCI124291.

182. Lee GQ, et al. Prevalence and clinical impacts of HIV-1 intersubtype recombinants in Uganda revealed by near-full-genome population and deep sequencing approaches. *AIDS*. 2017;31(17):2345–2354.

183. Trombetta JJ, et al. Preparation of Single-Cell RNA-Seq Libraries for Next Generation Sequencing. *Current Protocols in Molecular Biology* (John Wiley & Sons, Inc., Hoboken, NJ, USA), p 4.22.1-4.22.17.

184. Rosikiewicz W, Suzuki Y, Makałowska I. OverGeneDB: A database of 5′ end protein coding overlapping genes in human and mouse genomes. *Nucleic Acids Res*. 2018;46(D1):D186–D193.

185. Rittweger M, Arasteh K. Clinical pharmacokinetics of darunavir. *Clin Pharmacokinet*. 2007;46(9):739–56.

186. Cottrell ML, Hadzic T, Kashuba ADM. Clinical pharmacokinetic, pharmacodynamic and drug-interaction profile of the integrase inhibitor dolutegravir. *Clin Pharmacokinet*. 2013;52(11):981–994.

187. Gruber S, Haering CH, Nasmyth K. Chromosomal cohesin forms a ring. *Cell*. 2003;112(6):765–777.

188. Caserta S, et al. Chronic infection drives expression of the inhibitory receptor CD200R, and its ligand CD200, by mouse and human CD4 T cells. *PLoS One*. 2012;7(4):e35466.

189. Wright GJ, et al. Characterization of the CD200 Receptor Family in Mice and Humans and Their Interactions with CD200. *J Immunol*. 2003;171(6):3034–3046.

190. Navarro J, et al. Impact of low-level viraemia on virological failure in HIV-1-infected patients with stable antiretroviral treatment. *Antivir Ther*. 2016;21(4):345–352.

191. Podsadecki TJ, Vrijens BC, Tousset EP, Rode RA, Hanna GJ. Decreased Adherence to Antiretroviral Therapy Observed prior to Transient Human Immunodeficiency Virus Type 1 Viremia. *J Infect Dis*. 2007;196(12):1773–1778.

192. Li JZ, et al. Incomplete adherence to antiretroviral therapy is associated with higher levels of residual HIV-1 viremia. *AIDS*. 2014;28(2):181–186.

193. Tobin NH, et al. Evidence that Low-Level Viremias during Effective Highly Active Antiretroviral Therapy Result from Two Processes: Expression of Archival Virus and Replication of Virus. *J Virol*. 2005;79(15):9625–9634.

194. Gonzalez-Serna A, et al. A single untimed plasma drug concentration measurement during low-level HIV viremia predicts virologic failure. *Clin Microbiol Infect*. 2016;22(12):1004.e9-1004.e16.

195. Günthard HF, et al. Human immunodeficiency virus replication and genotypic resistance in blood and lymph nodes after a year of potent antiretroviral therapy. *J Virol*. 1998;72(3):2422–8.

196. Martinez-Picado J, et al. Antiretroviral resistance during successful therapy of HIV type 1 infection. *Proc Natl Acad Sci U S A*. 2000;97(20):10948–53.

197. Hermankova M. HIV-1 Drug Resistance Profiles in Children and Adults With Viral Load of <50 Copies/mL Receiving Combination Therapy. *JAMA*. 2001;286(2):196.

198. Havlir D V, et al. Prevalence and predictive value of intermittent viremia with combination hiv therapy. *JAMA*. 2001;286(2):171–9.

199. Bull ME, et al. Monotypic low-level HIV viremias during antiretroviral therapy are associated with disproportionate production of X4 virions and systemic immune activation. *AIDS*. 2018;32(11):1389–1401.

200. Karlsson AC, et al. Immunologic and virologic evolution during periods of intermittent and persistent low-level viremia. *AIDS*. 2004;18(7):981–989.

201. Reus S, et al. Low-level HIV viremia is associated with microbial translocation and inflammation. *J Acquir Immune Defic Syndr*. 2013;62(2):129–134.

202. Michaelis C, Ciosk R, Nasmyth K. Cohesins: chromosomal proteins that prevent premature separation of sister chromatids. *Cell*. 1997;91(1):35–45.

203. Losada A, Yokochi T, Kobayashi R, Hirano T. Identification and characterization of SA/Scc3p subunits in the Xenopus and human cohesin complexes. *J Cell Biol*. 2000;150(3):405–416.

204. Sumara I, Vorlaufer E, Gieffers C, Peters BH, Peters JM. Characterization of vertebrate cohesin complexes and their regulation in prophase. *J Cell Biol*. 2000;151(4):749–761.

205. Lara-Pezzi E, et al. Evidence of a transcriptional co-activator function of cohesin STAG/SA/Scc3. *J Biol Chem*. 2004;279(8):6553–9.

206. Rijkers ESK, et al. The inhibitory CD200R is differentially expressed on human and mouse T and B lymphocytes. *Mol Immunol*. 2008;45(4):1126–1135.

207. Vaine CA, Soberman RJ. The CD200-CD200R1 inhibitory signaling pathway: immune regulation and host-pathogen interactions. *Adv Immunol*. 2014;121(3):191–211.

208. Lewinski MK, et al. Genome-wide analysis of chromosomal features repressing human immunodeficiency virus transcription. *J Virol*. 2005;79(11):6610–9.

209. Shan L, et al. Influence of Host Gene Transcription Level and Orientation on HIV-1 Latency in a Primary-Cell Model. *J Virol*. 2011;85(11):5384–5393.

210. Lenasi T, Contreras X, Peterlin BM. Transcriptional Interference Antagonizes Proviral Gene Expression to Promote HIV Latency. *Cell Host Microbe*. 2008;4(2):123–133.

211. Han Y, et al. Orientation-Dependent Regulation of Integrated HIV-1 Expression by Host Gene Transcriptional Readthrough. *Cell Host Microbe*. 2008;4(2):134–146.

212. Kuo HH, et al. Anti-apoptotic Protein BIRC5 Maintains Survival of HIV-1-Infected CD4+ T Cells. *Immunity*. 2018;48(6):1183–1194.e5.

213. Cummins NW, et al. Maintenance of the HIV Reservoir Is Antagonized by Selective BCL2 Inhibition. *J Virol*. 2017;91(11):1–12.

214. Huang S-H, et al. Latent HIV reservoirs exhibit inherent resistance to elimination by CD8+ T cells. *J Clin Invest*. 2018;128(2):876–889.

215. Battivelli E, et al. Distinct chromatin functional states correlate with HIV latency reactivation in infected primary CD4+ T Cells. *Elife*. 2018;7:242958.

216. Chen H-C, Martinez JP, Zorita E, Meyerhans A, Filion GJ. Position effects influence HIV latency reversal. *Nat Struct Mol Biol*. 2016;24(November):1–11.

217. Wang Z, et al. Expanded cellular clones carrying replication-competent HIV-1 persist, wax, and wane. *Proc Natl Acad Sci*. 2018;(13):201720665.

218. Laskey SB, Pohlmeyer CW, Bruner KM, Siliciano RF. Evaluating Clonal Expansion of HIV-Infected Cells: Optimization of PCR Strategies to Predict Clonality. *PLoS Pathog*. 2016;12(8):1–17.

219. Salantes DB, et al. HIV-1 latent reservoir size and diversity are stable following brief treatment interruption. *J Clin Invest*. 2018;128(7):3102–3115.

220. Neumann AU, et al. HIV-1 rebound during interruption of highly active antiretroviral therapy has no deleterious effect on reinitiated treatment. Comet Study Group. *AIDS*. 1999;13(6):677–83.

221. García F, et al. Dynamics of viral load rebound and immunological changes after stopping effective antiretroviral therapy. *AIDS*. 1999;13(11):F79-86.

222. Martinez-Picado J, et al. Selection of drug-resistant HIV-1 mutants in response to repeated structured treatment interruptions. *AIDS*. 2002;16(6):895–9.

223. Schweighardt B, et al. Emergence of drug-resistant HIV-1 variants in patients undergoing structured treatment interruptions. *AIDS*. 2002;16(17):2342–4.

224. Piketty C, et al. A high HIV DNA level in PBMCs at antiretroviral treatment interruption predicts a shorter time to treatment resumption, independently of the CD4 nadir. *J Med Virol*. 2010;82(11):1819–28.

225. Steingrover R, et al. HIV-1 viral rebound dynamics after a single treatment interruption depends on time of initiation of highly active antiretroviral therapy. *AIDS*. 2008;22(13):1583–8.

226. Colby DJ, et al. Rapid HIV RNA rebound after antiretroviral treatment interruption in persons durably suppressed in Fiebig i acute HIV infection brief-communication. *Nat Med*. 2018;24(7):923–926.

227. Archin NM, et al. Immediate antiviral therapy appears to restrict resting CD4+ cell HIV-1 infection without accelerating the decay of latent infection. *Proc Natl Acad Sci*. 2012;109(24):9523–9528.

228. Ananworanich J, et al. Impact of multi-targeted antiretroviral treatment on gut t cell depletion and hiv reservoir seeding during acute hiv infection. *PLoS One*. 2012;7(3). doi:10.1371/journal.pone.0033948.

229. Josefsson L, et al. The HIV-1 reservoir in eight patients on long-term suppressive antiretroviral therapy is stable with few genetic changes over time. *Proc Natl Acad Sci*. 2013;110(51):E4987–E4996.

230. Strain MC, et al. Effect of Treatment, during Primary Infection, on Establishment and Clearance of Cellular Reservoirs of HIV-1. *J Infect Dis*. 2005;191(9):1410–1418.

231. Buzon MJ, et al. Long-Term Antiretroviral Treatment Initiated at Primary HIV-1 Infection Affects the Size, Composition, and Decay Kinetics of the Reservoir of HIV-1-Infected CD4 T Cells. *J Virol*. 2014;88(17):10056–10065.

232. WHO. *Guideline on when to start antiretroviral therapy and on pre-exposure prophylaxis for HIV*.

233. Samri A, et al. Polyfunctional HIV-specific T-cells in post-treatment controllers. *AIDS*. 2016; doi:10.1097/QAD.0000000000001195.

234. Halvas EK, et al. Nonsuppressible viremia on ART from large cell clones carrying intact proviruses *(CROI abstract 23, 2019)*.

235. Patro S, et al. A method to determine both the integration sites and sequences of HIV-1 proviruses *(CROI abstract 338, 2019)*.

236. Günthard HF, et al. Residual human immunodeficiency virus (HIV) Type 1 RNA and DNA in lymph nodes and HIV RNA in genital secretions and in cerebrospinal fluid after suppression of viremia for 2 years. *J Infect Dis*. 2001;183(9):1318–27.

237. Haddad DN, et al. Evidence for late stage compartmentalization of HIV-1 resistance mutations between lymph node and peripheral blood mononuclear cells. *AIDS*. 2000;14(15):2273–81.

238. Ball JK, Holmes EC, Whitwell H, Desselberger U. Genomic variation of human immunodeficiency virus type 1 (HIV-1): molecular analyses of HIV-1 in sequential blood samples and various organs obtained at autopsy. *J Gen Virol*. 1994;75 (Pt 4)(4):67–79.

239. van't Wout AB, et al. Analysis of the temporal relationship between human immunodeficiency virus type 1 quasispecies in sequential blood samples and various organs obtained at autopsy. *J Virol*. 1998;72(1):488–96.

240. Imamichi H, et al. Lack of compartmentalization of HIV-1 quasispecies between the gut and peripheral blood compartments. *J Infect Dis*. 2011;204(2):309–314.

241. Evering TH, et al. Absence of HIV-1 evolution in the gut-associated lymphoid tissue from patients on combination antiviral therapy initiated during primary infection. *PLoS Pathog*. 2012;8(2). doi:10.1371/journal.ppat.1002506.